Institut für Veterinärpharmakologie und -toxikologie
der Vetsuisse-Fakultät Universität Zürich

Direktor: Prof. Dr. Felix Althaus

Arbeit unter wissenschaftlicher Betreuung von

Dr. Kristijan Ramadan

# Chromatin-associated protein degradation: influence of p97/VCP on key factors in the DNA damage response

## Inaugural-Dissertation

zur Erlangung der Doktorwürde der

Vetsuisse-Fakultät Universität Zürich

vorgelegt von

**Sebastian Martin Koller**

Tierarzt

von Wil SG

genehmigt auf Antrag von

Prof. Dr. Hanspeter Nägeli

Prof. Dr. Ulrich Hübscher

**2013**

# Table of Contents

# 1 Summary

DNA double strand breaks (DSBs) are life-threatening lesions which can lead to chromosomal rearrangements and consequently to genomic instability, cancer or cell death. Cells respond to DSBs and other types of DNA damage with a signaling cascade called DNA damage response (DDR) in order to repair the lesions or to induce apoptosis. The AAA ATPase p97/VCP, which has diverse cellular functions linked to the ubiquitin system, has recently emerged as a crucial player in the DDR, acting as an ubiquitin-dependent remodeling factor at sites of DSBs. In this study, we investigated how MDC1, BRCA1 and 53BP1, the central DDR proteins, as well as poly-ubiquitin conjugates on chromatin, are influenced by p97 using RNA interference (siRNA), γ-irradiation (IR) and biochemical fractionation in human embryonic kidney (HEK293) cells. We observed that the three monitored DDR proteins undergo degradation upon IR in a p97-independent manner. On the other hand, p97 is demonstrated to control the total cellular level of 53BP1 as well as its localization to the tightly chromatin-associated protein fraction. We also show that impaired p97 function leads to accumulation of poly-ubiquitin conjugates on chromatin and thus confirm the importance of p97 in chromatin-associated protein degradation. As DDR proteins, p97 and the ubiquitin system are already established as druggable targets for cancer treatment, our findings have potential relevance for diagnosis, prognosis and therapy of neoplastic diseases.

# 2 Introduction

## 2.1 DNA damage

### 2.1.1 Biological and medical significance

DNA is the only biologic molecule that cannot be remanufactured but relies solely on repair of existing molecules. It is represented just by one copy in most cells, if maternal and paternal DNA is considered to be distinct. Therefore, it must be kept intact, at least in germline and proliferating cells, to function properly (1). The integrity of DNA is continuously endangered by spontaneous or endogenous alterations originating from normal metabolism, as well as by various exogenous genotoxic agents, such as ionizing radiation (IR), ultraviolet (UV) light and chemicals (2; 3; 4). It is estimated that a single cell of a metazoan organism accumulates tens of thousands of various DNA lesions every day (1; 2; 3). In a cell exposed to strong sunlight, additional 100'000 DNA lesions per hour can be induced by UV light (3). Inflammation also causes high levels of oxidative damage locally (1; 3).

DNA lesions can block replication and transcription, and they can ultimately lead to life-threatening mutations and genome aberrations (3; 5). Mutations are permanent changes in the genome which are passed to descendant cells and can lead to loss of tumor-suppressor genes or improper activation of oncogenes. The latter set off uncontrolled cellular proliferation and the development of cancer. While some types of DNA damage are primarily mutagenic, others are mainly cytotoxic or cytostatic (1) because they trigger cell death or permanent cell cycle arrest known as cellular senescence (6; 7). For instance, progressive loss of protective telomeric repeats with every round of replication limits the dividing potential of most somatic cells and functions as an anti-cancer barrier. Thus, DNA damage not only initiates cancer, but can protect against cancer as well. The downside of this protection, however, is aging. Importantly, damaging DNA is the most frequent strategy of cancer therapies (1; 3).

There are also some examples of physiological, programmed DNA lesions, arising during V(D)J recombination and class-switch recombination in developing B and T lymphocytes, respectively, to generate immunoglobulin and T-cell receptor diversity, or during meiosis to allow recombination events in developing germ cells (3; 5).

### 2.1.2 Spontaneous or endogenous damage

Misincorporation of deoxynucleotide triphosphates during DNA replication, interconversion between DNA bases caused by deamination, loss of DNA bases following DNA depurination, and modification of DNA bases by alkylation are examples for endogenous or spontaneous DNA lesions (2). Additionally, reactive oxygen and nitrogen species, which arise from normal cellular metabolism, cause several kinds of DNA single-strand breaks (SSBs) and a large variety of oxidative base and sugar products (1). DNA breaks also can be a consequence of abortive topoisomerase activity (3).

### 2.1.3 Environmental or exogenous damage

#### 2.1.3.1 Physical agents

UV light is the most pervasive environmental DNA-damaging agent, although the ozone layer absorbs the most dangerous part (UV-C) of the solar ultraviolet spectrum (3). UV radiation can induce pyrimidine dimers and 6-4 photoproducts in the DNA molecule. IR can cause oxidation of DNA bases as well as single-strand and double-strand DNA breaks (SSBs and DSBs, respectively). Sources of IR are e.g. cosmic radiation and medical treatments employing X-rays or radiotherapy (2). Some IR also results from decay of naturally occurring radioactive elements (3).

#### 2.1.3.2 Chemical agents

Chemical mutagens such as benzo[α]pyrene from combustion products are another important environmental source of DNA damage (8). Cigarette smoking as a common mechanism of self-inflicted DNA damage causes a wide variety of adducts and oxidative damage in lung and other tissues (2). Carcinogenic chemicals also can contaminate foods, for example aflatoxins found in peanuts and heterocyclic amines in over-cooked meat (3). Substances used in cancer chemotherapy can cause various types of DNA lesions, too: Alkylating agents such as methyl methanesulfonate (MMS) and temozolomide attach alkyl groups to DNA bases. Crosslinking agents, for example mitomycin C (MMC), cisplatin, psoralen, and nitrogen mustard, introduce covalent links between bases of the same DNA strand (intrastrand crosslinks) or of different DNA strands (interstrand crosslinks, ICLs) (2). The latter prevent strand separation, thus effectively arresting transcription and replication (1). The topoisomerase inhibitors camptothecin (CPT) and etoposide, which inhibit topoisomerase I or II, respectively, induce the formation of SSBs or DSBs by trapping topoisomerase-DNA covalent complexes (2).

### 2.1.4 Genome maintenance

Proper genome maintenance is a prerequisite for normal development as well as for prevention of premature aging and diverse diseases including cancer (6). Genome maintenance systems are evolutionary highly conserved, continuously monitor genomes for DNA damage and guarantee the high level of genome integrity under physiological conditions (8). They prevent genomic instability (9), which is a hallmark of cancer, and ensure faithful transmission of genetic information to progeny as well as functional integrity of DNA in long-lived, non-dividing cells (1).

The genome maintenance apparatus consists of multiple repair pathways, each focusing on a specific category of DNA lesions, and various checkpoint, signal-transduction, and effector systems connected with replication, transcription, recombination, chromatin remodeling and differentiation. It also includes a complex telomere-processing machinery (1). Genome maintenance systems thus coordinate DNA repair with cell cycle progression (9) and determine a cell's fate: survival, replicative senescence, or death (1).

### 2.1.5 Principles of the DNA damage response

The DNA damage response (DDR) is a signal transduction pathway that senses DNA damage or replication stress and sets in motion a choreographed response to protect the cell or avert the threat to the organism. Localization of DDR factors to sites of DNA damage is initiated by sensor proteins that recognize specific DNA lesions (2). Furthermore, the DDR involves the recruitment of DNA damage mediator, transducer and effector proteins (4).

The sequential accrual and function of sensing, signaling and repair proteins at sites of DNA damage is orchestrated by dynamic post-translational modifications (6) including phosphorylation, acetylation, methylation, ubiquitination, SUMOylation and PARylation (5; 10). Some of these modifications regulate structural chromatin changes ("chromatin remodeling") in order to make DNA accessible for repair factors (9; 11). The ability of the DNA-repair machinery to access the DNA can has a significant impact on genomic stability within specific chromatin regions. The mechanisms of chromatin remodeling include posttranslational modifications of histones as well as ATP-driven shifting and removal of nucleosomes, or their replacement with specialized histone variants. Four responsible ATPase families, SWI/SNF, CHD, INO80, and ISWI, have been identified in eukaryotes (12).

If the above-mentioned events allow effective DNA repair, the DDR subsides, allowing the resumption of normal cell functioning. Otherwise chronic DDR signaling triggers apoptosis or cellular senescence (3), both of which are tumor suppression mechanisms (8). Mutations in DDR genes are associated with hereditary cancer predisposition, as well as other severe pathologies (2; 3; 13).

### 2.1.6 Overview of DNA repair pathways

The simplest form of DNA repair, which is direct reversal of the lesion, is represented by $O^6$-methylguanine DNA methyltransferase (MGMT) (14). It repairs a single $O^6$-methylguanine lesion by transferring the methyl from a guanine in DNA to a cysteine in the enzyme (1). The resulting conformational change targets the protein for degradation. High MGMT expression in tumor cells is associated with resistance to alkylating chemotherapeutics (14).

The genomic maintenance system also includes multistep repair pathways, each covering a specific subclass of DNA lesions (1). In mismatch repair (MMR), detection of mismatches and insertion/deletion loops triggers a single-strand incision that is then processed by nuclease, polymerase and ligase enzymes (3). Base-excision repair (BER) removes subtle modifications of DNA, including oxidative lesions, small alkylation products, and different kinds of single-strand breaks (1). BER and SSB repair are often assumed to be synonymous, because BER-mediated excision of damaged bases indirectly results in SSB, and because both repair mechanisms involve the same components (14).

Nucleotide-excision repair (NER) eliminates helix-distorting DNA damage, a broad category of damage that affects one of the two DNA strands (1). There are two sub-pathways of NER that differ in the mechanism of lesion recognition: transcription-coupled NER, which specifically targets lesions that block transcription, and global-genome NER (3).

DSBs can be repaired by at least four independent pathways, which will be described in more detail in chapter 2.2.2: Nonhomologous end joining (NHEJ) does not require resection of the broken DNA ends, whereas homologous recombination (HR), microhomology-mediated end joining (MMEJ) and single-strand annealing (SSA) rely on end processing to a different extent (2). NHEJ and HR are regarded as the two principal repair mechanisms (15), with 53BP1 and BRCA1 (see chapter 2.2.3) playing a key role in the choice between these pathways (12).

ICL repair probably involves a combination of pathways, using part of the HR machinery in conjunction with Fanconi's anemia proteins and one of the NER endonucleases. Finally, DNA lesions that escape detection by repair proteins can be bypassed by specialized translesional polymerases, which have, however, a somewhat elevated mutation rate (1).

## 2.2 DNA double strand breaks

### 2.2.1 Biological significance

DSBs are the most deleterious form of DNA damage because they do not leave an intact complementary strand as a repair template (5). Persistent or inaccurately repaired DSBs can lead to mutations and chromosomal aberrations, which are associated with genomic instability and cancer (15) or trigger cell death (9). Broken DNA ends are vulnerable to further physical and chemical attacks resulting in lost or damaged bases or the formation of abnormal DNA structures. The physical discontinuity of DNA also presents a serious challenge for cell division since it endangers the equal partitioning of replicated genomes into daughter cells (16).

The cellular response to DSBs is characterized by accumulation of numerous DDR proteins in the vicinity of the lesion (15), which occurs within minutes and results in the formation of microscopically visible foci (17). These subnuclear compartments are also called ionizing radiation-induced foci (IRIF) since they can be induced by IR. It is thought that IRIF identify one or more DSBs undergoing repair (9).

### 2.2.2 DSB repair pathways

#### 2.2.2.1 Nonhomologous end joining

NHEJ, as the most straightforward way to repair a DSB, simply rejoins the broken ends regardless of the genetic sequence at the break. DSBs with flushed 5'-phosphorylated ends or complementary overhangs can be re-ligated efficiently with relatively high fidelity by NHEJ (16). However, since bases may be lost or added, NHEJ is an inaccurate process that takes place mostly before replication, in the absence of an identical copy of DNA (1). While NHEJ plays a critical role in maintaining the structural integrity of DNA, it does not guarantee preservation of genetic integrity but can be mutagenic (16). Nevertheless, it is the prevalent DSB repair pathway in higher eukaryotes (5), responsible for rapid repair of up to 85% of IR-induced DSBs (14).

The NHEJ apparatus is also responsible for the repair of programmed DSBs during V(D)J recombination and class-switch recombination (CSR) in developing B and T lymphocytes (3; 18). These crucial events generate immunoglobulin and T-cell receptor diversity, allowing effective recognition of diverse antigens (3). Consequently, besides causing ionizing radiation hypersensitivity, NHEJ defects yield in severe combined immune-deficiency (2; 3).

#### 2.2.2.2 Microhomology-mediated end joining

If poly-peptides are covalently attached to a broken DNA end, for example after treatment of cells with the topoisomerase inhibitor CPT, these DNA ends are not recognized by the Ku sensor heterodimer (see 2.2.3.1) and therefore cannot be processed by normal NHEJ. They are repaired by a Ku-independent mechanism called MMEJ or alternative end joining (alt-NHEJ): The blocked DNA end is removed and one strand of the break is resected until a small region of complementary base pairs is revealed. The broken ends are then stabilized through base-pairing, the displaced DNA flap is removed and ligation occurs (16). As NHEJ, MMEJ is an error-prone pathway since it always results in sequence deletions (3). Moreover, abnormal activity of MMEJ in the absence of functional NHEJ induces chromosomal translocations in mammalian cells, underscoring the importance of a correct balance between DSB repair pathways (2).

#### 2.2.2.3 Homologous recombination

NHEJ and MMEJ are functional throughout all phases of the cell cycle, but, however, are not error-free (3). As cells progress through S-phase, a second copy of the genome is produced in the form of a sister chromatid (16). Hence, after replication, HR can use the sister chromatid to properly align the broken ends and unerringly insert missing information (1). Resection of broken DNA ends, which involves multiple factors at different steps, is essential for HR (2). Whereas NHEJ and MMEJ require just local processing of DNA ends for ligation, HR relies on extensive end resection, resulting in a 3' single-stranded DNA tail onto which the central recombinase protein RAD51 can load. RAD51 forms a nucleoprotein filament which initiates the search for homology in the sister chromatid and promotes the exchange of homologous DNA strands to form heteroduplex DNA. After replication, the HR pathway can diverge towards a number of different outcomes, as shown in Figure 1 (16). Besides DSB repair, HR is also used to restart stalled replication forks and to repair ICLs (3).

#### 2.2.2.4 Single-strand annealing

SSA acts in the presence of repetitive DNA sequences and, as HR, requires end resection on a large scale (2). It basically anneals two ends of a DSB when the same sequences are found on both strands. Annealing of the resected DNA is catalyzed by RAD52, if RAD51 does not inhibit this function (19), and is followed by removal of DNA flaps (2). SSA is a non-conservative repair pathway, because not all bases that are removed during end processing are replaced, and because SSA causes translocations in the genome if the similar sequences that are found are incorrectly aligned (19).

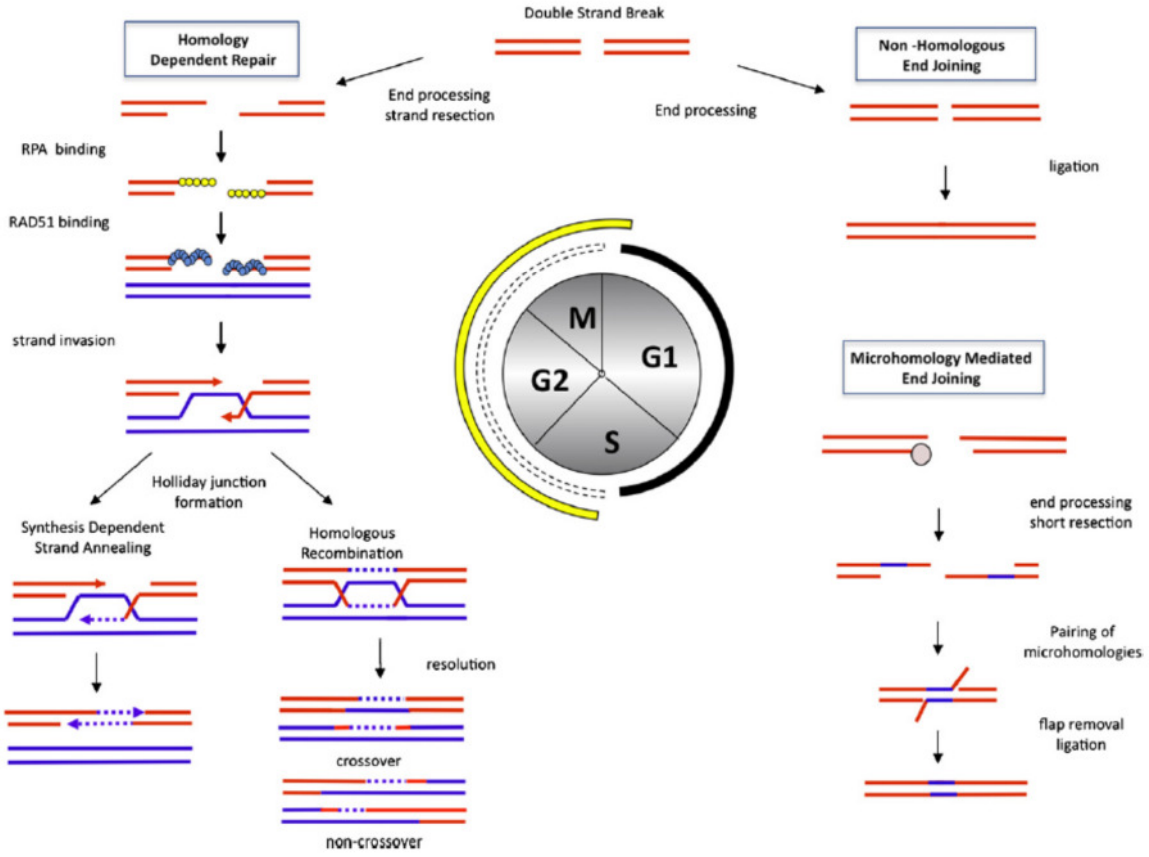


Figure 1: Pathways for repairing DSBs. Homologous recombination, here called homology directed repair, acts during the G2 phase of the cell cycle when a sister chromatid is available, and relies on extensive processing of the broken DNA ends. Non homologous end joining and microhomology-mediated end joining can basically take place in every cell cycle stage. Adapted from (16).

### 2.2.3 Key players in the DSB signaling pathway

#### 2.2.3.1 Sensor proteins

Poly(ADP-ribose) polymerases (PARP1 and PARP2) recognize DSBs (as well as SSBs) and catalyze the addition of poly(ADP-ribose) chains on proteins, such as histones and PARP1 itself (2; 20). PAR chains provide a quick transient signal and are rapidly hydrolyzed by PARG. They contribute to the recruitment of chromatin remodeling factors (2; 12). In the response to DSB, PARP1 promotes MMEJ, but seems to be dispensable for NHEJ (21). PARP1/2 also detect disrupted replication forks and promote their repair by HR (20). PARP1 is thought to compete with Ku binding to DNA ends and to mediate the initial accumulation of the MRN complex at DSBs in a γ-H2AX- and MDC1-independent manner. Recruitment of ATM by MRN and PARP1 could then contribute to the activation of the γ-H2AX cascade and stabilization of DDR factors at sites of damage (2).

DSBs are also recognized by the Ku heterodimer (Ku70 and Ku80), which binds and activates the catalytic subunit of the DNA protein kinase DNA-PK (DNA-PKcs) to initiate NHEJ (2; 16). Ku heterodimers at different DNA ends can associate and contribute to the tethering of broken DNA ends, especially if there is no complementary base pairing to facilitate their direct interaction (16). Moreover, Ku is thought to repress HR by protecting the DNA ends from resection by MRE11 and CtIP (22). Conversely, end resection blocks NHEJ, as Ku cannot bind to resected ssDNA (23).

The MRN complex, consisting of meiotic recombination 11 (MRE11), RAD50 and Nijmegen breakage syndrome 1 (NBS1), is another sensor of DSBs (24). MRE11 and RAD50 provide direct association with DNA ends, with MRE11 dimerization ensuring stable DNA binding, and RAD50 dimerization tethering DNA ends together (5; 24). MRE11 exhibits endonuclease as well as exonuclease activities and performs initial steps of DNA end resection that is essential for HR (2; 24). NBS1 promotes recruitment and activation of ATM (2) and also binds MDC1, which in turn controls retention of MRN at sites of DNA damage (24).

Replication protein A complex (RPA) recognizes ssDNA ends that arise from DSB resection involving MRN, CtIP, RECQ family helicases as well as EXO1 and DNA2 nucleases (5). RPA-coated ssDNA serves as a scaffold for activation of signaling factors such as the ATR kinase (see 2.2.3.2) and factors that are critically involved in the HR process such as RAD51, BRCA1 and BRCA2 (15). CDK-dependent phosphorylation of BRCA2, which is limited to S and G2 phases of the cell cycle, and CHK1-mediated RAD51 phosphorylation are important regulation mechanisms of HR (2).

#### 2.2.3.2 ATM, ATR, DNA-PK and checkpoint kinases

Phosphatidylinositol 3-kinase-related kinases (PIKK) assume a key role in the DDR signaling cascades. These include DNA dependent protein kinase (DNA-PKcs), ataxia telangiectasia-mutated (ATM), and ATM and Rad3-related (ATR). DNA-PKcs and ATM are primarily involved in DSB repair, whereas ATR responds to a wide range of DNA lesions, especially those associated with DNA replication (25). A common substrate of the DDR kinases is the histone variant H2AX, phosphorylation of which is a central event of IRIF formation (5).

As mentioned above, DNA-PKcs, activated by Ku, mediates NHEJ. Loading of DNA-PKcs to the DNA termini results in the recruitment of the XLF-XRCC4-LigaseIV complex, which promotes re-ligation of the broken ends (5). DNA-PK protects DNA ends via auto-phosphoryation on its PQR cluster, but also can destabilize its interaction with DNA ends by auto-phosphorylation on the ABCDE cluster, thus providing access to end processing enzymes. ABCDE phosphorylation can be induced by ATM as well and promotes HR when NHEJ fails (2).

ATM has emerged as the master kinase for phosphorylation of H2AX and many other phosphorylation events required for the formation of protein complexes at sites of DNA damage. Besides activation by MRN, auto-phosphorylation of ATM, allowing its binding to MDC1 and retention in IRIF, is an important mechanism of ATM function at DSB (15). In particular, factors that contribute DNA end resection, as BRCA1, CtIP, EXO1, BLM and ARTEMIS, are ATM targets, explaining how ATM is involved in HR and MMEJ regulation (2).

ATR is recruited by RPA at ssDNA regions, via its partner protein, ATRIP (5). Loading of the RAD9-HUS1-RAD1 (9-1-1) complex onto DNA ends adjacent to RPA-coated ssDNA regions sets in motion the ATR cascade, which is the central pathway orchestrating DNA replication responses and for instance promotes restart of stalled or collapsed replication forks (2).

Both, ATM and ATR, have a crucial role in connecting the DDR to cell-cycle progression. As part of fast-acting signaling axes, ATM and ATR phosphorylate and thereby activate the checkpoint kinases CHK2 and CHK1, respectively (26), which in turn reduce cyclin-dependent kinase (CDK) activity to slow down or arrests cell-cycle progression at the G1-S, intra-S and G2-M cell-cycle checkpoints, thus increasing the time available for DNA repair before replication or mitosis ensues (3). To achieve a maintained cell cycle arrest, ATM-mediated phosphorylation of p53 initiates transcription-based mechanisms of CDK inhibition in addition to the fast-acting kinase-driven pathway (26).

#### 2.2.3.3 γ-H2AX

The histone H2A variant H2AX, which is a component of the nucleosome core, comprises 10-15% of total cellular H2A in higher organisms (15; 27). Phosphorylation of H2AX on Ser139 by DDR kinases, then called γ-H2AX, spreads up to several mega base pairs from damaged sites (9; 28), but is strictly confined to the damaged chromosome (27). γ-H2AX foci appear within a minute after damage. Therefore, γ-H2AX is currently the DSB biomarker of choice. However, hypoxia can lead to MRN-independent activation of ATM, as well as activation of DNA-PK, and subsequent H2AX phosphorylation in absence of DSBs (28).

MDC1 directly binds the phospho-Ser139 of H2AX via its carboxy-terminus (2). A complex of MRN, MDC1, and γ-H2AX recruits additional ATM and facilitates spacious propagation of the γ-H2AX signal (25). In addition, chromatin remodeling enzymes, such as INO80 and SWI/SNF, are recruited to DSBs in a γ-H2AX-dependent manner (2). Inactivation of different chromatin remodeling factors blocks ubiquitination of histone H2A/H2AX by RNF8/RNF168 and inhibits subsequent loading of several effector proteins, including BRCA1, 53BP1 and RAD51 (see next sections), onto chromatin (12).

Besides Ser139 phosphorylation, other modifications of H2AX may also play important roles in regulating formation and dynamics of IRIF. H2AX Tyr142 is constitutively phosphorylated by the WSTF kinase, but is de-phosphorylated upon DNA damage (15). Interestingly, MDC1 binding to γ-H2AX was shown to depend on Tyr142 de-phosphorylation, whereas the pro-apoptotic kinase JNK1 was reported to associate with H2AX phosphorylated on both Ser139 and Tyr142. Thus, Tyr142 phosphorylation of γ-H2AX might provide a molecular switch between JNK-mediated apoptosis and MDC1-dependent DSB repair (2).

#### 2.2.3.4 MDC1

Mediator of DNA damage checkpoint protein 1 (MDC1) has been reported to mediate NHEJ as well as HR (2) and can be regarded as the master organizer of protein assembly at IRIF. As mentioned before, MDC1 binds to γ-H2AX via its C-terminal tandem BRCT repeats. It not only serves as a recruitment platform for downstream factors, but also protects γ-H2AX from de-phosphorylation and thus determines the dynamic extension of IRIF (15).

The FHA domain of MDC1 associates with NBS1 and thus influences MRN complex retention at sites of DNA damage (24). MRN facilitates further amplification of γ-H2AX signaling by ATM (11). MDC1 also might bind ATM directly (17), but further evidence for this mechanism is needed (27). Formation of extensive γ-H2AX regions is important for sustaining the DDR, as H2AX is not required for the initial localization of NBS1, BRCA1, and 53BP1 at DSBs via PARP but rather for the maintenance of these DDR factors at sites of damage (2). ATM also phosphorylates MDC1, and this allows binding of the E3 ubiquitin ligase RNF8 (29; 11).

#### 2.2.3.5 RNF8, RNF168 and other E3 ubiquitin ligases

RNF8 contains an N-terminal FHA domain, which is required for its association to phosphorylated MDC1, as well as a C-terminal RING finger domain typical of E3 ubiquitin ligases (9). RNF8 is responsible for the activation of a DDR-induced ubiquitination cascade (2) and cooperates with UBC13, the only known E2 conjugating enzyme that catalyzes the formation of non-proteolytic Lys63-linked (K63) ubiquitin chains (29). Initial polyubiquitin marks generated by RNF8 serve as docking sites for another E3 ligase, RNF168, which harbors motifs interacting with ubiquitin (MIU) (13; 29). Cooperative action of RNF8 and RNF168 results in the formation of non-proteolytic K63 ubiquitin chains on histones and facilitates assembly of BRCA1 and 53BP1 at IRIF (11; 30). The latter make the decision about HR or NHEJ repair (31; 23). Notably, BRCA1 again is an ubiquitin ligase (5).

Mutations in RNF168 abolishing its recruitment to IRIF were identified to be the cause of the RIDDLE syndrome, which is characterized by radiosensitivity, immunodeficiency, dysmorphic features and learning difficulties (13; 32).

Contrary to the former model, the “priming” ubiquitination conducted by RNF8 and required for RNF168 recruitment seems not to target histones but a non-nucleosomal protein, because efficient K63-linked poly-ubiquitination of H2A by RNF8 only takes place after initial ubiquitination by RNF168 (11). In the past few years it came to light that RNF8 also plays an essential role in the formation of K48-linked ubiquitin chains at sites of DNA damage (33; 34; 35), see chapter 4. It is now supposed that the RNF8/RNF168-dependent K63 pathway mainly controls NHEJ, whereas the RNF8-dependent K48 pathway controls HR (34).

The bunch of E3 ligases at DSB sites is further expanded by HERC2 and RAD18 (29). HERC2 interacts with RNF8 in a phosphorylation-dependent manner and facilitates the assembly of the RNF8-UBC13 complex (2). Since RNF8 also is capable of interacting with other E2 enzymes, HERC2 could be required to promote the specific E2-E3 interaction of RNF8 and UBC13, ensuring the formation of K63-linked ubiquitin chains at sites of DNA damage (15). RAD18 is supposed to associate with the K63 chains generated by RNF8 and RNF168. Its function remains elusive but might be linked to HR (29).

Latest reports suggest that ubiquitination not only plays a role downstream of MDC1, but already at a very early step of the DDR: Following DNA damage, the E3 ubiquitin ligase RNF2 and its adaptor BMI1 catalyze mono-ubiquitination of H2AX at Lys119 and Lys120. This modification is necessary for recruitment of ATM, and consequently, for efficient formation of γ-H2AX (11).

#### 2.2.3.6 BRCA1 complexes

Breast cancer susceptibility protein 1 (BRCA1) is a tumour suppressor and was first identified as a key genetic lesion associated with familial breast cancer. Mutations in the BRCA1 gene are detected in up to 50% of human patients with inheritable breast and ovarian cancer (36). BRCA1 as well as BRCA2, a second gene that often is affected by mutations leading to hereditary breast and ovarian cancer, are crucial factors for HR (2).

BRCA1 is a large protein, including an N-terminal RING domain and two C-terminal BRCT repeats that mediate interactions with different adaptors and provide for the localization of BRCA1 to sites of DNA damage (37). BRCA1 is part of at least three distinct complexes (BRCA1-A, -B and -C), the composition of which is determined by the binding of mutually exclusive adaptor proteins. BRCA1 associates with Abraxas (ABRA1), Fanconi anemia group J (FANCJ) and CtBP-interacting protein (CtIP) in the A, B and C complex, respectively (9).

BRCA1 and its interacting partner, BARD1 (BRCA1-associated RING domain), comprise the first mammalian E3 enzyme shown to function within IRIF (5). BRCA1 becomes phosphorylated during S-phase of the cell cycle and accumulates in the nucleus. In addition, BRCA1-BARD1 is phosphorylated by ATM and ATR upon different types of DNA damage and can shuttle between different subcellular localizations (36).

Few BRCA1 ubiquitination targets have been identified so far, but one of these is CtIP (5). During the S and G2 phases of the cell cycle, ubiquitination of CtIP in the BRCA1-C complex facilitates its association with damage sites, where it promotes DNA end resection for HR. In G1, CtIP carries out limited end resection for MMEJ, but in a BRCA1-independent manner (2). Phosphorylation by CDK in the S phase is an additional mechanism that boosts the interaction of CtIP with BRCA1 and, consequently, its end resection activity. Moreover, CtIP becomes more abundant during S phase (16).

A large proportion of the BRCA1 that localizes to DSB sites is part of the BRCA1-A complex (38). This complex has structural similarities to the proteasome lid and is recruited to DNA lesions through the ubiquitin interacting motifs of receptor associated protein 80 (RAP80), which bind to the K63-ubiquitin chains generated by RNF8 and RNF168. Ubiquitin binding activity has also been shown for other subunits of the BRCA1-A complex, including ABRA1, BRE, BRCC36 and NBA1 (2). BRCC36 (BRCA1-BRCA2-containing complex subunit 36) is a de-ubiquitinating enzyme (9) which could contribute to the remodeling of DSB-associated K63 chains, steering the DDR towards HR (22). However, it has also been suggested that the BRCA1-A complex does not promote, but limits end resection to prevent potentially deleterious HR events that would counteract genome integrity (39).

#### 2.2.3.7 53BP1

53BP1 (p53 binding protein 1) was originally identified in a screen looking for proteins that interact with the p53 tumor suppressor. Subsequent studies established 53BP1 as a substrate for ATM and that it localizes to IRIF (18). It was generally assumed that, in contrast to the BRCA1-A complex, 53BP1 does not directly interact with the K63-linked ubiquitin chains at DSB, but binds to methylated histones (15). Nevertheless, RNF8 as well as RNF168 ligase activity are strictly required for 53BP1 foci formation (13). Therefore, it was suggested that the ubiquitination events at DSB lead to structural changes which render 53BP1 binding sites accessible (17).

More precisely, the tandem tudor domains of 53BP1 bind to methylated Lys79 of histone H3 (H3K79) and methylated Lys20 of histone H4 (H4K20). Di-methylated H4K20 (H4K20me2) is meanwhile regarded as the most likely physiological binding site (15). Both mentioned lysine residues map to the nucleosome core and their methylation state is not changed by DNA damage, explaining the need for ubiquitination as an additional signal required for efficient recruitment of 53BP1 (40). However, an alternative model is suggested by work demonstrating that increased MMSET histone methyltransferase activity at sites of DNA damage enables 53BP1 foci formation via de novo methylation of H4K20. This might only be relevant for newly synthesized chromatin, because 98% of new histone H4 is di-methylated at K20 within 2-3 cell cycles following deposition in S-phase, with little to no detectable turnover of this modification in vivo (18).

Besides H2AX phosphorylation, RNF8-mediated ubiquitination and constitutive methylation of histones, damage-induced histone acetylation by TRRAP/TIP60 is another prerequisite for retention of 53BP1 at IRIF, with the latter modification also facilitating BRCA1 retention (41). Moreover, a recent study revealed that 53BP1 yet is able to recognize a RNF168-generated ubiquitination mark, namely histone H2A ubiquitinated on Lys 15 (H2AK15ub), directly via its carboxy-terminal ubiquitination-dependent recruitment (UDR) motif. It was proposed that the engagement of H4K20me2 by the tudor domain positions the UDR in the correct orientation to contact the epitope formed by H2AK15ub. Hence, 53BP1 seems to be a bivalent histone modification reader. It binds to nucleosomes minimally as a dimer and thus may alter nucleosomal array structure or crosslink nucleosomes (42). The mechanisms of 53BP1 recruitment are further discussed in chapter 5.5.

As mentioned before, 53BP1 plays a crucial role in DNA repair via NHEJ: On the one hand, 53BP1 is thought to promote NHEJ by increasing the stability and mobility of DSBs to find each other for productive ligation (2), especially over large ranges (12). During long-range V(D)J or CSR repair, 53BP1 might facilitate the clustering of DNA regions subject to programmed breakage via binding of methylated chromatin within these loci and subsequent oligomerization to bring them together. Indeed, the methylation status of histones significantly affects the outcome of CSR and V(D)J (18). On the other hand, 53BP1 inhibits DNA end resection and thus negatively regulates the HR pathway. A recently identified factor that contributes to this mechanism is RIF1, which is recruited to IRIF through 53BP1 phosphorylated by ATM (23). Loss of 53BP1 partially rescues the HR defect of BRCA1 mutant cells. Hence, the defective DSB resection in BRCA1 mutant cells, which results in NHEJ-dependent chromosomal rearrangements, is compensated by 53BP1 loss (31). Tumors with BRCA1 or BRCA2 mutations are significantly associated with low levels of 53BP1, indicating that 53BP1 mutation confers a survival advantage in the absence of BRCA1 and BRCA2 (2).

53BP1 is also involved in phosphorylation of CHK2 and activation of p53 after DNA damage (43). This role in cell cycle checkpoint activation, however, is rather subtle: 53BP1 binds to the MRN complex via RAD50 and thus contributes to MRN-ATM concentration at IRIF. At low doses of damage, this function is critical to maintain a certain level of ATM per DSB that is sufficient for checkpoint activation. At high levels of DSBs, 53BP1 is dispensable for maintaining ATM activity and cell cycle arrest (18).

## 2.3 Ubiquitination

### 2.3.1 Principle

Ubiquitin, a protein of 76 amino acids with a molecular weight of 8.5kDa, belongs to a family of ubiquitin-like proteins (UBLs) together with SUMO and others (44). Ubiquitination is a highly conserved and essential post-translational protein modification process that regulates protein function or expression in the eukaryotic cell (45). For example, it can lead to conformational changes, shifts in subcellular localization, modulation of enzyme activity, alteration in protein-protein interactions, or a change in the lifespan of the modified protein (29). The process of ubiquitination is ATP-dependent and results in formation of an isopeptide bond between the C-terminal glycine of ubiquitin (44) and the ε-amino group of a lysine residue in the target protein. Under certain circumstances, ubiquitin can also be conjugated to the N-terminal or even non-lysine residues of proteins (46).

Ubiquitination is catalyzed by sequential action of an ubiquitin-activating enzyme (E1), an ubiquitin-conjugating enzyme (E2) and an ubiquitin ligase (E3) (46; 47). Ubiquitin E3 ligases are divided into two families, which use different mechanisms to transfer ubiquitin from the E2 enzyme to the target protein: The RING (really interesting new gene) E3 family comprises more than 600 potential members in mammals whereas the smaller HECT (homologous to the E6AP carboxyl-terminus) family has about 30 members (11). A family of de-ubiquitinating enzymes (DUBs) mediates reversibility of the ubiquitination process (29). Ubiquitin can also bind non-covalently to interacting partners at specific domains called ubiquitin-binding domains (UBDs) (11).

### 2.3.2 Types of ubiquitination

Target proteins can be modified by a single ubiquitin molecule (mono-ubiquitination), several ubiquitin molecules on different sites (multiple mono-ubiquitination), or an ubiquitin chain (oligo- and poly-ubiquitination) (29). The seven lysine residues of ubiquitin provide for the formation of different isopeptide chain linkages, which adopt different three-dimensional structures, and all of which are represented in eukaryotic cells (48). Attachment to the N-terminal amino group is also possible, resulting in linear chains. Taken into account that branched ubiquitin chains might be employed by the cell additionally, there seems to emerge a proper “ubiquitin code” (29). Some E2 enzymes show specificity for a certain linkage type, while others can promote the formation of several types (44). Different linkages result in different chain topologies, which can be recognized by specialized UBDs, thus conferring specificity to the system (29). In some cases, ubiquitin chain elongation factors called E4 enzymes are required in addition to E1, E2 and E3 for efficient ubiquitination (49).

Strikingly different biological outcomes can be dictated by the different types of ubiquitin chain topologies. For example, conjugation of K48-, K29- and K11-linked poly-ubiquitin chains typically target proteins for degradation by the proteasome. In contrast, mono-ubiquitination or K63-linked ubiquitin conjugates act as regulatory signals in several cellular pathways (47). Mono-ubiquitination is involved in endocytosis, DNA repair and replication, transcriptional regulation and modulation of the histone code, whereas chains of the K63 type play a role in DNA repair signal transduction, protein trafficking and ribosomal protein synthesis (29). Additionally, the latter promote degradation of misfolded proteins in the aggresome-autophagy pathway and lysosomal degradation of cell surface proteins (45), with the latter pathway also involving K29 chains (29).

### 2.3.3 Ubiquitin-dependent degradation pathways

#### 2.3.3.1 Endolysosomal degradation

The endolysosomal protein degradation pathway is the principle means by which a cell turns over plasma membrane proteins, such as receptors or channels. Endocytosed proteins are either recycled to the plasma membrane or captured into lumenal vesicles of the multivesicular body (MVB) as it matures from the sorting endosome, before fusing directly with lysosomes. Ubiquitination serves as an internalization signal for some receptors. It also directs internalized proteins towards lysosomal degradation by engagement with endosomal sorting complexes required for transport (48).

#### 2.3.3.2 The ubiquitin proteasome system

The ubiquitin-proteasome system (UPS) is responsible for the constitutive degradation of most cellular proteins and regulates diverse processes by conditionally degrading proteins that control those processes (50). Typically, proteins are targeted for proteasomal degradation by K48-linked poly-ubiquitin chains (11; 46; 32). Notably, recent studies show that all linkage types except K63 accumulate in the cell after proteasome inhibition, suggesting that they also play a role in this pathway (48). To be recognized by the proteasome, ubiquitin chains must consist of at least four moieties (44; 48).

The proteasome is a protease of over 2.5 mega Dalton. It is composed of a 20S core particle comprised of 28 subunits and a 19S regulatory particle, also called PA700, consisting of 19 subunits. The core particle has a barrel-like structure whose subunits are arranged in four stacked seven-membered rings. The catalytic sites are sequestered within its large interior space. The access of substrates into this space is controlled by the regulatory particles, which can bind to both ends of the core cylinder (51).

The regulatory particle recognizes and unfolds the ubiquitinated substrate, opens a narrow channel in the cylinder end of the core particle and translocates the substrate through this channel (51). It comprises three DUBs, which remove the ubiquitin marks before degradation to maintain the cellular ubiquitin pool, and probably also to save certain substrates from disposal (48). Several sub-functions of the regulatory particle depend on ATP and have been linked to one or more of six distinct PA700 subunits which are ATPases of the AAA family (see 2.5.1) (50). The proteasome does not degrade its substrates to amino acids, but to peptides, some of which serve as raw material for adaptive cell-mediated immunity in the MHC pathway of mammals. To alter the product spectrum of the proteasome, certain subunits can be replaced, resulting e.g. in so called immune-proteasomes. In rare instances, regulatory proteins are subjected to partial proteolysis by the proteasome, which activates them through the removal of inhibitory domains (51).

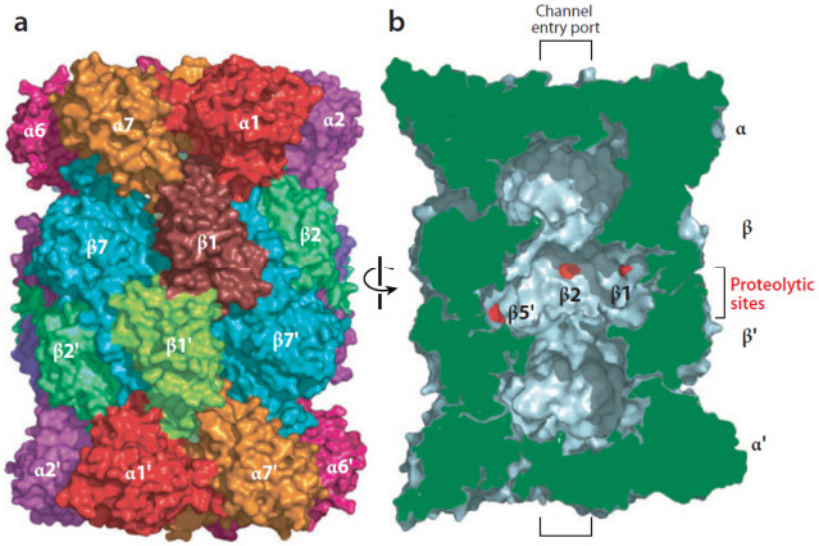


Figure 2: (a) Surface representation of the proteasome core particle, showing its organization into four heptameric rings of subunits. (b) Free, closed-channel state of the core particle showing sequestration of the proteolytic sites in the closed channel. A medial section is shown, with the slice surface in green. Adapted from (51).

### 2.3.3.3 Autophagy

The autophagy pathway is responsible for degradation of misfolded proteins that aggregate in the cytosol (45) and that are incompatible with unfolding by the proteasome, as well as for disposal of whole organelles (48). Aggregate formation is pronounced under certain pathological conditions referred to as “conformational diseases” and can be induced by protein overexpression or by pharmacological inhibition of the proteasome (50).

In the process of autophagy, the substrates are enveloped with a double-membrane compartment derived from the pre-autophagosomal structure. The resulting autophagosome can then directly fuse with late endosomes or lysosomes to form the autolysosome, wherein the double-membrane structure is digested. Ubiquitin plays a critical role in the selective removal of certain structures by autophagy (48). Aggregate proteins are ubiquitinated by the E3 ligase Parkin, which appears to prefer building K63-linked chains. This ubiquitin signal promotes retrograde transport of the misfolded proteins to the aggresome, which is located at the microtubule-organizing center. p62, which harbors a ubiquitin association domain, facilitates the recruitment of autophagic membranes to form the autophagosome (45).

### 2.3.4 Ubiquitination in context of DNA damage and repair

Ubiquitination is a common regulation pattern in DNA repair pathways, damage-avoidance mechanisms and cell cycle checkpoint responses. For example, the UPS accounts for the degradation of stalled RNA polymerases at damaged DNA templates or for the degradation of DDR proteins after completed repair (52). The latter could be an important mechanism for cell cycle resumption, also known as checkpoint recovery (53). Crucial DDR proteins, such as MDC1, NBS1, 53BP1 and BRCA1, are poly-ubiquitinated after IR (32). Proteasomal degradation in response to IR was demonstrated for MDC1 (54) and BRCA1 (55). MDC1 and 53BP1 were shown to be protected from accelerated degradation by the DUB enzyme USP28 in response to DNA damage. Inactivation of USP28 leads to the attenuation of DNA-damage signals and resistance to damage-induced apoptosis (56). Turnover of RNF168 is regulated by the E3 ligases UBR5 and TRIP12, depletion of which causes hyper-accumulation of RNF168 and ubiquitin conjugates, as well as widespread accumulation of 53BP1 and BRCA1 (57; 58). Importantly, several studies demonstrate the physical presence of the proteasome at sites of DNA damage (32). There are also ubiquitin receptor proteins that shuttle DDR factors targeted for degradation to the proteasome, such as yeast Rad23, Dsk2, and Ddi1, as well as p97 complexes (44), see chapters 2.5 and 4.

Besides its function in protein turnover, ubiquitin has additional regulatory functions in the DDR: The role of ubiquitination in the recruitment of DDR proteins to DSB is pointed out in chapters 2.2.3.5 and 4. Another example is the switching of repair pathways by alternating PCNA ubiquitination (59). PCNA (proliferating cell nuclear antigen) acts as a processing factor for DNA polymerases and as a platform for proteins that mediate replication-linked functions. If damaged DNA leads to stalled replication forks and generation of ssDNA during the S phase, RPA recruits the E3 enzyme RAD18, which mono-ubiquitinates PCNA. This mediates error-prone translesion synthesis of DNA. In contrast, if translesion synthesis fails, poly-ubiquitination of PCNA results in a recombination-related error-free bypass (52). In the Fanconi anemia pathway, mono-ubiquitination of the factors FANCI and FANC2 is a prerequisite for their recruitment to ICL-induced foci (44).

Since the UPS regulates many proteins that control cellular processes relevant for tumorigenesis, such as cell-cycle progression, apoptosis, receptor down-regulation and gene transcription, inhibition of the proteasome can be exploited for anti-cancer therapy (32). In addition to the development and clinical validation of a proteasome inhibitor, bortezomib, in myeloma therapy, recent studies have demonstrated that it is possible to develop inhibitors for specific ubiquitination and de-ubiquitination enzymes (46).

## 2.4 SUMOylation

### 2.4.1 General

SUMO is a small ubiquitin-like modifier of around 100 amino acid residues. SUMOylation has been reported to play a role in regulation of transcription, in various aspects of genome stability and in the control of nucleo-cytoplasmic transport (29). SUMO and ubiquitin have only limited sequence identity but they fold in a similar manner (44). The process of protein SUMOylation follows the same enzymatic cascade as ubiquitination (29). SUMO proteins bind the activating enzyme E1 (SAE1 and SAE2 in mammals) in an ATP-dependent manner and are transferred to the conjugating enzyme UBC9, which is the only E2 dedicated to SUMO conjugation. UBC9 is able to transfer SUMO to targets in absence of an E3, though E3-like proteins facilitate the process by enhancing the affinity of UBC9 for its substrates (44). As ubiquitination, SUMOylation is reversible and therefore suitable for regulatory purposes (52). Mammals have three types of SUMO conjugates, namely SUMO1, SUMO2 and SUMO3. The latter two are often referred to as SUMO2/3, because they are very similar and considered to be functionally equivalent (29). SUMO2/3 can form poly-SUMO chains, but not so SUMO1. SUMOylation often targets a lysine residue within a consensus sequence, but other lysine residues can be modified as well (52). Moreover, RNF4 represents a so far unique case of a SUMO-targeted ubiquitin ligase (60), which contains SUMO-interacting motifs (SIMs) that enable it to bind poly-SUMOylated proteins and to attach ubiquitin to the SUMO chains on those proteins, thus producing hybrid SUMO-ubiquitin chains (61).

### 2.4.2 SUMOylation in context of DNA damage and repair

Numerous DDR proteins, including human BLM, XRCC4, and RPA, as well as budding yeast Sgs1, Ku70, and Rad52, have been identified as SUMOylation targets (5). All three mammalian SUMO types are recruited to DSB sites. Furthermore, the SUMO E3 ligases PIAS1 and/or PIAS4, as well as the E2 UBC9, are required for the recruitment of RNF168, 53BP1 and BRCA1 to DNA damage foci. Interestingly, 53BP1 and BRCA1 were shown to be SUMOylation targets themselves. It was suggested that RNF8, RNF168 and/or BRCA1-BARD1 might require pre-SUMOylation of their targets or that SUMOylation regulates their ubiquitin-ligase activities (62).

In addition, RNF4 is recruited to DSBs in a manner requiring its SIMs, the SUMO E3 ligases PIAS1 and PIAS4, and different DSB-responsive proteins (63). RNF4 ubiquitinates SUMOylated MDC1 (60; 63), BRCA1 (60), RPA and BLM, recruits the proteasome component PSMD4 to sites of DNA damage (63), and is needed for HR as well as for NHEJ, pointing to an amazing interplay between ubiquitin and SUMO in the DDR (60; 63). RNF4 was also shown to be critical for the recruitment of RAP80 and BRCA1 to damage sites (61).

Further interesting examples for the regulatory function of SUMO in DNA repair are DSB-induced SUMOylation of the HR mediator RAD52, preventing it from accelerated degradation perhaps by sequestering it into repair foci (52), or PCNA SUMOylation, which prevents the formation of DSBs and the occurrence of inappropriate recombination events at stalled DNA replication forks (44).

## 2.5 The AAA ATPase p97/VCP

### 2.5.1 Nomenclature and characteristics

The ATPase p97 is one of the most abundant proteins in the cell, since it accounts for more than 1% of the proteome. The protein has a molecular weight of 97kDa and forms ring-shaped homo-hexamers (64), which is typical for AAA (ATPases associated with various cellular activities) family members (65). Since p97 has two ATP-binding cassettes, it is a class II member of the AAA ATPases (66). Also known as valosin containing protein (VCP) in mammals and plants, TER94 in insects, Cdc48 in yeast and VAT in Archaea, p97 is highly conserved among all kingdoms of life (64).

Together with a growing number of adaptors which mediate its interaction with substrates, p97 has a broad range of essential cellular functions (45). Most if not all of them are based on the ability to bind to ubiquitinated proteins and to segregate them from binding partners, or to extract them from complexes. This “segregase” function is mediated by the ATPase activity, which results in mechanical forces that move and partially rotate the outside rim of the enzyme (67). In addition, p97 has been proposed to assist the proteasome in unfolding a subset of substrates to facilitate their degradation. p97 is also able to edit ubiquitin modifications with the help of certain cofactors and thus introduces an important additional level of regulation and plasticity to ubiquitin-mediated processes (68).

### 2.5.2 Structure of p97

p97 has a modular structure: The amino terminal region (N), comprised of 187 amino acids, mediates interactions with substrates and various cofactors (64). The two ATPase domains, D1 and D2, form the center of p97. Each ATPase domain is comprised of approximately 250 amino acids and contains Walker A and Walker B motifs (45), which are responsible for ATP binding and hydrolysis, respectively (66). N and D1, as well as D1 and D2, are joined by short linker fragments. The carboxy-terminal tail (C) is highly disordered (64) and therefore allows access to Tyr796 and Tyr805 for phosphorylation, see 2.5.4 (69). It also recruits certain adaptors and contributes to hexamer stability (65).

In the homo-hexamer, the D1 domain of each monomer is stacked on top of the D2 in a head to tail packing, resulting in a D1 ‘‘disc’’ on top of a D2 ‘‘disc’’ (65) with the N domain facing away from D1 and C extending from D2 (45). D1 is believed to have a primarily structural function, facilitating hexameric assembly, but it shows increased ATPase activity at elevated temperatures. D2 is likely responsible for the majority of ATPase activity under physiological conditions (66).

There are a number of models explaining how nucleotide binding and hydrolysis in D2 may change p97 and/or adaptor conformation and result in the application of mechanical force on substrates. The central pore of the hexamer is blocked by a $Zn^{2+}$ ion in the D1 region, so substrates probably do not pass through this channel (45).

### 2.5.3 p97 adaptors

The functional diversity of p97 depends on a large number of cofactors, many of which function as ubiquitin adaptors, although p97 has ubiquitin-binding activity itself and can interact with unmodified stretches of the substrate. Proteins containing an ubiquitin-X (UBX) domain or UBX-like domain constitute the largest family of cofactors. These domains assume an ubiquitin fold and interact with the N-domain of p97 (68). Unlike p47 (Shp1/Ubx1 in yeast), which is the founding member of the UBX family (67), the majority of the UBX proteins does not possess ubiquitin-associated domains (UBA) and therefore probably does not interact directly with ubiquitinated proteins. These cofactors may have a regulatory influence on others or even mediate ubiquitin-independent activities of p97 (45). p47 binds to the p97 N-domains as a trimer, preventing other cofactors from binding (66).

The most functionally diverse (66) and best studied adaptor is the UFD1-NPL4 heterodimer (ubiquitin fusion degradation 1, nuclear protein localization homolog 4) (68). NPL4 harbors a UBX related motif called UBD (ubiquitin D) and binds to the same amino terminal region of p97, but this requires prior interaction with UFD1, which has a p97 binding domain, too (45).

The PUB domain is found in adaptor proteins such as PNGase, UBXD1 (UBX domain-containing protein 1), and RNF31 (RING finger protein 31). PNGase is a well characterized PUB domain-containing protein that is involved in the de-glycosylation of ERAD substrates (69), see 2.5.5.3. UBXD1 has both, a UBX and a PUB domain, but probably, only the latter mediates binding to p97 (45). As the PUB motif, the PUL domain binds to the C region of the ATPase. It is found in PLAP (Ufd3/Doa1 in yeast), which is thought to be involved in ubiquitinated protein degradation (69). Other p97 interaction domains include the SHP box (present in yeast Shp1), VIM (VCP interacting motif) and VBM (VCP binding motif), which are thought to contact p97 in the N and/or D1 region (45). Ufd2, a yeast E4 chain elongation enzyme, competes with Ufd3 for binding to the D2 domain of Cdc48 and can also be antagonized by the DUB Otu1 (VCIP135 in vertebrates) (67).

The current model of p97 adaptor relationships is a hierarchical system in which UFD1-NPL4, p47 and UBXD1 represent the mutually exclusive major cofactors, which form the p97 core complexes (68; 57). These major cofactors modulate p97 activity or govern assembly of additional adaptors. Hence, each core complex can act in several pathways by associating with alternative sets of accessory proteins that determine localization or provide additional enzymatic activities (68).

In competition experiments, it was shown that binding of ATP to the D1 domain (rather than hydrolysis) strengthened the UFD1-NPL4 association with the N domain, favoring the recruitment of UFD1-NLP4 instead of p47. This novel role of ATP links the multiple functions of p97 to the metabolic status of the cell (65).

Functionally, p97 accessory proteins can be divided in substrate recruiting or localization cofactors and substrate modifying or processing cofactors (66). Substrate recruiting factors harbor UBA domains and, in contrast to substrate processing factors, have no enzymatic activities. In many cases, the latter also contain UBA domains (45). Because p97-substrate processing factors can directly determine the fate of substrates by extending the ubiquitin chain (as the E4 ligase Ufd2) or removing ubiquitin (as the DUB VCIP135), p97 may also be considered a recruiting platform for ubiquitin-regulated processes (34). A special type of substrate processing, namely de-glycosylation, is given in the case of PNGase. It seems likely that many adaptors have dual functions in substrate recruitment and modulation, either by themselves or via associating partners (45).

### 2.5.4 p97 modifications

p97 is subject to a variety of posttranslational modifications, but their functions remain unknown in many cases, with the exception of Tyr805 phosphorylation (66). This modification in the C domain abolishes the interaction of p97 with PLAP and PNGase. Impaired binding to PNGase probably inhibits de-glycosylation and subsequent degradation of ERAD substrates (69). Tyrosine phosphorylation also regulates the transitional association of p97 with the ER membrane in vitro. Moreover, it has been shown that p97 is one of the first proteins that undergo tyrosine phosphorylation in response to T-cell stimulation (64).

The putative phosphorylation of serine residues in the D2 and C domains could lead to conformational changes with consequent alterations of p97 function. Phosphorylation of p97 is involved in cell cycle progression and serves as a localization signal (69). In yeast, Cdc48 generally attaches to the ER, but relocates into the nucleus after phosphorylation in a cell cycle-dependent manner (57). The finding that p97 localizes to sites of DNA damage upon phosphorylation at Ser784 is of special interest: After IR, p97 is phosphorylated by DNA-PK and/or ATM, whereas after UV exposure, ATR is the responsible kinase. It was also shown that p97 associates with the chromatin-enriched cell fraction upon irradiation (70).

Acetylation, particularly known to be important for chromatin rearrangement, has been proposed as an additional regulation mechanism for p97, since a number of potential acetylation sites were identified. Moreover, the histone de-acetylases HDAC6 were shown to interact with p97, its adaptor PLAP and poly-ubiquitinated proteins. It is therefore speculated that acetylation of p97 could regulate certain ubiquitin-degradation pathways (69).

### 2.5.5 Functions of p97

#### 2.5.5.1 General

As other AAA proteins, p97 acts as a molecular chaperone in many seemingly unrelated cellular activities. However, almost all of them are directly or indirectly linked to the UPS (64). Generally, p97 catalyzes remodeling of ubiquitinated client proteins to facilitate downstream steps (68). As mentioned before, these functions can be divided into three categories (45), namely extraction of substrates from diverse cellular locations ("segregase"), unfolding of substrates to promote their proteasomal degradation ("unfoldase") (57), and modulation of substrate ubiquitination in both a positive and negative manner (45) to control the fate of substrates (67).

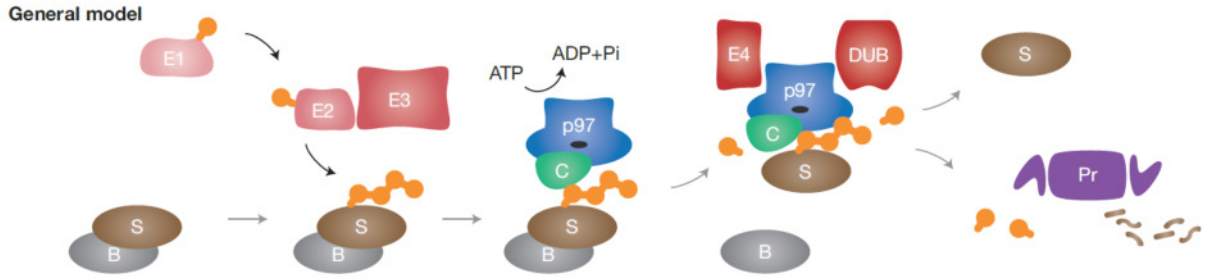


Figure 3: General model for p97 in substrate segregation and ubiquitin chain editing. A target substrate (S) modified with ubiquitin (orange) by a cascade of the ubiquitin activating enzyme (E1), a ubiquitin-conjugating enzyme (E2) and a ubiquitin ligase (E3). p97 binds to the ubiquitinated substrate with the help of ubiquitin-binding cofactors (C). p97 then employs ATP hydrolysis to remodel the target in order to segregate it from binding partners (B) or cellular surfaces. Interactions with ubiquitin-editing factors, such as an E4 enzymes or DUBs, may help the ubiquitin modification process to either recycle the substrate or direct it to the proteasome (Pr) for degradation. Adapted from (68).

#### 2.5.5.2 Degradation of soluble proteins

The discovery of Ufd1 and Ufd2 as essential yeast genes required for degradation of soluble substrates in the ubiquitin fusion degradation (UFD) pathway gave the first hint to the function of Cdc48/p97 in the UPS (57). Meanwhile, it is known that p97 and/or its adaptors participate in degrading a number of presumably properly folded natural substrates in human cells, for example IκBα (see 2.5.5.6), or HIF1α (45; 71) which is a crucial transcription factor initiating cellular responses to hypoxia and is degraded in a p97-dependent manner under normoxic conditions (49). It remains unclear however, if p97 in this context just serves as scaffold for ubiquitin ligases, if it segregates the modified substrate from interacting partners, or if it is needed for substrate unfolding (45).

#### 2.5.5.3 Endoplasmic-reticulum-associated degradation

ER-associated protein degradation (ERAD) is the best described p97-dependent proteolytic pathway (49). During this process, abnormal ER proteins, which cannot be restored by the various chaperone systems, are ubiquitinated, retro-translocated from the ER lumen or extracted from the ER membrane, and degraded by cytosolic proteasomes (45). ERAD also can act on normal proteins for regulatory purposes (67).

p97 is required to maintain protein misfolding, or perhaps even further denaturation, and to move the misfolded protein through the ER channel (45). Recruitment of p97 to the ER membrane is mediated by a group of accessory factors including UBXD2 (49) (Erasin, Ubx2 in yeast), which anchors the ATPase to the ER membrane. The NPL4-UFD1 heterodimer couples p97 to the ubiquitinated substrate. PNGase de-glycosylates misfolded glycoproteins. E4B (Ufd2 in yeast) further poly-ubiquitinates the substrate. YOD1 (Otu1 in yeast) as a DUB is required for substrate translocation. The role of Ubx4 remains undefined (45). Rad23 or its homolog Dsk2 serve as escort factors (67). The interaction between p97 and two E3 ubiquitin ligases, gp78 and Hrd1, also plays an important role in ERAD (72). Reflecting its essential role, p97 inactivation elicits the unfolded protein response, which can trigger ER-stress-induced apoptosis (68).

#### 2.5.5.4 Mitochondria-associated degradation

Recent studies in yeast and C. elegans point to the involvement of p97/Cdc48 in a proteolytic pathway that, in analogy to ERAD, operates at the outer mitochondrial membrane (OMM) to prevent mitochondrial stress. This pathway is called mitochondria-associated degradation (MAD) (49). Upon oxidative stress, the cofactor Vms1, which is also involved in some ERAD sub-pathways, forms a complex with Cdc48 and Ufd1 to mediate proteasomal degradation of OMM proteins. Moreover, Cdc48 collaborates with the E3 ligase Parkin, which is mutated in an autosomal recessive form of Parkinson's disease (72), to control the fate of defective mitochondria by prohibiting fusion and in turn promoting autophagy (49).

#### 2.5.5.5 Aggresome-autophagy pathway

p97 depletion results in the accumulation of autophagosomes which are unable to mature into autolysosomes (see 2.3.3.3). The same phenotype is caused by p97 mutations found in IBMPFD patients (see 2.5.6.1). The mechanism is still unclear, but could be linked to HDAC6, which is involved in transport of the misfolded proteins towards the microtubule-organizing center (45) and interacts with p97 as well as with ubiquitin (66). In yeast, p97 associated with Shp1/p47 is involved in autophagosome biogenesis (72).

#### 2.5.5.6 Transcription and translation control

p97 not only participates in the activation of soluble transcription factors (see 2.5.5.2 and 2.5.5.9) but also in the activation of membrane-bound transcription factors (64). The inactive precursor of yeast Spt23 is anchored to the ER membrane and homodimerizes upon shortage of unsaturated fatty acids. One of the two molecules is then ubiquitinated and its transmembrane domain is removed by the proteasome. The active protein has to be separated from its uncleaved partner by Cdc48-Ufd1-Npl4 and can then set off transcription of the fatty acid de-saturase Ole1 (67). The same mechanism is employed for another yeast transcription factor, Mga2 (72).

A different mechanism of transcription control is given in the case of the yeast transcription repressor Matα2, which, after poly-ubiquitination, is rapidly removed from the DNA promoter region by p97 to induce the mating type-specific gene expression program (34).

Transactive response DNA-binding protein 43 (TDP-43) is a highly conserved RNA-binding protein involved in regulation of transcription, pre-mRNA splicing, RNA transport and translation. p97 was suggested to extract TDP-43 from ribonucleoprotein complexes during translation and to transfer it back to the nucleus. This would provide an explanation for TDP-43-positive inclusions found in IBMPFD and ALS patients, see 2.5.6.1 (72).

#### 2.5.5.7 Membrane fusion

During mitosis of eukaryotic cells, the nuclear membrane, the ER and the Golgi apparatus are fragmented to ensure a proper partitioning of the organelles to daughter cells. There, reassembly of the organelles takes place by homotypic fusion of the vesicles. p97 is involved in fusion of the ER and Golgi membranes together with its adaptors p47 and VCIP135. For nuclear envelope assembly, the UFD1-NPL4 adaptor is required first. Later, p47 cooperates with p97 to feed additional membranes into the growing nuclear envelope. The involvement of ubiquitin-binding p97 cofactors suggests that ubiquitination plays a role in membrane fusion (64). However, the target is still unknown. Interestingly, p47 is regulated by phosphorylation during the cell cycle. Removal of the phosphate group at the end of mitosis allows p47 to participate in the described events (45).

#### 2.5.5.8 Cell cycle control

As its name indicates, yeast Cdc48 was initially identified as a protein required for progression through the cell division cycle (67). Depletion of p97, UFD1 and/or NPL4 leads to a delay of the cell cycle, replication stress and DNA replication checkpoint activation. p97 mediates degradation of cyclin E and the G1-CDK inhibitor Far1, which regulate G1/S transition (57; 72).

p97 also removes the poly-ubiquitinated DNA licensing factor CDT1 from PCNA and delivers it to the proteasome at the onset of the S phase (34). In fission yeast, Cdc48 promotes separation of sister chromatids and thus facilitates metaphase-to-anaphase transition (57; 72). Moreover, p97-UFD1-NPL4 is important for disassembly of the mitotic spindle (73) and extracts the ubiquitinated Aurora B kinase from chromatin during the exit of cells from mitosis, allowing chromatin de-condensation and nuclear envelope formation (74). On the other hand, p97-Shp1 promotes nuclear accumulation of the PP1 phosphatase to counteract Aurora B kinase activity in yeast (57; 72). Findings as the rapid phosphorylation of p97 upon T cell stimulation or high expression levels in fast dividing and cancer cells additionally support the notion that p97 is a pro-proliferation factor (64).

p97 also interacts with three DNA helicases, namely DNA unwinding factor (DUF) in Xenopus egg extracts, human Werner syndrome protein (WRNp), and HIM-6, a C. elegans homologue of human Bloom syndrome helicase (BLM). p97 might play an important role in disassembly of the helicase complexes from DNA during the processes of DNA replication, repair and/or recombination. Alternatively, p97 may be required for chromatin remodeling during cell division processes (72).

#### 2.5.5.9 Apoptosis

Important regulators of apoptotic pathways are degraded by the UPS. This is consistent with the observation that proteasome inhibitors induce apoptosis. Several lines of evidence suggest that p97 acts as an anti-apoptotic agent (64) by promoting degradation of IκBα, which is an inhibitor of the pro-survival functions of NF-κB (45). In unstimulated cells, NF-κB is sequestered in the cytoplasm, associated with IκB proteins. Upon stimulation, IκBα is phosphorylated and poly-ubiquitinated. p97 then mediates its proteasomal degradation, allowing NF-κB to translocate to the nucleus and to regulate its target genes (64).

#### 2.5.5.10 DNA repair

p97 was associated with DNA damage repair for the first time when its physical interaction with BRCA1 was shown by immunoprecipitation. In vitro studies further revealed that p97 binds to BRCA1 via its N domain (75). Later, it was demonstrated that WRNp, as mentioned before, forms a tight molecular complex with p97. This interaction depends on ATP and is disrupted by chemical agents that confer DNA damage, suggesting that p97 plays a role in the signal-dependent release of WRNp from its nucleolar sequestration site (76). As already described in 2.5.4, it was also found that p97 is phosphorylated upon DNA damage (70).

Recently, p97 emerged as an important player in DSB signaling and repair (33; 34). These findings will be discussed in chapter 4.

Furthermore, p97 controls gap-filling DNA synthesis after UV damage and excision of thymine dimers by the NER machinery. Similar as under physiological conditions, p97-UFD1-NPL4 extracts PCNA-bound CDT1 and mediates its proteasomal degradation (57). p97 is also involved in the disassembly of RNA polymerase II complex that is stalled at UV-induced DNA lesions. In this case, it mediates extraction and degradation of the ubiquitinated subunit Rbp1 (34; 57; 72). In addition, p97 is recruited to stalled DNA replication by DNA damage-associated VCP/p97 cofactor 1 (DVC1; also known as SPARTAN or C1orf124) and extracts DNA polymerase delta and eta. DVC1 seems to play a role only in response to replication-related DNA damage, but not upon IR-induced DSBs, and links p97 to translesion DNA synthesis (57).

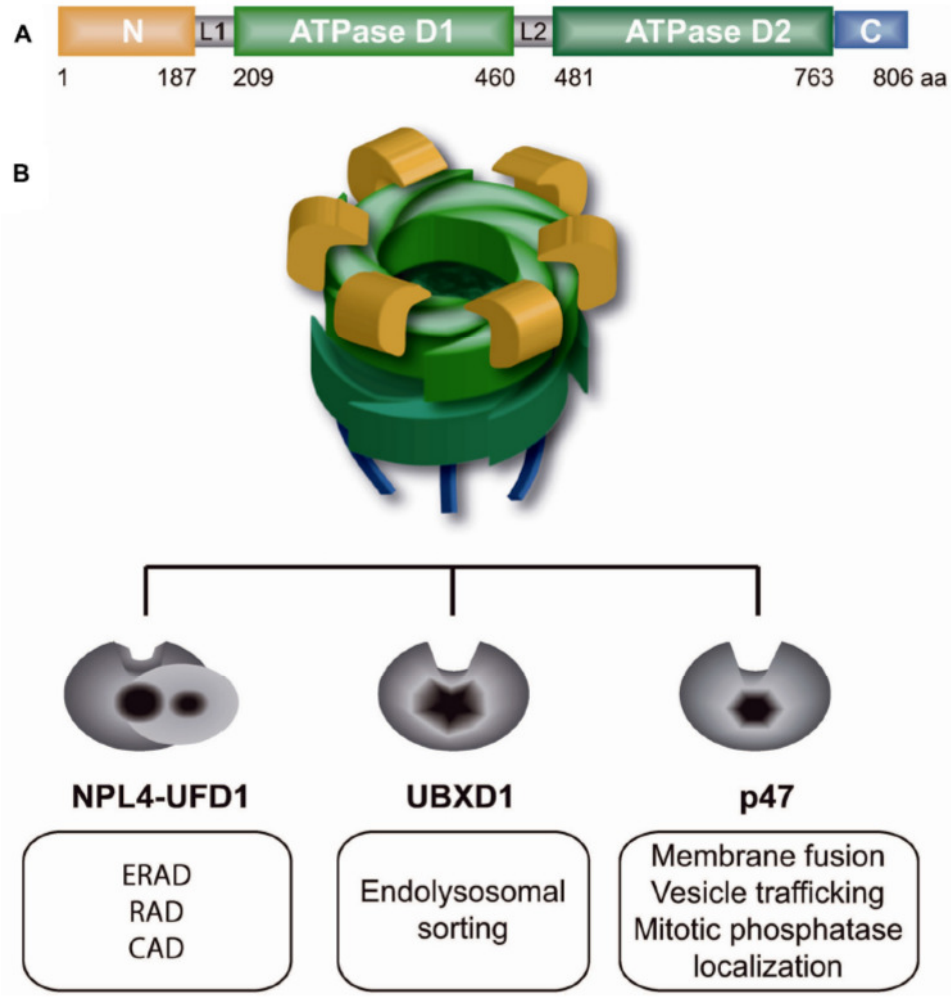


Figure 4: (A) Domain structure of the p97 monomer showing the N-terminal domain (N), linker regions (L1, L2), ATPase cassettes (D1, D2) and the C-terminal extension (C). (B) Ring-shaped p97 hexamer and mutually exclusive core adaptors that mediate specific cellular functions. ERAD (endoplasmic reticulum-associated degradation), RAD (ribosome-associated degradation), CAD (chromatin-associated degradation). Adapted from (57).

### 2.5.6 Medical significance of p97

#### 2.5.6.1 Degenerative diseases

p97 protects cells from the cytotoxic effects of damaged or misfolded proteins. As such, it is essential for cellular homeostasis, especially under stress conditions (68). Missense mutations in the p97 gene are the cause of human inclusion body myopathy (IBM) associated with Paget's disease of the bone (PDB) and frontotemporal dementia (FTD), briefly IBMPFD (77). This rare, hereditary, ultimately lethal multisystem disorder features muscle weakness as the most common symptom, but also musculoskeletal pain, pathological fractures and pre-senile dementia in some patients (78). The mutation is located in the N region of p97, namely at position 155, in most of the affected families (77), but thirteen causative mutations have been found at the interface of D1 and N meanwhile. The mutations that have been studied all lead to increased ATPase activity and altered nucleotide affinity, which also has structural implications. How these observations relate to pathology remains an area of intense study (66). It is thought that imbalanced cofactor association of p97 rather than increased ATPase activity results in IBMPFD (72). Some studies claim that both, UPS function and autophagy, are compromised, while other studies claim that only autophagy is lost (66).

The presence of ubiquitin-positive inclusions in the affected tissues links IBMPFD to other aggresome-associated disorders (77). Recently, familial cases of amyotrophic lateral sclerosis (ALS) have also been associated with p97 mutation (79). In addition, p97 is proposed to counteract human age-related diseases including Huntington's disease and Parkinson's disease, which are causally connected to imbalanced proteostasis in the ER or mitochondria, respectively (49). Huntington's disease is caused by accumulation of huntingtin harboring an expanded poly-glutamine region (ex-polyQ). This region binds to gp78, an ubiquitin ligase that is involved in ERAD, and sterically interferes with p97 binding to gp78, thus leading to ER stress and apoptosis. Another polyQ-related disorder is Machado-Joseph disease (MJD), also called spinocerebellar ataxia type 3 (SCA3) (66). It is caused by an ex-polyQ in the DUB enzyme ataxin-3 (72), leading to aggregates which co-localize with p97. However, it is unclear if p97 plays a direct role in pathogenesis (66).

#### 2.5.6.2 Cancer

There is strong evidence suggesting that p97 and/or some of its adaptors play a role in cancer, since they have been implicated in the direct regulation of some key cancer relevant proteins, such as degradation of HIF1α, IκBα and Aurora B kinase (45; 57; 71; 74).

Removal of IkBα by p97 can be up-regulated by pre-B-cell leukemia transcription factor 1 or E74-like factor 2. These transcriptional programs lead to increased survival and proliferation. Moreover, p97 antagonizes the p53 pathway and thus, cellular senescence. Elevated levels of p97 have been linked to a poor prognosis in many different forms of cancer including prostate cancer, non-small-cell lung carcinoma, pancreatic cancer, breast cancer, and leukemia (66), also see chapter 6.5. However, considering that p97's targets are likely to comprise both growth inhibitory and promoting proteins, the significance of the p97 expression data is hard to assess. They could be explained by protein damage-induced stress signals that are elevated in cancer cells (45; 80). The identification of p97 as a novel regulator of several DNA repair pathways anyhow accentuates its relevance in terms of cancer (57).

#### 2.5.6.3 p97 as a therapeutic target

The clinical success of the proteasome inhibitor bortezomib highlighted that tumors can be sensitive to perturbations of proteostasis, driving efforts to identify additional targets in these pathways (81). Hence, p97 might offer therapeutic possibilities for cancer treatment (34). Current studies focus on inhibition of p97 ATPase activity with promising results (66; 72), also see chapter 6.5. The late onset of diseases caused by p97 mutation indicates that partial loss of its function could be tolerated for a prolonged time, but p97 inhibitors were shown to kill cancer cells efficiently (81). However, there are many possible off-pathway targets because the p97 ATP-binding pocket is highly conserved. Furthermore, the abundance of p97 may necessitate large quantities of the inhibitor, increasing the likelihood of side effects. Better understanding of p97 mechanics and cofactor interactions might open therapeutic approaches for other diseases, especially proteinopathies. This is unlikely to require inhibition, but regulation of p97. For instance, in the case of IBMPFD, a small molecule that restores the interaction between N and D1, perhaps only to a small extent, may be a useful treatment (66).

# 3 Materials and methods

## 3.1 Buffers and solutions

### 3.1.1 Cell culture solutions

3.1.1.1 Selective growth medium

DMEM containing 4.5g/l glucose, 0.1g/l sodium pyruvate and L-glutamine (SIGMA)

substituted with:

10% (v/v) FCS (GIBCO)

100U/ml Penicillin (GIBCO)

100µg/ml Streptomycin (GIBCO)

0.2µg/ml Hygromycine B (INVITROGEN)

15µg/ml Blasticidin S HCl (INVITROGEN)

3.1.1.2 Puck's EDTA saline solution

137mM NaCl (SIGMA)

5.4mM KCl (MERCK)

5.6mM Glucose (SIGMA)

4.2mM $NaHCO_3$ (APPLICHEM)

0.7mM EDTA (APPLICHEM)

in aqua dest.

pH adjusted to 7.4 with HCl

sterilized by filtering

3.1.1.3 Normal growth medium

DMEM containing 4.5g/l glucose, 0.1g/l sodium pyruvate and L-glutamine (SIGMA)

substituted with:

10% (v/v) FCS (GIBCO)

100U/ml Penicillin (GIBCO)

100µg/ml Streptomycin (GIBCO)

3.1.1.4 Trypsin solution

2.5% (w/v) trypsin (GIBCO)

1:30 in Puck's EDTA saline sol. (3.1.1.2)

### 3.1.2 Buffers for extraction, fractionation and immunoprecipitation

3.1.2.1 25x protease inhibitor cocktail

5 tbl. Complete Mini EDTA-free (ROCHE)

in aqua dest.

3.1.2.2 25x phosphatase inhibit. cocktail

5 tbl. PhosSTOP (ROCHE)

in aqua dest.

3.1.2.3 Total extraction buffer

300mM KCl (MERCK)

25mM tris pH 7.5 (APPLICHEM)

5mM $MgCl_2$ (FLUKA)

1% (v/v) TritonX-100

5% (v/v) glycerol (APPLICHEM)

2mM β-mercaptoethanol (FLUKA)

4% (v/v) 25x prot. inh. cocktail (3.1.2.1) [A]

10mM N-ethylmaleimide (SIGMA) [A]

4% (v/v) 25x phos. inh. cockt. (3.1.2.2) [A]

in aqua dest.

A: added just before usage

3.1.2.4 Fractionation buffer A

10mM HEPES pH 7.5 (SIGMA)

10mM KCl (MERCK)

1.5mM $MgCl_2$ (FLUKA)

340mM sucrose (APPLICHEM)

10% (v/v) glycerol (APPLICHEM)

1mM DTT (FLUKA) [A]

1mM PMSF (FLUKA)

4% (v/v) 25x prot. inh. cocktail (3.1.2.1) [A]

10mM N-ethylmaleimide (SIGMA) [A]

0.1% (w/v) digitonin (SIGMA) [B]

in aqua dest.

A: added just before usage

B: only for the cytoplasmic extraction and the first washing step (see 3.4.2.5)

3.1.2.5 Fractionation buffer B

3mM EDTA (APPLICHEM)

0.2mM EGTA (FLUKA)

1mM DTT (FLUKA) [A]

0.1mM PMSF (FLUKA)

4% (v/v) 25x prot. inh. cocktail (3.1.2.1) [A]

10mM N-ethylmaleimide (SIGMA) [A]

in aqua dest

A: added just before usage

3.1.2.6 IP buffer

120mM KCl (MERCK)

50mM tris pH 7.5 (APPLICHEM)

5mM $MgCl_2$ (FLUKA)

0.5% (v/v) TritonX-100

5% (v/v) glycerol (APPLICHEM)

2mM β-mercaptoethanol (FLUKA)

4% (v/v) 25x prot. inh. cocktail (3.1.2.1) [A]

10mM N-ethylmaleimide (SIGMA) [A]

in aqua dest.

A: added just before usage

3.1.2.7 10x SDS-PAGE sample buffer

600mM tris pH 6.8 (APPLICHEM)

25mM DTT (FLUKA)

20% (w/v) SDS (SIGMA)

20% (v/v) glycerol (APPLICHEM)

20% (v/v) β-mercaptoethanol (FLUKA)

0.05% (w/v) bromophenol blue sodium salt (APPLICHEM)

in aqua dest.

3.1.2.8 Phosphate buffered saline (PBS)

137mM NaCl (APPLICHEM)

2.7mM KCl (MERCK)

10mM $Na_2HPO_4 \cdot 7H_2O$ (SIGMA)

1.76mM $K_2HPO_4$ (FLUKA)

in aqua dest.

pH adjusted to 7.4 with HCl

### 3.1.3 Buffers for SDS-PAGE and semi-dry western blot

3.1.3.1 4x loading gel buffer

0.5M tris (APPLICHEM)

in aqua dest.

pH adjusted to 6.8 with HCl

0.4% (w/v) SDS (SIGMA)

small pinch of bromophenol blue sodium salt (APPLICHEM)

3.1.3.2 4x separating gel buffer

1.5M tris (APPLICHEM)

in aqua dest.

pH adjusted to 8.8 with HCl

0.4% (w/v) SDS (SIGMA)

3.1.3.3 SDS-PAGE running buffer

25mM tris (APPLICHEM)

192mM glycin (APPLICHEM)

0.1% (w/v) SDS (SIGMA)

in aqua dest.

3.1.3.4 Transfer buffer

25mM tris (APPLICHEM)

192mM glycin (APPLICHEM)

20% (v/v) methanol (MERCK)

0.1% (w/v) SDS (SIGMA)

in aqua dest.

3.1.3.5 PBS-T

0.05% (v/v) Tween-20 (SIGMA)

in PBS (3.1.2.8)

3.1.3.6 Blocking buffer

1% (w/v) BSA (SIGMA)

in PBS-T (3.1.3.5)

3.1.3.7 Primary antibody solution

1% (w/v) BSA (SIGMA)

0.05% (w/v) $NaN_3$ (APPLICHEM)

Antibody diluted according to 3.2.1

in PBS-T (3.1.3.5)

3.1.3.8 Secondary antibody solution

1% (w/v) BSA (SIGMA)

Antibody diluted according to 3.2.2

in PBS-T (3.1.3.5)

## 3.2 Antibodies

### 3.2.1 Primary antibodies

| Target protein | Actual size | Appar. size | Species | Dilution | Supplier |
|---|---|---|---|---|---|
| 53BP1 | 350kDa | > 250kDa | Rabbit | 1:500 | SANTA CRUZ |
| 53BP1 | 350kDa | >250kDa | Mouse | 1:2000 | BD BIOSCIENCES |
| BRCA1 | 220kDa | > 213kDa | Mouse | 1:500 | SANTA CRUZ |
| MDC1 | 225kDa | > 250kDa [A] | Mouse | 1:1000 | SIGMA |
| Vinculin | 123kDa | 123kDa | Mouse | 1:2000 | NOVUS |
| p97 | 97kDa | 97kDa | Rabbit | 1:2000 | H. Meyer, ETHZ |
| L3MBTL1 | 84kDa | 100kDa [B] | Rabbit | 1:1000 | ABCAM (ab51880) |
| L3MBTL1 | 84kDa | 84kDa [B] | Rabbit | 1:1000 | ABCAM (ab97304) |
| FK2 ubiquitin | var. | var. | Mouse | 1:1000 | BIOMOL |
| α-Tubulin | 55kDa | >50kDa | Mouse | 1:10'000 | SIGMA |
| PCNA | 29kDa | 30kDa | Mouse | 1:2000 | ABCAM |
| Cyclophilin A | >15kDa | > 15kDa | Goat | 1:333 | NOVUS |
| Histone H2A | 14kDa | > 10kDa [C] | Rabbit | 1:1000 | CELL SIGNALING |
| γ-H2AX | 17kDa | >15kDa | Mouse | 1:1000 | MILLIPORE |

Table 1: Primary antibodies used for immunodetection (3.4.3.4). (A) 2-3 bands according to the supplier's datasheet. (B) The supplier provides contradictious information about the apparent size. According to our experience, the sensitivity of both antibodies is not sufficient to detect endogenous levels of L3MBTL1, see chapter 5.5. (C) A strong double band at approx. 35kDa is indicated as histone H2A in chapter 5.4. It could correspond to cross-reacting Histone H1, since the antibody against histone H1 revealed a similar pattern (results not shown).

### 3.2.2 Secondary antibodies

| Target species | Coupled enzyme | Species | Class | Dilution | Supplier |
|---|---|---|---|---|---|
| Mouse | Peroxidase | Goat | IgG | 1:10'000 | SIGMA |
| Rabbit | Peroxidase | Goat | IgG | 1:10'000 | SIGMA |
| Goat | Peroxidase | Rabbit | IgG | 1:10'000 | SIGMA |

Table 2: Secondary antibodies used for immunodetection (3.4.3.4).

## 3.3 Strep-p97-transfected HEK 293 cells

The experiments were carried out with two lines of human embryonic kidney (HEK 293) cells, stably transfected with strep-p97-WT (wildtype, further on refered to as “WT”) and strep-p97-E578Q, respectively. The latter, further on referred to as “EQ”, is a dominant negative mutant of p97 that contains a single amino-acid mutation (glutamic acid to glutamine at position 578) in the ATPase cassette and therefore lacks ATPase activity. The cell lines were designed according to the Flip-In T-Rex 293 system protocol (INVITROGEN) and kindly provided by Hemmo Meyer, ETH Zürich. The cells were grown in medium containing Hygromycine B and Blasticidin S as selective antibiotics (3.1.1.1). The expression of the strep-p97-WT and strep-p97-EQ constructs, used for the co-precipitation experiment in chapter 5.4, was induced by addition of Doxycyclin (3.4.1.3). For the other experiments, non-induced WT cells were used.

## 3.4 Procedures

### 3.4.1 Cell culture

#### 3.4.1.1 General

Cells were kept in a HERA cell 240 incubator at 37°C and 5% $CO_2$. All cell culture procedures were carried out under sterile conditions in a SKAN VST-2000-120 laminar flow hood. Media and buffers were warmed up to 37°C before they were applied on the cells, except if negligible volumes were used. The cells were checked on every working day with a NIKON Diaphot microscope.

#### 3.4.1.2 Maintenance and splitting

HEK cells were maintained in cell culture bottles (NUNC) or dishes (CORNING and TPP) with selective growth medium (3.1.1.1). Depending on the purpose, they were split in time intervals from two to five days and in a ratio from 1:4 to 1:20. Usually, the cells were split if they reached a confluence of 90-100%. The splitting procedure was carried out as follows: The growth medium was removed and the cell layer was washed carefully with Puck’s EDTA saline solution (3.1.1.2). The cells were then incubated with a small amount of trypsin solution (3.1.1.4) for about 1min. Detachment of cells was accelerated by slight knocking. Afterwards, fresh selective growth medium was filled up to the original volume to inactivate the trypsin and the cell suspension was refined by pipetting. Finally, the requested amount was diluted with fresh selective growth medium in a new vessel. For the experiments, cells were grown in dishes with a diameter of 10cm, containing 10ml of medium.

#### 3.4.1.3 Induction of p97 expression

The expression of strep-p97-WT and strep-p97-EQ, respectively, was induced 24h before harvesting with 1µg Doxycyclin hyclate (SIGMA) per ml selective growth medium (3.1.1.1). Whereas induction causes microscopically visible vacuolization in p97-EQ-transfected U2OS cells (K. Ramadan, personal communications), it had no obvious effect on the strep-p97-EQ-transfected HEK cells used for this work.

#### 3.4.1.4 Treatment with MG132

To inhibit proteasome activity, the cells were treated with 5nM MG132 (SIGMA) for 14h. Since MG132 was applied as a stock solution of 10mM in DMSO, the control cells were treated with the corresponding amount of pure DMSO (SIGMA). Treatment with MG132 caused rounding and detachment of cells, whereas DMSO-treated cells did not show changes in morphology.

#### 3.4.1.5 siRNA transfections

Depletion of proteins by RNAi was performed using Lipofectamine RNAiMAX transfection reagent from INVITROGEN according to the manufacturer's forward transfection protocol: The siRNA was incubated with transfection reagent in OptiMEM I (GIBCO) for 15-20min before it was added to the cell culture dishes containing normal growth medium (3.1.1.3). If necessary, additional medium was filled up after 24h. At the time of transfection, the cells had a confluence of about 10-20%. They were harvested after 3 days when they had reached a confluence of 80-100%. The applied siRNA sequences are described in Table 3. Control cells were treated with transfection reagent, but not with siRNA.

| **Name** | **Sequence** | **Final conc.** | **Supplier** |
|---|---|---|---|
| #p97-1 | 5'-AAGUAGGGUAUGAUGACAUUG-3' | 20nM | MICROSYNTH |
| #p97-2 | 5'-AACAGCCAUUCUCAAACAGAA-3' | 20nM | QIAGEN |
| #MDC1 | 5'-AAUCCUGAGACCUCCUAAGGUUU-3' | 20nM | MICROSYNTH |
| #L3M-1 | 5'-GCCUGCACUUUGAUGGGUAUU-3' | 100nM | MICROSYNTH |
| #L3M-2 | 5'-GCUGGAGUCAUGGCUAUGAUU-3' | 100nM | MICROSYNTH |

Table 3: siRNA sequences used for depletion of p97, MDC1 and L3MBTL1 (abbreviated to L3M for reasons of space).

#### 3.4.1.6 Irradiation

Cells were irradiated for 3.5min in a PANTAK SEIFERT X-ray system set to 120kV and 19mA, which corresponds to a dose of 10Gy. They were then brought back to the incubator for recovery and harvested 60min after irradiation.

### 3.4.2 Preparation of samples

#### 3.4.2.1 General

During all procedures described below, cells and cell extracts, respectively, were kept on ice. An EPPENDORF centrifuge 5810R was used for 15ml and 50ml FALCON tubes, whereas 0.5ml and 1.5ml EPPENDORF tubes were centrifuged in an EPPENDORF centrifuge 5415R.

#### 3.4.2.2 Harvesting of cells

The cell culture medium was removed and the cell layer was washed with few ml of Puck's EDTA saline solution (3.1.1.2). The medium as well as the washing solution was collected in a FALCON tube. Few ml of trypsin solution (3.1.1.4) were subsequently added on to the cells to detach them. The trypsin solution was inactivated with at least the same amount of cell culture medium (3.1.1.3) and remaining cells were detached by pipetting. The cell suspension was transferred to the FALCON tube and centrifuged at 1000g, 4°C for 3min. The supernatant was removed and the cell pellet was washed in PBS (3.1.2.8). After repetition of the centrifugation step the resulting cell pellet was processed according to the following protocols.

#### 3.4.2.3 Total extraction

The cell pellet was suspended in total extraction buffer (3.1.2.3) by pipetting or vortexing and transferred to a 1.5ml EPPENDORF tube. For a cell pellet from a 10cm dish, 400µl of total extraction buffer were used. After an incubation time of 20min, the cell suspension was sonicated for 17min with high power, time intervals 30sec, using a DIAGENODE BIORUPTOR with a cooling device from THERMO SCIENTIFIC. The protein concentration was measured as described in 3.4.2.6. Finally, the total cell extract was mixed with SDS-PAGE sample buffer (3.1.2.7), boiled at 95°C for 5min using an EPPENDORF ThermoStat plus and stored at -20°C.

#### 3.4.2.4 2-step fractionation

The cell pellet (from a 10cm cell culture dish) was suspended in 300µl of total extraction buffer (3.1.2.3) as described in the total extraction protocol (3.4.2.3). After 20min incubation, the suspension was centrifuged at 16'000g, 4°C for 15min. The supernatant (S = soluble fraction) was collected whereas the pellet, considered as chromatin, was washed twice in total extraction buffer to remove remaining soluble proteins. The centrifugation conditions were the same as before. The pellet (P) was re-suspended in 100µl of total extraction buffer and sonicated as described in chapter 3.4.2.3. Both fractions (S and P) were subsequently processed like the total extracts in 3.4.2.3: Measurement of protein concentration (3.4.2.6), addition of sample buffer, boiling and storage.

#### 3.4.2.5 3-step fractionation

The freshly harvested cell pellet was suspended in fractionation buffer A containing digitonin (3.1.2.4) by pipetting. The amount of buffer corresponded to 1.5x to 2x the volume of the pellet. After an incubation period of 5-10min, the suspension was centrifuged at 1000g, 4°C for 5min. The supernatant (CE = cytoplasmic extract) was collected and the pellet, supposed to consist of cell nuclei, was washed twice. The first washing step was carried out with fractionation buffer A containing digitonin and the resulting supernatant was added to the CE sample. For the second washing step, fractionation buffer A without digitonin was used and the supernatant was discarded. Centrifugation conditions were the same as before.

Next, the pellet was re-suspended in fractionation buffer B (3.1.2.5) by pipetting and vortexing. The amount of buffer again corresponded to 1.5x to 2x the volume of the pellet. The suspension was incubated for 15min, centrifuged at 1500g, 4°C for 5min and the supernatant (NE = nucleoplasmic extract) was collected. The chromatin pellet was washed twice in fractionation buffer B using the same centrifugation conditions. The supernatant from the first wash was added to the NE sample, whereas the second was discarded.

Afterwards, the chromatin pellet was re-suspended in 1.5x to 2x the volume of IP buffer (3.1.2.6), transferred to EPPENDORF tubes, incubated for 15min and sonicated as described in the total extraction protocol (3.4.2.3). The resulting chromatin extract (CH), together with the other samples, was centrifuged at 16'000g, 4°C for 10min. An aliquot of CE, NE and CH, each, was processed as described for the total extracts in 3.4.2.3: Measurement of the protein concentration, addition of sample buffer, boiling and storage at -20°C. The major parts of the samples were blast-frozen in liquid nitrogen and stored at -20°C for isolation of strep-tagged p97 (3.4.2.7).

#### 3.4.2.6 Measurement of protein concentrations

Protein concentrations of the samples were determined using BIO-RAD protein assay solution diluted 1:5 in aqua dest., an AMERSHAM Ultrospec 2100 pro photometer and 1ml photometer cuvettes from RATIOLAB. The samples, as well as BSA standards of known concentration, were diluted 1:500 and 1:50, respectively, in protein assay solution. The light absorbance at 595nm wavelength was measured and, by linear regression from the standard values, protein concentrations of the samples and required loading amounts for SDS-PAGE were calculated using MICROSOFT Office Excel 2010.

#### 3.4.2.7 Isolation of strep-tagged p97

Step-Tactin Sepharose beads from IBA were used for precipitation of step-tagged p97. The beads were always centrifuged at 1000g, 4°C for 1min.

Since the beads are supplied in a 1:1 suspension, they were first centrifuged and the supernatant was discarded. The beads were re-suspended in IP buffer (3.1.2.6), incubated for 5min on a rotor at 4°C and spun down. This washing procedure was repeated again twice. To prevent unspecific binding of proteins, the beads were subsequently incubated with IP buffer containing 5% BSA for 150min on the rotor at 4°C. After this blocking step, they were washed again in IP buffer twice, as described above.

Prepared like this, the beads were re-suspended in an equal volume of IP buffer and 30µl of this suspension were added to each sample. The latter, after thawing on ice and centrifugation at 16'000g, 4°C for 20min, had been diluted with IP buffer, so that all samples contained 0.5mg of total protein. An aliquot for the input sample (IN) had been taken in advance. The samples containing beads were incubated for 1h on a rotor at 4°C to allow binding of step-tagged p97. Afterwards, the flow through (FT) was collected and the beads were washed 3x in 300µl of IP buffer with 5min rotation at 4°C, each. At the end, the beads were mixed with an equal volume of 2x SDS-PAGE sample buffer (10x SDS-PAGE sample buffer, 3.1.2.7, diluted 1:5 in aqua dest.) and boiled at 95°C for 3min to elute bound proteins (EL sample). The IN an FT samples had been mixed with 1/9 the volume of 10x SDS-PAGE sample buffer and were boiled, too. All samples were stored at -20°C.

### 3.4.3 Analysis of samples

#### 3.4.3.1 Sodium dodecylsulfate polyacrylamide gel electrophoresis (SDS-PAGE)

SDS-PAGE was performed using gel systems from BIO-RAD with 10 loading wells per gel and a diameter of 1mm. Gels were prepared according to Table 4.

| Compound/percentage | loading gel | 5% | 8% | 10% | 12% | 15% |
|---|---|---|---|---|---|---|
| Aqua dest. | 1.58ml | 4.69ml | 4.13ml | 3.77ml | 3.38ml | 2.82ml |
| 4x loading gel buffer (3.1.3.1) | 0.63ml | - | - | - | - | |
| 4x separating gel buff. (3.1.3.2) | - | 1.87ml | 1.87ml | 1.87ml | 1.87ml | 1.87ml |
| 40% acrylamide 4K solution (APPLICHEM) | 0.24ml | 0.94ml | 1.5ml | 1.86ml | 2.25ml | 2.82ml |
| 10% APS (APPLICHEM) | 20µl | 50µl | 50µl | 50µl | 50µl | 50µl |
| TEMED (APPLICHEM) | 5µl | 10µl | 10µl | 10µl | 10µl | 10µl |

Table 4: Composition of polyacrylamide gels.

For certain purposes, two-step gels with different percentages of acrylamide were prepared. Thus, a good separation over wide molecular weight ranges could be achieved. Usually, two gels were prepared and run together. The gel apparatus was set up as prescribed by the manufacturer and filled with SDS-PAGE running buffer (3.1.3.3). The samples were boiled at 95°C for 5min, using an EPPENDORF ThermoStat plus, directly before loading. Usually, 40µg of proteins were loaded per well. As an exception, the EL samples from IP were loaded entirely, since their protein concentration was not known. All Blue Protein Standards from BIO-RAD were used as molecular weight marker. The gels were run at constant 40mA for 55-80min until the marker bands reached the desired positions. If the voltage exceeded 180V, the current was decreased to 30mA.

#### 3.4.3.2 Semi-dry transfer

Semi-dry transfer was used if small proteins, such as histones, should be detected, and for the experiments shown in chapter 5.4.

It was performed immediately after SDS-PAGE, using a trans-blot semi-dry transfer cell, PVDF membranes and extra thick blot paper from BIO-RAD. The PVDF membrane was activated in methanol (MERCK) for 30sec, washed twice in aqua dest., and equilibrated twice for 10min in transfer buffer (3.1.3.4). The blot paper was pre-wetted in the same buffer. The gel sandwich was prepared according to the manufacturer's instructions and remaining air bubbles were pressed out. The transfer was run with constant 240mA for 10-15min and 260mA for additional 30min. Afterwards the membranes were labeled with a ballpoint, washed briefly in PBS-T (3.1.3.5) and stored in blocking buffer (3.1.3.6) overnight at 4°C.

#### 3.4.3.3 Wet transfer

Wet transfer, according to our experience, is the most suitable transfer method for large proteins and was used for most experiments shown in chapters 5.1, 5.2, 5.3, and 5.5.

It was performed immediately after SDS-PAGE, using a Western blot system, PVDF membranes and filter paper from BIO-RAD. The PVDF membrane was activated in methanol (MERCK) for 30sec, washed twice in aqua dest., and equilibrated twice for 10min in transfer buffer (3.1.3.4). The filter papers and the foam pads belonging to the gel holder cassettes were pre-wetted in the buffer. The gel sandwich was prepared according to the manufacturer's instructions and remaining air bubbles were pressed out. The transfer was run with constant 60V for 75min. Afterwards, the membranes were washed briefly in PBS-T (3.1.3.5) and stored in blocking buffer (3.1.3.6) overnight at 4°C.

#### 3.4.3.4 Immunodetection of proteins

An EB SM-30 shaker was used for the antibody incubation and for the washing steps. After blocking, the membranes were washed twice in PBS-T. Usually, the membranes were cut and the pieces were incubated with different antibodies. The incubation in primary antibody solution (3.1.3.7) lasted for at least 90min and was followed by three washing steps. After at least 45min incubation in secondary antibody solution (3.1.3.8), the membranes were washed again three times. The washing steps usually lasted for 5-10min, but occasionally, the procedure was interrupted there and the membranes were stored in PBS-T at 4°C. The membranes were developed using SuperSignal West Dura Extended Duration Substrate or SuperSignal West Femto Maximum Sensitivity Substrate from THERMO SCIENTIFIC. Digital pictures were taken with an Image Reader LAS-3000 from FUJIFILM. After development, the membranes were again washed three times and stored at 4°C. In some cases they were treated with Restore™ Western Blot Stripping Buffer from THERMO SCIENTIFIC, blocked again and developed with another antibody.

#### 3.4.3.5 Quantification of immunoblots

Digital pictures (JPG) of immunoblots were quantified using the freeware program ImageJ. The polygon tool was used to adjust the selection frame to the protein bands. In case of ubiquitin, as well as MDC1 and BRCA1 in P fractions, a bigger part of the lane ("smears") was measured instead of single bands. The resulting mean pixel values were corrected by the loading amount of the corresponding sample, which was determined by measurement of the loading control on the same membrane (α-Tubulin or PCNA). Values from S and P samples are depicted in percent of the untreated control ($S^{-RNAi\ -IR}$ and $P^{-RNAi\ -IR}$, respectively), because a direct comparison between S and P fractions is unsuitable due to big differences in the protein amounts. Mean percent values from two independent experiments are shown in the diagrams in chapter 5. Error bars indicate standard errors of the mean. MICROSOFT Office Excel 2010 was used for calculations and creation of diagrams.

# 4 Aim of the study

DSBs are considered as the most cytotoxic form of DNA damage (5; 3) and trigger accumulation of numerous DNA damage signaling and repair proteins in a highly ordered fashion, forming IRIF (15). The accrual and function of DDR factors is orchestrated by a myriad of posttranslational modifications, including ubiquitination (6).

While the role of non-proteolytic K63-linked ubiquitin chains in the DDR is established, recent studies revealed that also K48-linked ubiquitin chains as well as protein degradation contribute to proper DNA damage signaling and repair (33; 34; 35). In other words, the removal of repair proteins from DNA should be considered as equally important as their recruitment (82). Since protein degradation by the UPS is virtually involved in any cellular process, it is not surprising that the UPS also participates in turnover of chromatin-bound proteins (32). For instance, MDC1 is removed from sites of DNA damage via K48 poly-ubiquitination and is subsequently degraded by the proteasome in human cells. Impairment of MDC1 removal through proteasome inhibitors seems to prevent BRCA1 foci formation after IR (54), although this observation also could be due to depletion of free ubiquitin in the nucleus (10; 9). Another study on Xenopus egg extracts showed that DNA containing DSBs accumulates members of the Skp1-Cul1-F-box complex (E3 ubiquitin ligase complex) as well as K48-linked poly-ubiquitinated proteins, and that K48 poly-ubiquitination of Ku80 is a crucial signal for its removal from DNA. Importantly, removal and subsequent proteasomal degradation of Ku80 are distinct events (82). On the other hand, there is also evidence for the physical presence of the proteasome at sites of DSBs (32).

A further level of complexity was brought into the field by the finding that ubiquitin-like modifiers (SUMO) are required for efficient recruitment of RNF168, 53BP1 and BRCA1 to damage sites (62) and that there is an interplay of SUMO and ubiquitin systems in the DDR, probably to promote degradation of certain factors (63; 60). Thus, in the past few years, ubiquitin and ubiquitin-like proteins were recognized to play a crucial role in coordinating the DDR (11). In attempt to understand how DDR proteins are regulated by the ubiquitin system, we focused on p97.

Because of its function as an ubiquitin-dependent segregase and a recruitment platform for ubiquitin-editing factors, p97 is known as a central component of the UPS (67). The large diversity of p97 activities has recently been expanded by chromatin-associated functions and its involvement in DNA repair (68). The first process in which p97 was shown to act as an ubiquitin-dependent segregase on chromatin was extraction of the kinase Aurora B, promoting exit from mitosis (74). Indirect hints that link p97 to DNA repair came from studies describing its physical interaction with BRCA1 (75) and the WRNp helicase (76). It also was reported that p97 is phosphorylated upon DNA damage and that it is present at DSB sites (70).

Driven by these previous findings, our laboratory discovered that p97 is rapidly recruited to sites of DSBs together with the UFD1-NPL4 adaptor, and that it is necessary for proper localization of the important DNA repair factors 53BP1, BRCA1 and RAD51 to damage sites. Recruitment of p97 is mediated by previously unappreciated K48 poly-ubiquitin chains at DSB, formation of which depends on RNF8, but not on RNF168. p97 is involved in processing of these K48 chains, because they persist for 1h following DSB induction under physiological conditions but could be detected for 4h or longer in cells expressing the ATPase-deficient p97-EQ mutant. The crucial role of p97 in orchestration of IRIF was confirmed by the observation that cells with impaired p97 activity show a reduced survival after IR (33).

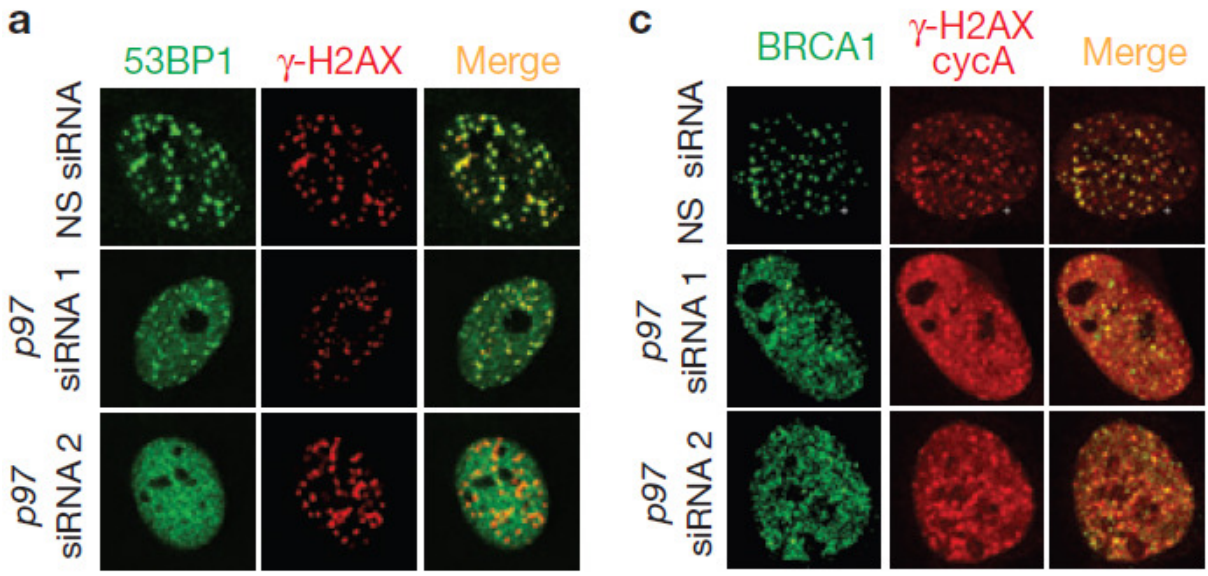


Figure 5: Immunoflourescence pictures of U2OS cells showing impaired 53BP1 and BRCA1 foci formation upon depletion of p97, 1h after irradiation with 3Gy. Treatment with siRNA against p97 (sequences depicted in 3.4.1.5) or non-silencing siRNA (NS) lasted for 2 days. Adapted from (33).

These discoveries lead to the model of chromatin-associated protein degradation (CAD) in which p97, in analogy to ERAD, extracts ubiquitinated and SUMOylated substrates from chromatin to maintain protein homeostasis. Impaired p97 function leads to accumulation of its substrates on chromatin, which disturbs essential DNA metabolic processes such as replication, transcription and repair, resulting in protein-induced chromatin stress (PICHROS) and genomic instability. Thus, p97 is emerging as a genome caretaker (57).

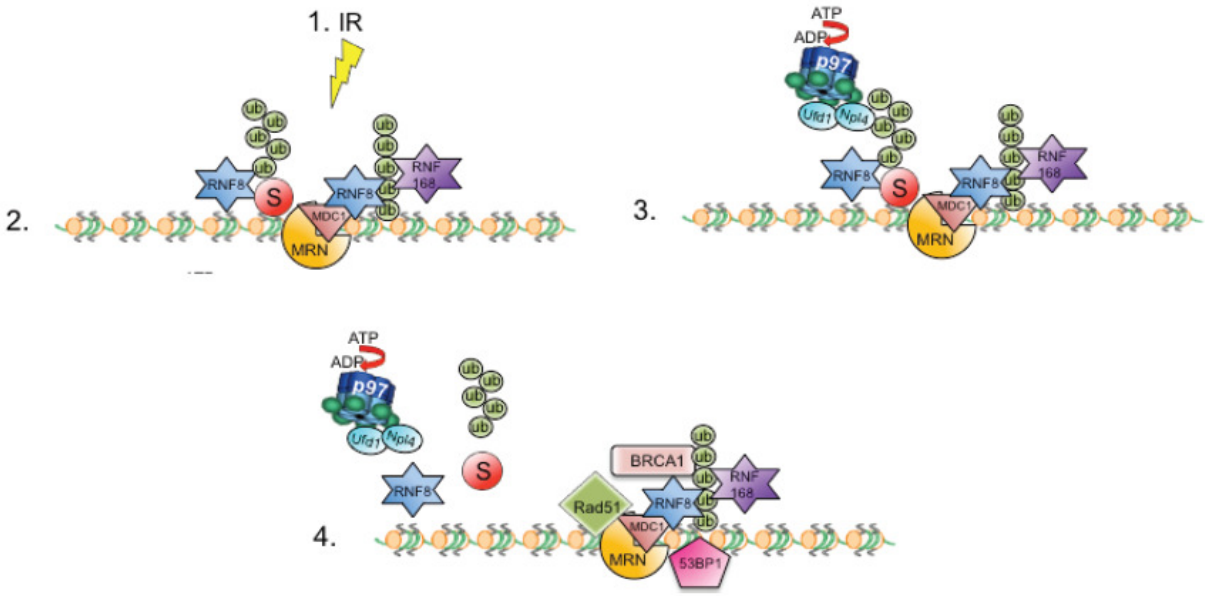


Figure 6: Model of p97 function in the DDR: IR induces a DSB (1). ATM-mediated phosphorylation stimulates recruitment of the MRN complex, MDC1, RNF8 and RNF168. The latter forms K63 poly-ubiquitin chains on histones, while RNF8, eventually together with another ligase, mediates K48-linked ubiquitination of yet unidentified chromatin-bound substrates (2). p97-UFD1-NPL4 is recruited to the DSB by K48 chains (3) and hydrolyzes ATP to remove the ubiquitinated substrates from chromatin, allowing assembly of downstream factors such as 53PB1, BRCA1 and RAD51 (4). Adapted from (33).

In the present study, biochemical methods were applied to further investigate the influence of p97 on key factors of the DDR in human cells under physiological and genotoxic conditions. We focused on MDC1, the central recruitment platform for ubiquitin ligases at DSB, as well as on 53BP1 and BRCA1, the mediators of the two major DSB repair pathways, NHEJ and HR. Employing RNA interference and cell fractionation, we wanted to clarify whether inactivation of p97 affects the total level or localization of these DDR proteins. Since it has been demonstrated that depletion of p97 increases the total level of poly-ubiquitinated substrates in the cell due to failed proteasomal degradation (20), we also asked if impaired p97 function leads to an increased level of poly-ubiquitin conjugates on chromatin as a correlate of PICHROS and p97's role in CAD.

In summary we aimed to:

1) Investigate the role of p97 in the recruitment and turnover of MDC1, 53BP1 and BRCA1 on chromatin under physiological and IR-damaged conditions

2) Establish a simple biochemical approach to investigate the function of p97 in chromatin-related processes

# 5 Results

## 5.1 p97 and the ubiquitin proteasome system control the total level of 53BP1

To characterize our experimental tools and to determine whether the total levels of our target proteins are controlled by the UPS and p97, we treated HEK293 cells with the proteasome inhibitor MG132 and with two different siRNA sequences against p97. Additionally, the siRNA sequence against MDC1, which was used for further experiments described in chapter 5.3, was tested. Total extracts of the cells were analyzed by immunoblot.

Figure 7A shows efficient and equal depletion of p97 by both siRNA sequences, #p97-1 and #p97-2, whereas the level of p97 is not affected in the other conditions. The efficacy of MDC1 depletion using this siRNA sequence is not shown here, since we were not able to detect a sufficient signal from MDC1 and BRCA1 antibodies, but it was confirmed in many other independent experiments (see chapter 5.3.1).

As expected, proteasome inhibition as well as depletion of p97 causes a strong accumulation of poly-ubiquitin conjugates, detected with the FK2 antibody (Figure 7A lanes 2, 5, 6). This serves as a positive control for the respective treatments. The effect of sequence #p97-2 on the poly-ubiquitin level is slightly stronger than the effect of sequence #p97-1, which was already observed previously (K. Ramadan, personal communications). The depletion of MDC1 slightly increased the total ubiquitin level. This finding will be confirmed in chapter 5.3.

Interestingly, the total level of 53BP1 was strongly increased not only after inhibition of the proteasome, but also upon depletion of p97 with both siRNA sequences (Figure 7B). These findings indicate that the UPS and p97 regulate the steady state level of 53BP1 in mammalian cells under physiological conditions.

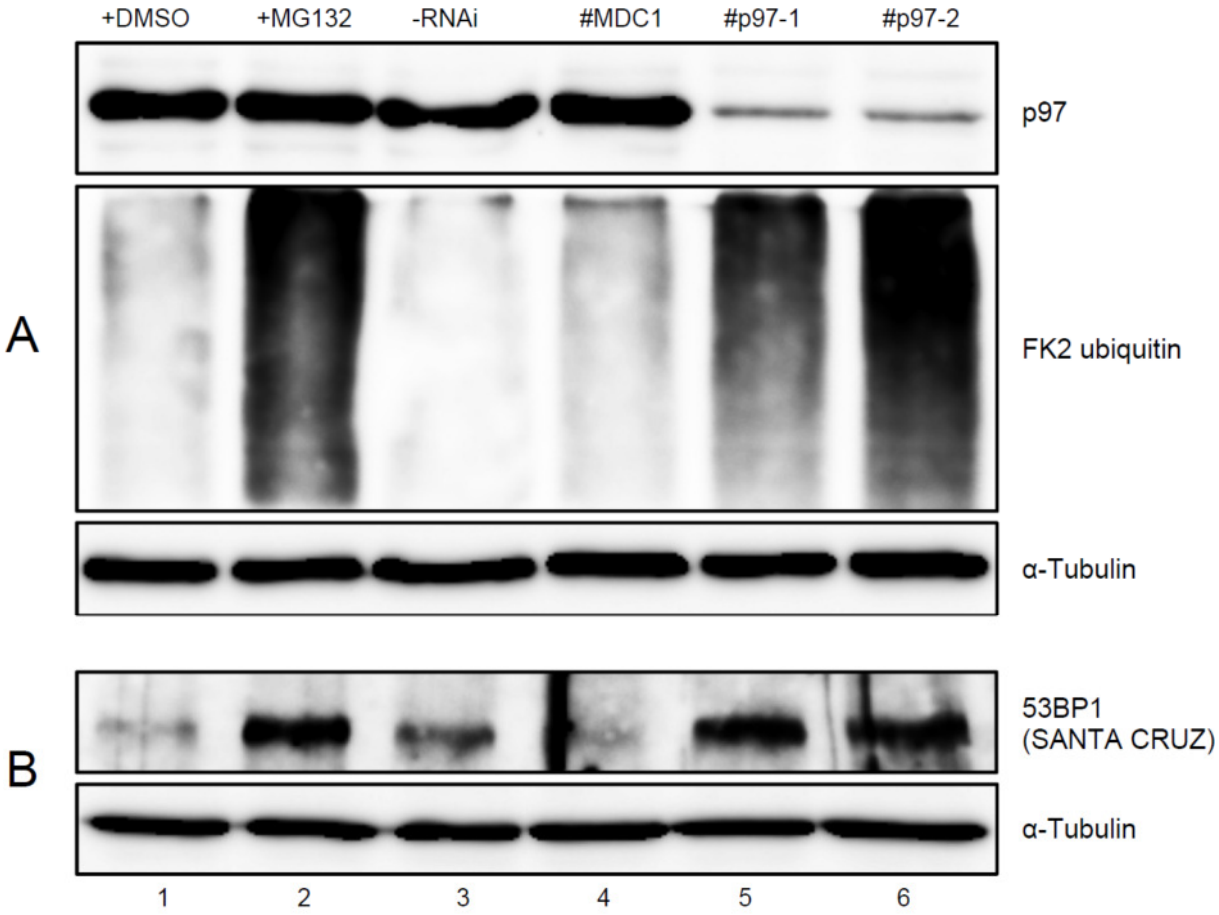


Figure 7: Immunoblots of total cell extracts from HEK293 cells. Treatment with the proteasome inhibitor MG132 lasted for 14h and the control cells were treated with pure DMSO. Treatment with the indicated siRNA sequences lasted for 3 days and transfection reagent without siRNA was applied to the control cells (-RNAi). Protein levels were analyzed with the indicated antibodies. α-Tubulin was used as loading control. For technical details refer to chapter 3.

## 5.2 Influence of p97 depletion and IR on protein turnover in the soluble cell fraction and in the tightly packed chromatin

Chromatin is not only a place for DNA replication, repair and transcription, but is also one of the largest protein assemblies in the cell that undergoes constant rearrangement (9; 32). Therefore we wanted to investigate how p97 regulates the turnover of DDR proteins on chromatin. We used a biochemical approach to separate the soluble and loosely bound chromatin proteins (S fraction) from the tightly bound chromatin proteins (P fraction). The extraction buffer for isolation of the S fraction contained a high salt concentration (300mM KCl) and 1% of TritonX-100. Therefore we assume that only proteins that are tightly associated to chromatin remain in the chromatin pellet, whereas proteins loosely bound to chromatin are extracted with the S fraction. To test the influence of p97 on protein dynamics in these fractions, we used the siRNA sequence #p97-2, which was shown to deplete p97 effectively in Figure 7. In addition, we exposed p97-depleted and control cells to IR (10Gy and 1h recovery time) to determine whether p97 acts on chromatin only after genotoxic stress or also under physiological conditions. The fractions were analyzed by conventional immunoblot.

### 5.2.1 p97 removes ubiquitinated substrates from chromatin

To confirm the efficacy of our fractionation method, we used the core histone H2A as a marker for the tightly bound chromatin (P) fraction and vinculin as a marker for the soluble (S) fraction. Vinculin is an adhesion protein that links integrin transmembrane molecules to the actin cytoskeleton (83) and therefore is only present in the S fraction, whereas histone H2A is only found in the P fraction (Figure 8A). The appearance of phosphorylated histone H2AX (γ-H2AX) indicates the presence of DSBs in the irradiated samples.

Figure 8B confirms the effective depletion of p97. Just a very small level of p97 is present in the P fraction, which only stands out from the background after long exposure (also see Figure 18, chapter 5.3.2).

As visible in Figure 8C and Figure 9, depletion of p97 strongly increases the level of total poly-ubiquitin conjugates and IR additionally increases their level in presence as well as in absence of p97. IR-induced poly-ubiquitination is detectable in both fractions, S and P. Notably, the accumulation of poly-ubiquitin conjugates upon p97 depletion is not limited to the S fraction, but is even more obvious in the tightly bound chromatin fraction of proteins (compare lanes 2 and 6, or 4 and 8 in Figure 8C). These results clearly indicate a crucial role of p97 in chromatin-associated degradation of ubiquitinated proteins.

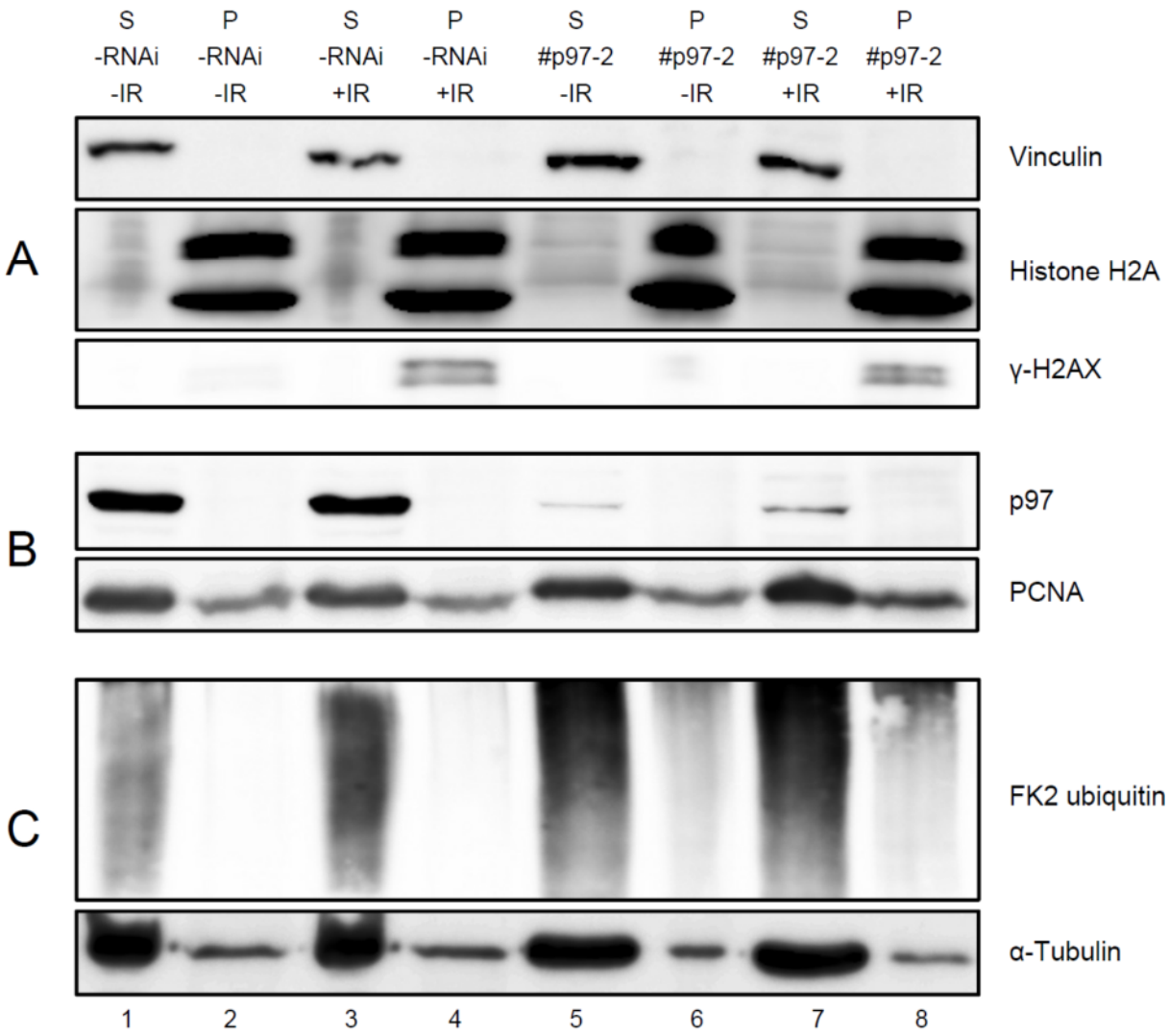


Figure 8: Immunoblots of S and P fractions from HEK293 cells subjected to the indicated treatments: RNAi of p97 (#p97-2) and control (-RNAi); irradiation with 10Gy (+IR) and control (-IR). Extraction took place 1h after irradiation. Vinculin and Histone H2A were used as fractionation controls, whereas γ-H2AX served as marker for IR-induced DSBs. p97 and total conjugated ubiquitin (FK2) levels were analyzed together with loading controls (PCNA and α-Tubulin, respectively). For technical details refer to chapter 3.

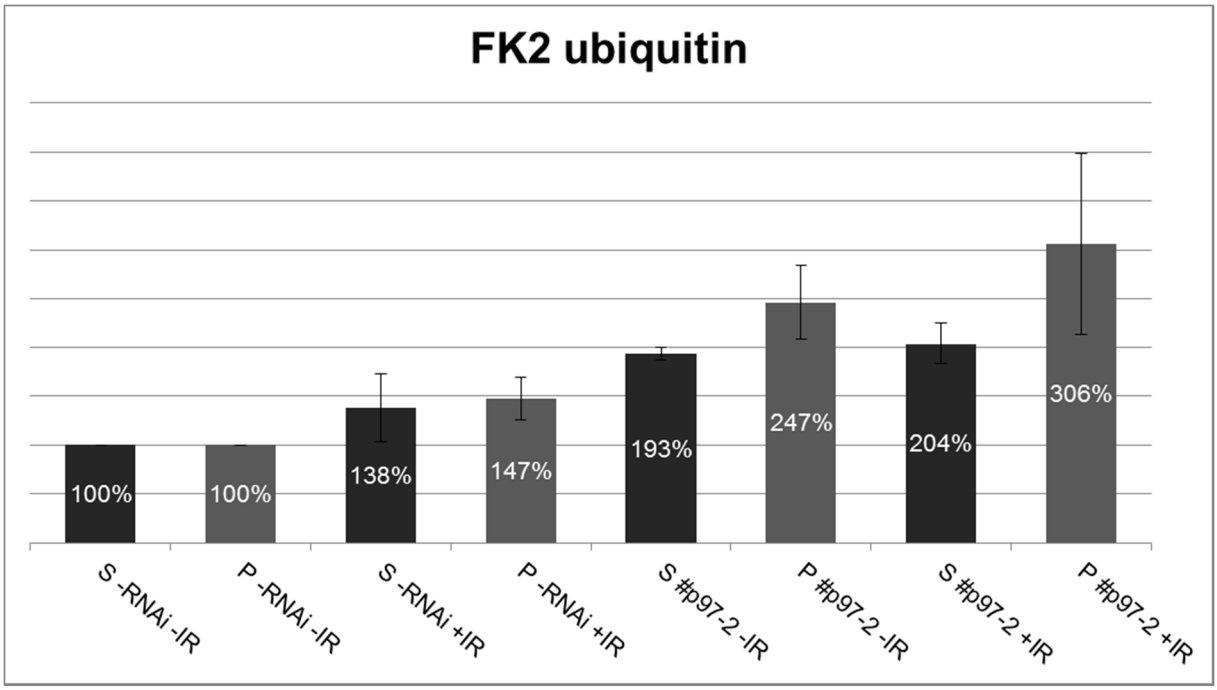


Figure 9: Quantification of total conjugated ubiquitin levels in the experiment shown in the previous figure and one additional, independent experiment. Protein levels in the S and P fractions were normalized to the loading control and are depicted as percentage of the corresponding untreated control (S $^{-RNAi\ -IR}$ and P $^{-RNAi\ -IR}$, respectively). The whole FK2 ubiquitin "smears" of a MW higher than approx. 100kDa were measured. For technical details refer to chapter 3.

### 5.2.2 p97 stabilizes MDC1 on chromatin

Analysis of MDC1 levels revealed that the major part of this protein is extracted in the S fraction with our stringent fractionation method, but a small amount is also detected in the P fraction under control conditions (Figure 10, lane 2). The total level of MDC1 is markedly reduced after irradiation, and this degradation takes place independently of p97 (Figure 10, lanes 1, 3, 5 and 7, low exposure). These results suggest that p97 does not control MDC1 degradation during recovery from genotoxic stress, but that this degradation could employ a p97-independent UPS pathway. In the P fraction, irradiation leads to an increased background signal ("smears") over the whole lanes, which might correspond to ubiquitinated and/or degraded MDC1 (compare lanes 2 and 4, or 6 and 8 in Figure 10). Note that for the quantification in Figure 11, those smears were measured instead of the bands. Since the protein samples were run in a two-step gel with 5% acrylamide in the upper part and 10% acrylamide in the lower part, the suspected MDC1 degradation products accumulate at the border of the two parts (Figure 10, high exposure, lower quarter of the picture). In the P fractions, no clear bands of MDC1 can be detected upon depletion of p97 (compare lines 2 and 6 or 4 and 8 in Figure 10), but the background signal is increased also in the non-irradiated sample (Figure 10, lane 6). This indicates that p97 stabilizes chromatin-associated MDC1, probably by extracting MDC1 from the tightly bound chromatin fraction or by removing MDC1-targeted E3 ubiquitin ligases.

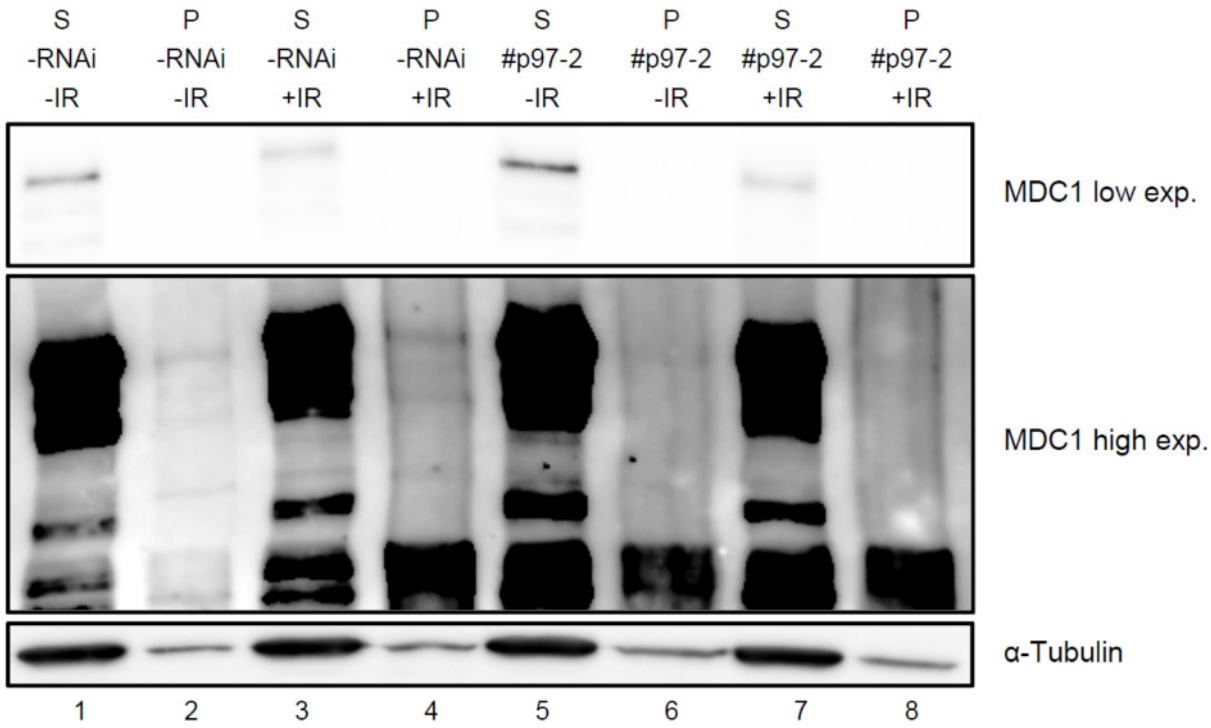


Figure 10: Immunoblots of S and P fractions from HEK293 cells subjected to the indicated treatments: RNAi of p97 (#p97-2) and control (-RNAi); irradiation with 10Gy (+IR) and control (-IR). Extraction took place 1h after irradiation. Fractionation controls are shown in Figure 8. MDC1 levels were analyzed together with α-Tubulin (loading control). For technical details refer to chapter 3.

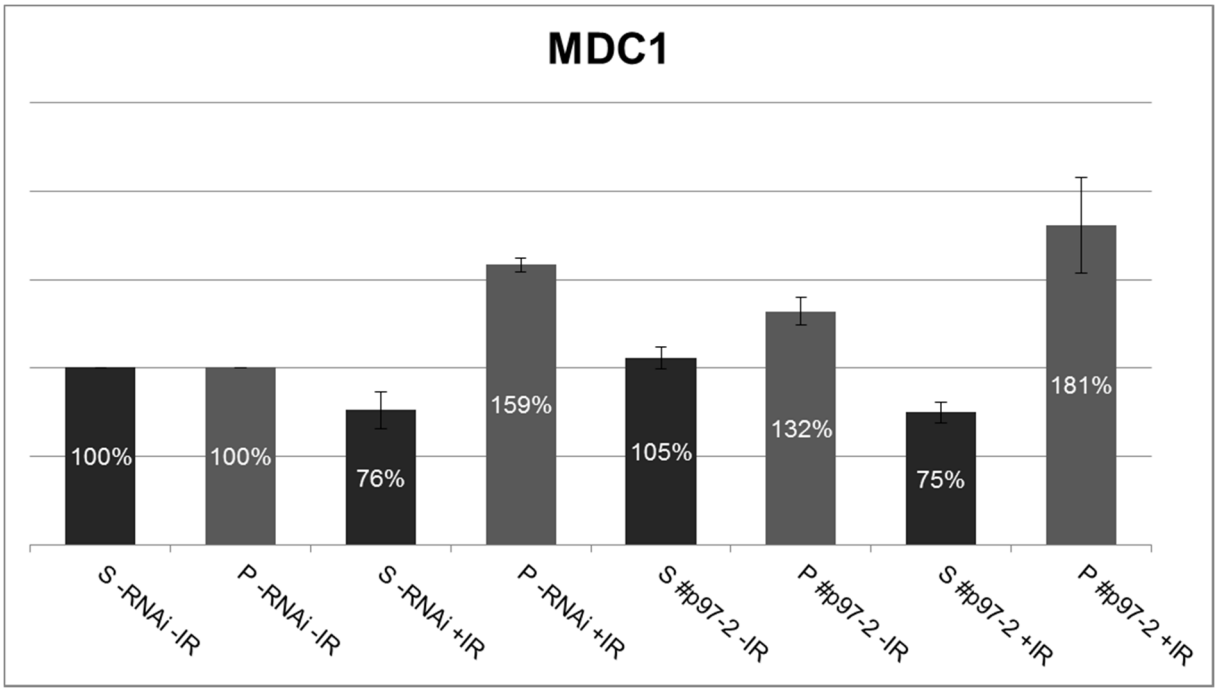


Figure 11: Quantification of MDC1 levels in the experiment shown in the previous figure and one additional, independent experiment. Protein levels in the S and P fractions were normalized to the loading control and are depicted as percentage of the corresponding untreated control (S $^{-RNAi\ -IR}$ and P $^{-RNAi\ -IR}$, respectively). Note that for the P fractions, the whole lanes ("smears"), considered as ubiquitinated and/or degraded MDC1, were measured instead of the bands. For technical details refer to chapter 3.

### 5.2.3 53BP1 recruitment to the chromatin depends on p97

Similar as for MDC1, we also observed an IR-induced and p97-independent degradation of 53BP1 (compare lanes 1 and 3 or 5 and 7 in Figure 12, low exposure). Furthermore, the accumulation of 53BP1 in absence of p97, which already was described in chapter 5.1, turns up again in the S fraction (compare lanes 1 and 5 or 3 and 7 in Figure 12, low exposure).

In the P fraction, 53BP1 is present under physiological conditions and its level halves upon IR in accordance with the S fraction (Figure 12, lanes 2 and 4). The localization of 53BP1 to the P fraction is strongly impeded by depletion of p97 (compare lanes 2 and 6 or 4 and 8 in Figure 12), indicating that p97 is required for recruitment of 53BP1 to tightly bound chromatin structures under both, genotoxic and physiological conditions.

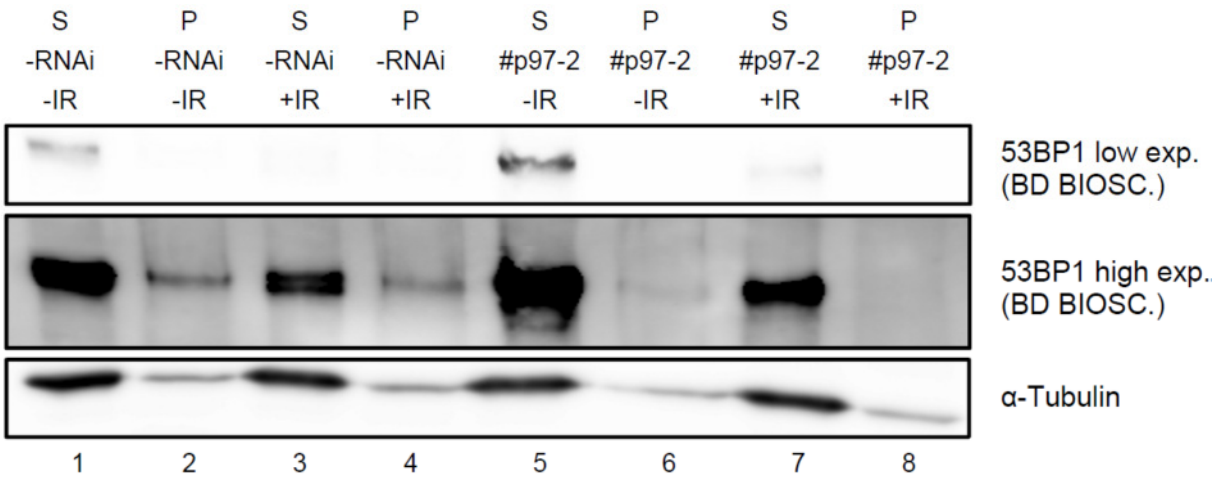


Figure 12: Immunoblots of S and P fractions from HEK293 cells subjected to the indicated treatments: RNAi of p97 (#p97-2) and control (-RNAi); irradiation with 10Gy (+IR) and control (-IR). Extraction took place 1h after irradiation. Fractionation controls are shown in Figure 8. 53BP1 levels were analyzed together with α-Tubulin (loading control). For technical details refer to chapter 3.

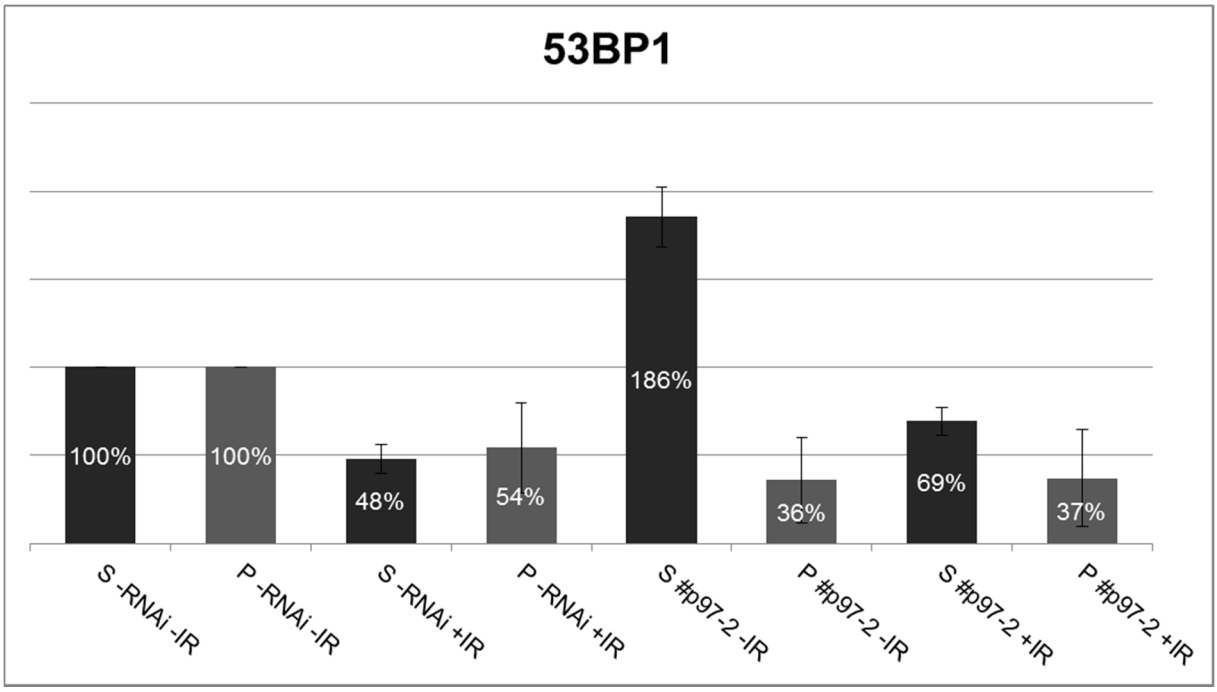


Figure 13: Quantification of 53BP1 levels in the experiment shown in the previous figure and one additional, independent experiment. Protein levels in the S and P fractions were normalized to the loading control and are depicted as percentage of the corresponding untreated control (S $^{-RNAi\ -IR}$ and P $^{-RNAi\ -IR}$, respectively). For technical details refer to chapter 3.

### 5.2.4 BRCA1 degradation upon exposure to IR

The third protein of interest, BRCA1, was observed to be degraded upon irradiation in a p97-independent manner as well, although this effect was not as clear as in case of MDC1 and 53PB1 (compare lines 1 and 3 or 5 and 7 in Figure 14).

In contrast to MDC1 and 53BP1, only a heavily modified form of BRCA1 ("smears") was detectable in the P fraction (Figure 14, lanes 2, 4, 6, 8). Therefore, as in case of MDC1, we measured these "smears", which could correspond to poly-ubiquitinated and/or SUMOylated BRCA1, for the quantification in Figure 15. Without determining the specificity of the "smears", the results give a hint that p97 plays a role in the recruitment of modified (poly-ubiquitinated or -SUMOylated) BRCA1 to chromatin as well as that DNA damage induced by IR might slightly increase this effect.

Together, these findings suggest that only a heavily modified form of BRCA1 exists in the tightly bound chromatin fraction and that p97 plays a role in the recruitment of BRCA1 to this fraction under physiological and genotoxic conditions.

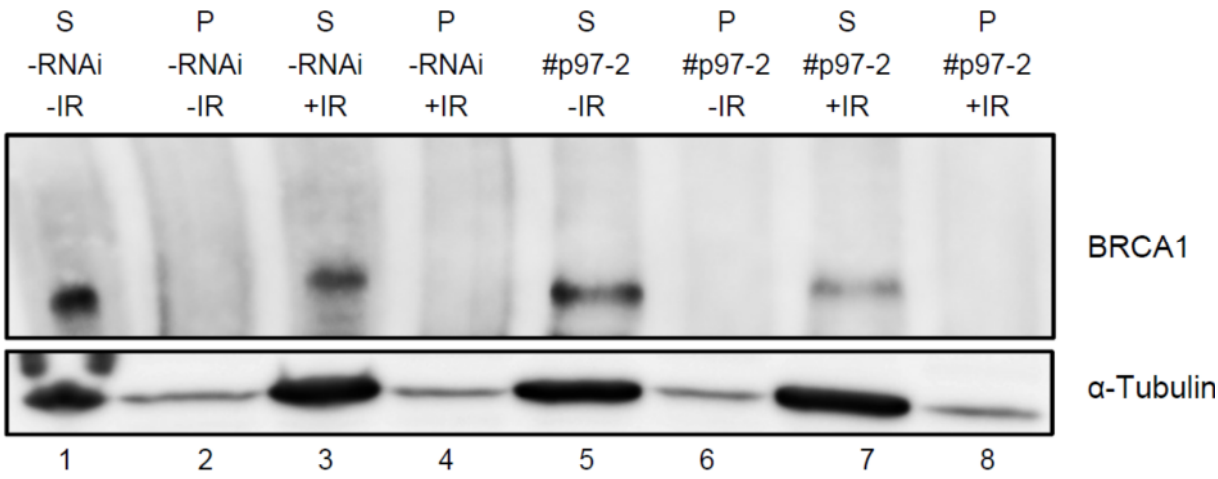


Figure 14: Immunoblots of S and P fractions from HEK293 cells subjected to the indicated treatments: RNAi of p97 (#p97-2) and control (-RNAi); irradiation with 10Gy (+IR) and control (-IR). Extraction took place 1h after irradiation. Fractionation controls are shown in Figure 8. BRCA1 levels were analyzed together with α-Tubulin (loading control). For technical details refer to chapter 3.

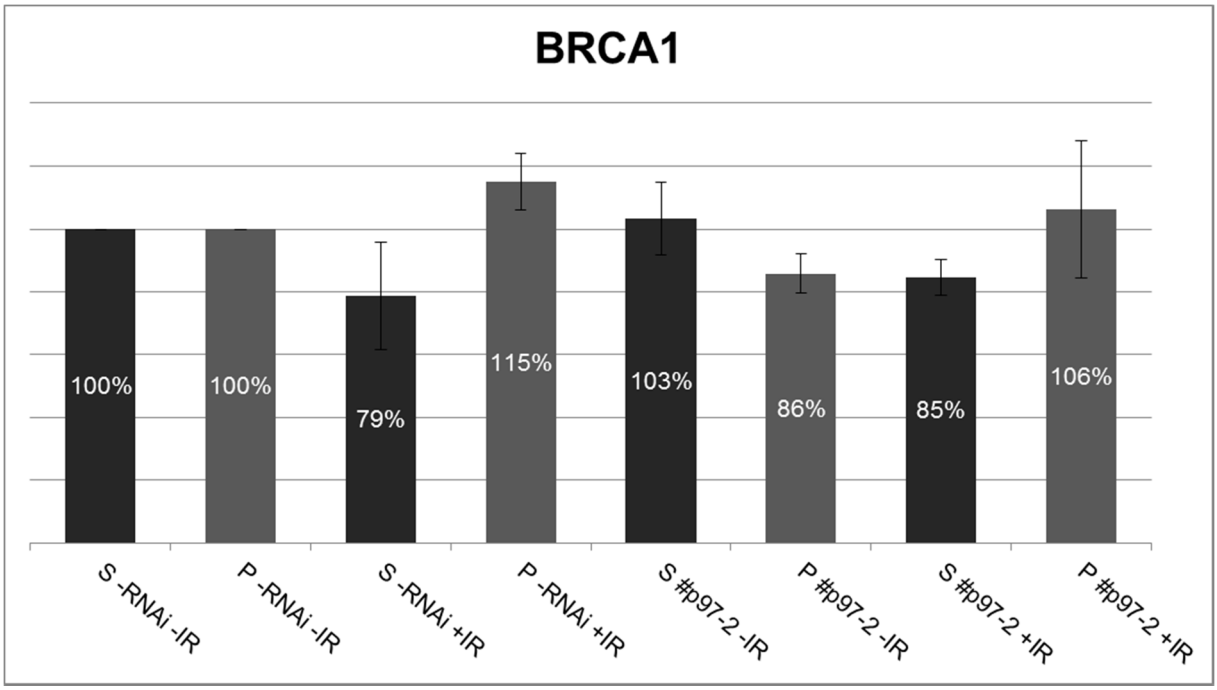


Figure 15: Quantification of BRCA1 levels in the experiment shown in the previous figure and one additional, independent experiment. Protein levels in the S and P fractions were normalized to the loading control and are depicted as percentage of the corresponding untreated control (S $^{-RNAi\ -IR}$ and P $^{-RNAi\ -IR}$, respectively). Note that for the P fractions, the whole lanes ("smears"), which might correspond to ubiquitinated and/or degraded BRCA1, were measured instead of the bands. For technical details refer to chapter 3.

## 5.3 Influence of MDC1 depletion and IR on protein turnover in the soluble cell fraction and in the tightly packed chromatin

The results shown in chapter 5.2.2 indicate that MDC1 is ubiquitinated and degraded in the P fraction upon IR. Indeed, it was reported that the MDC1 level at IRIF peaks about 30min after irradiation and subsequently decreases (84) and that K48-linked poly-ubiquitination and degradation of MDC1 are the responsible mechanisms (54). Therefore we speculated that the "smears" observed in our assay should disappear upon RNAi of MDC1 if they correspond to ubiquitinated and/or degraded MDC1. Since MDC1 is an integration platform of ubiquitination events that consequently controls the recruitment of 53BP1 and BRCA1 to sites of DSBs (11), we wanted to clarify whether FK2 ubiquitin, 53BP1 and BRCA1 levels are affected by MDC1 depletion. Thus, we performed another fractionation experiment analogous to the experiment described in chapter 5.2, but depleting MDC1 instead of p97.

### 5.3.1 MDC1 ubiquitination and degradation upon ionizing radiation

We again confirmed the quality of fractionation and the presence of DNA damage after IR by detection of vinculin, histone H2A and γ-H2AX (Figure 16A).

Effective depletion of MDC1 by the applied siRNA sequence is demonstrated in Figure 16B and the quantification in Figure 17. In accordance with previous results, the total level of MDC1 decreases after IR (compare lanes 1 and 3 in Figure 16B, low exposure), whereas the “smears” in the P fraction are enhanced (compare lanes 2 and 4, high exposure). These “smears” are markedly reduced in the samples depleted for MDC1 (lanes 6 and 8), meaning that they are attributable to MDC1 ubiquitination and degradation products.

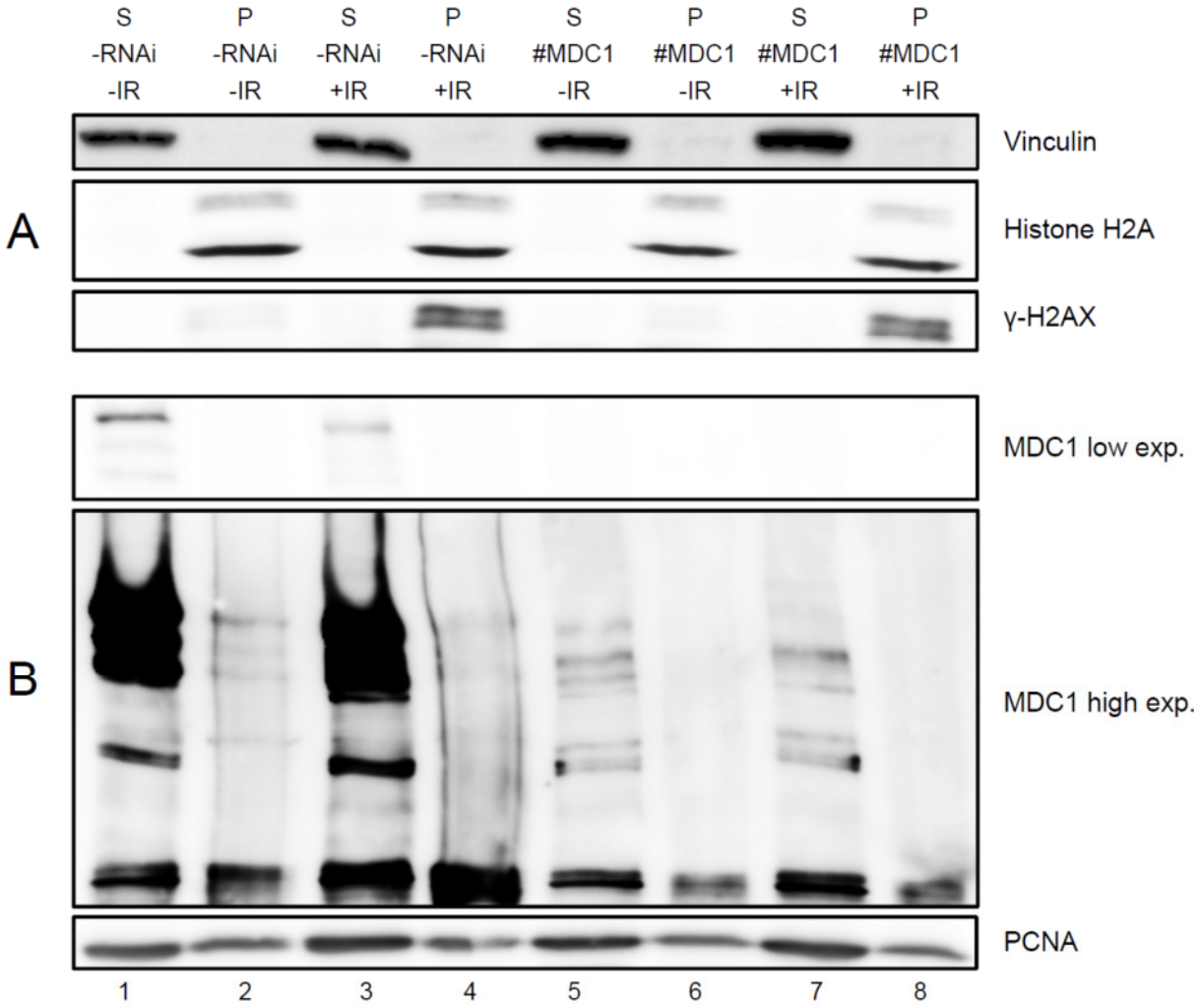


Figure 16: Immunoblots of S and P fractions from HEK293 cells subjected to the indicated treatments: RNAi of MDC1 (#MDC1) and control (-RNAi); irradiation with 10Gy (+IR) and control (-IR). Extraction took place 1h after irradiation. Vinculin and Histone H2A were used as fractionation controls, whereas γ-H2AX serves as marker for IR-induced DSBs. MDC1 levels were analyzed together with PCNA (loading control). For technical details refer to chapter 3.

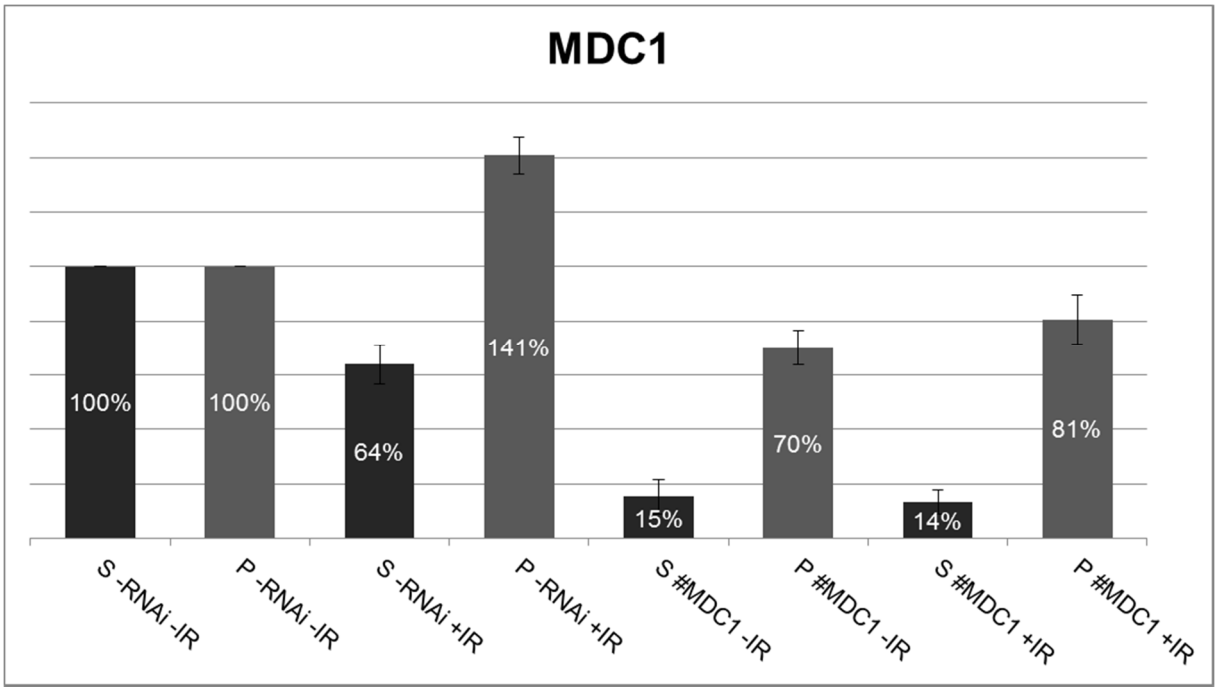


Figure 17: Quantification of MDC1 levels in the experiment shown in the previous figure and one additional, independent experiment (mean values). Protein levels in the S and P fractions were normalized to the loading control and are depicted as percentage of the corresponding untreated control ($S^{-RNAi\ -IR}$ and $P^{-RNAi\ -IR}$, respectively). Note that in the P fractions, the whole lanes ("smears"), considered as ubiquitinated and/or degraded MDC1, were measured instead of the bands. For technical details refer to chapter 3.

### 5.3.2 MDC1 depletion leads to ubiquitin accumulation on chromatin

Surprisingly, analysis of total ubiquitin levels revealed that depletion of MDC1 leads to accumulation of poly-ubiquitin conjugates in the soluble fraction and especially in the P fraction (Figure 18A and Figure 19). This finding suggests that some ubiquitination events on chromatin are happening upstream of MDC1 and that MDC1 not only serves as a mediator of the DDR, but also controls the turnover of ubiquitinated proteins on chromatin under physiological conditions. The slight increase of poly-ubiquitin levels induced by IR in the control samples (-RNAi, Figure 18A, lanes 3 and 4) is consistent with the previous results. In absence of MDC1, IR does not cause a considerable, additional increase of FK2 levels in the P fraction (compare lanes 6 and 8 in Figure 18A), as it has been observed after depletion of p97 (chapter 5.2.1). This can be explained based on the established knowledge according to which the major part of IR-induced ubiquitination events (DDR) on chromatin depends on MDC1 (54; 85).

In the S fraction, on the other hand, a slight IR-induced increase of ubiquitin is still detectable upon MDC1 depletion (compare lanes 5 and 7 in Figure 18), meaning that IR could cause MDC1-independent ubiquitination (and probably degradation) of loosely or non-chromatin-associated proteins.

Figure 18B and the corresponding quantification show that neither IR nor depletion of MDC1 affects the levels of p97. As noticed before, p97 is mainly present in the S fraction, but a small amount of p97 is localized in the P fraction. The discovery of our laboratory that p97 recruitment to microscopically visible sites of DNA damage (laser stripe) might raise the expectation that as a biochemical correlate, p97 levels in the P fraction should increase upon irradiation. There are two possible explanations for the fact that this is not the case: Firstly, the association of p97 to sites of DNA damage might be too weak to withstand the stringent extraction conditions in our assay, meaning that p97 is released from damaged DNA with the S fraction. Secondly, IR might not affect the chromatin level of p97 at all, but merely lead to a concentration of chromatin-associated p97 at sites of DNA damage.

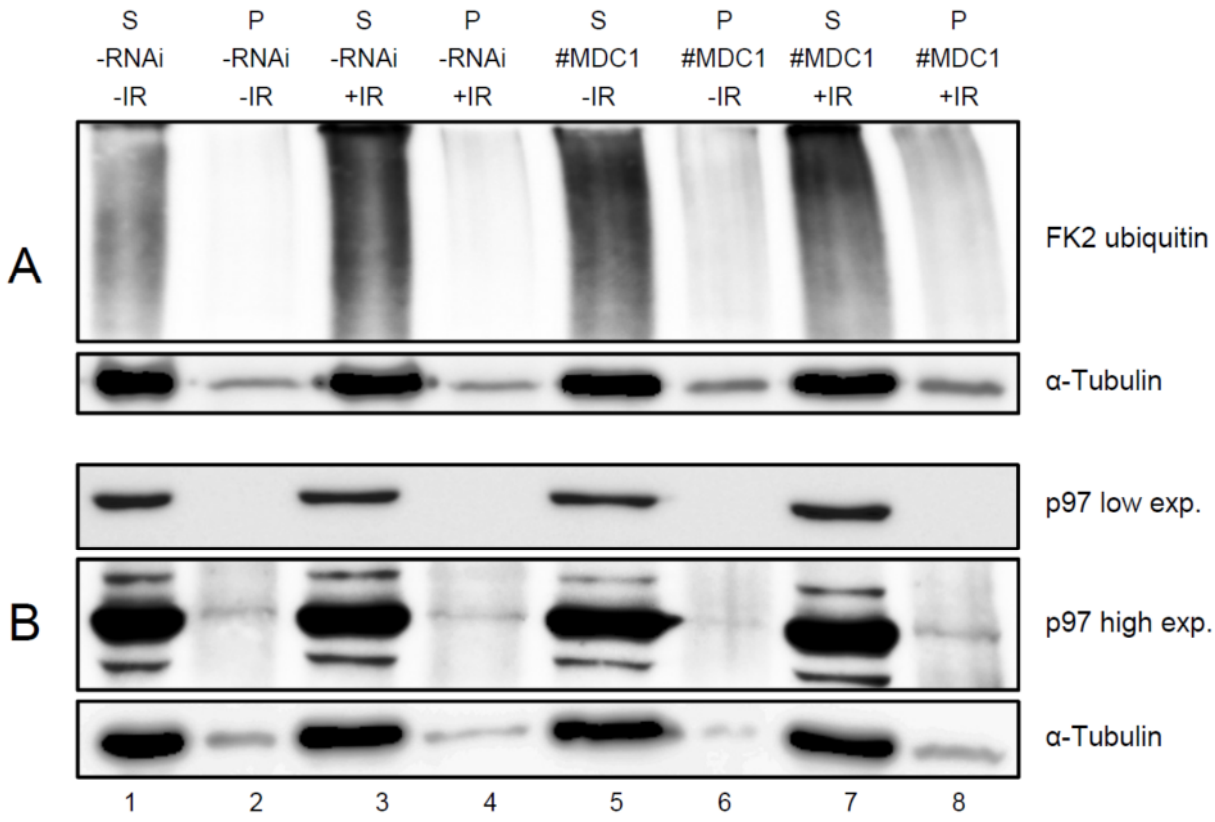


Figure 18: Immunoblots of S and P fractions from HEK293 cells subjected to the indicated treatments: RNAi of MDC1 (#MDC1) and control (-RNAi); irradiation with 10Gy (+IR) and control (-IR). Extraction took place 1h after irradiation. Fractionation controls are shown in Figure 16. Total conjugated ubiquitin (FK2) and p97 levels were analyzed together with α-Tubulin (loading control). For technical details refer to chapter 3.

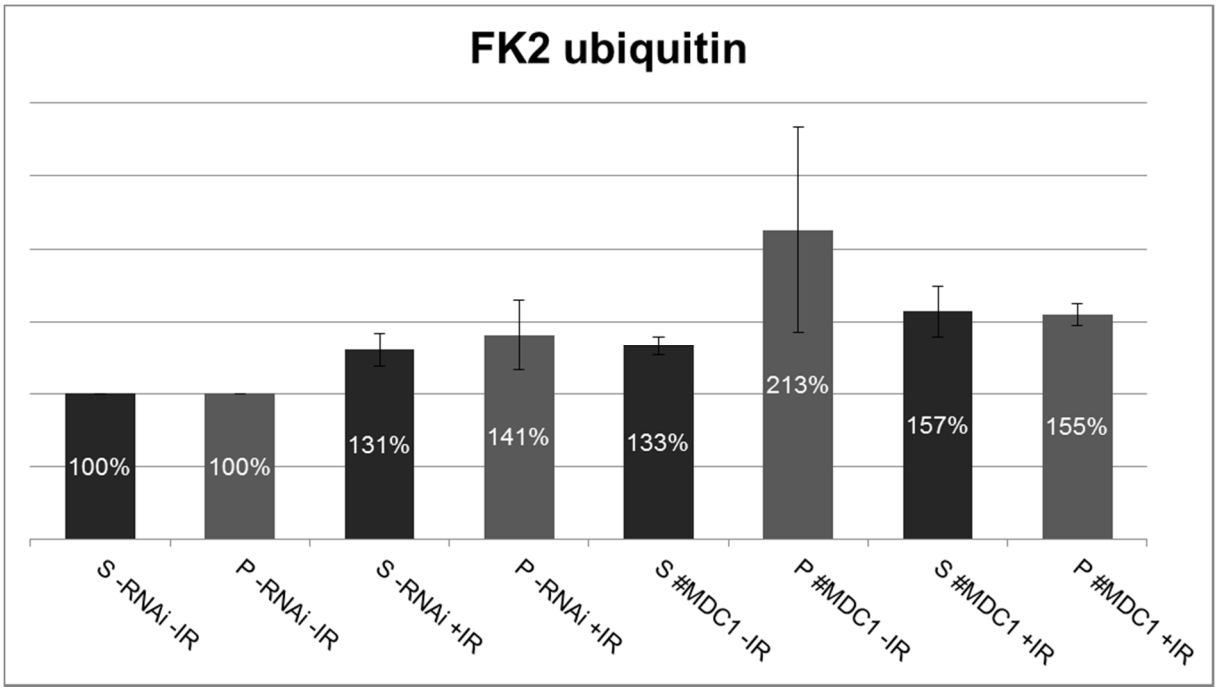


Figure 19: Quantification of total conjugated ubiquitin levels in the experiment shown in the previous figure and an additional, independent experiment (mean values). Protein levels in the S and P fractions were normalized to the loading control and are depicted as percentage of the corresponding untreated control (S $^{-RNAi\ -IR}$ and P $^{-RNAi\ -IR}$, respectively). For technical details refer to chapter 3.

### 5.3.3 MDC1 is required for the recruitment of 53BP1 to chromatin

The distribution of BRCA1 in Figure 20A resembles the picture shown in chapter 5.2.4 regarding IR-induced degradation. Again, BRCA1 bands are limited to the S fractions. MDC1 depletion might lead to a certain accumulation of BRCA1 (Figure 20A, lane 5). If the “smears” in the P fractions should correspond to ubiquitination and/or SUMOylation products of BRCA1, their level is decreased by MDC1 depletion (compare lanes 2 and 6 or 4 and 8 in Figure 20A). This notion is supported by the fact that MDC1 is an upstream factor of BRCA1 in the DDR (17) and thus could not only control its recruitment, but also its degradation. However, it would be required to demonstrate the specificity of the “smears” to allow this conclusion.

The impact of MDC1 depletion on 53BP1 surprisingly resembles the effect of p97 depletion as well (Figure 20B and quantification in Figure 21). 53BP1 accumulates in the S fraction in absence of MDC1, although to a lower extent than upon depletion of p97 (chapter 5.2.3). On the other hand, recruitment of 53BP1 to the P fraction is impaired in MDC1 depleted cells similar to p97-depleted cells. Whereas it is established that MDC1 governs the recruitment of 53BP1 in the DDR (17), our results indicate a more general role of MDC1 in regulation of 53BP1 levels, also under physiological conditions.

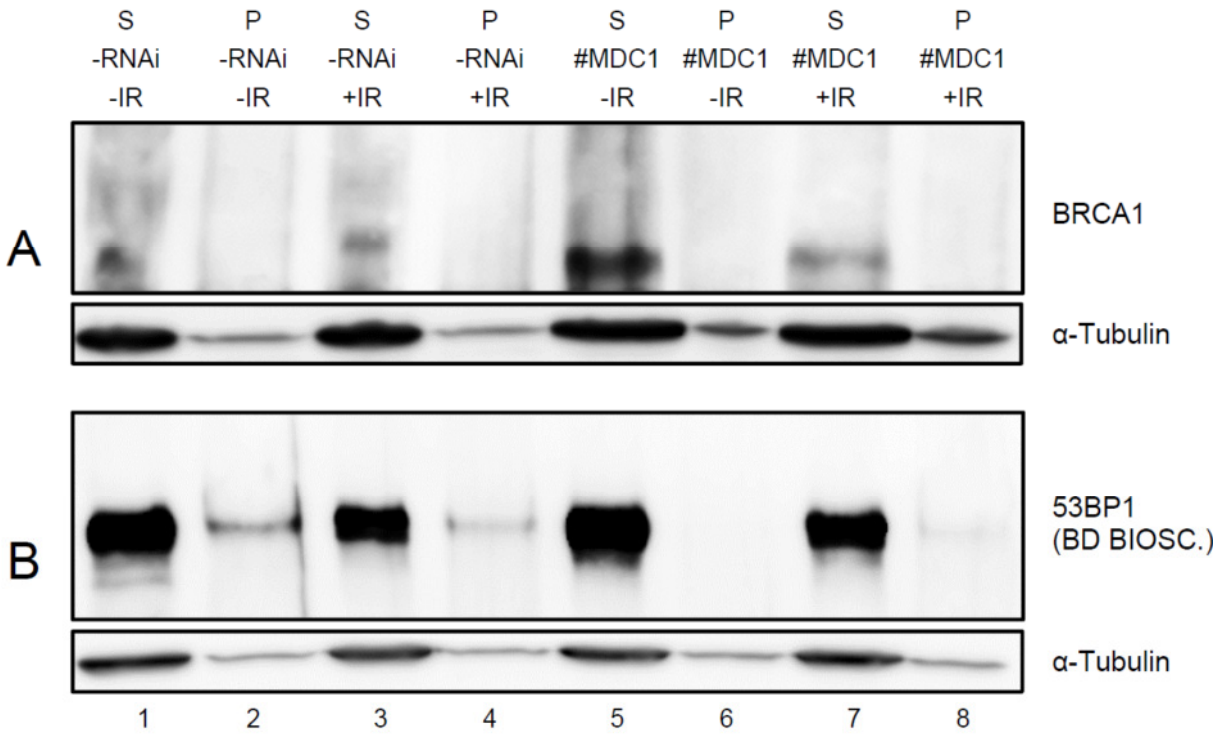


Figure 20: Immunoblots of S and P fractions from HEK293 cells subjected to the indicated treatments: RNAi of MDC1 (#MDC1) and control (-RNAi); irradiation with 10Gy (+IR) and control (-IR). Extraction took place 1h after irradiation. Fractionation controls are shown in Figure 16. BRCA1 and 53BP1 levels are were analyzed together with α-Tubulin (loading control). For technical details refer to chapter 3.

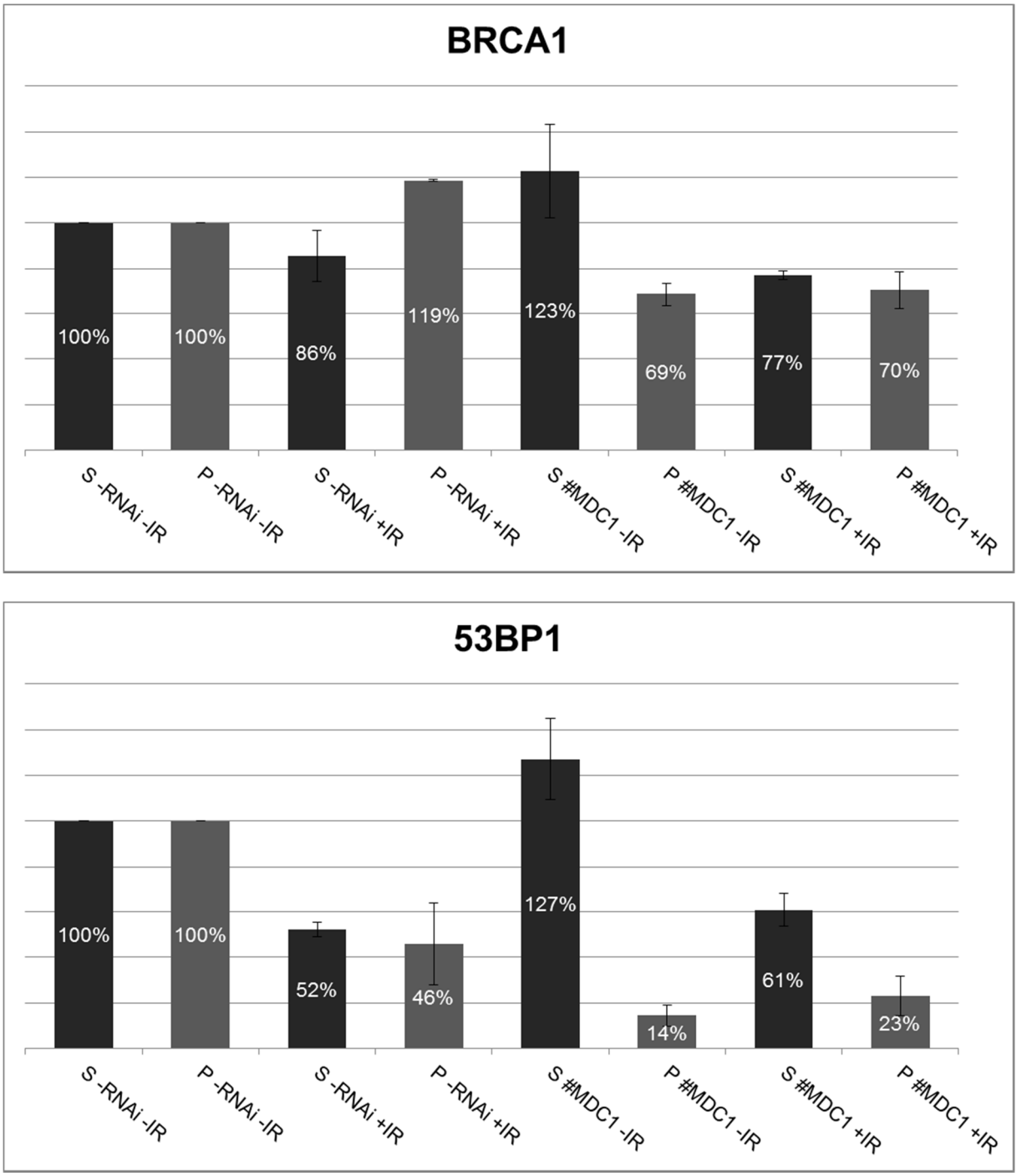


Figure 21: Quantification of BRCA1 and 53BP1 levels in the experiment shown in the previous figure and one additional, independent experiment (mean values). Protein levels in the S and P fractions were normalized to the loading control and are depicted as percentage of the corresponding untreated control (S $^{-RNAi\ -IR}$ and P $^{-RNAi\ -IR}$, respectively). For technical details refer to chapter 3.

## 5.4 Isolation of the p97 fraction from tightly packed chromatin

The previous results indicate that p97 influences the steady state level of 53BP1 and its recruitment to the tightly packed chromatin fraction. Thus, we wanted to address the question whether p97 controls 53BP1 via direct interaction. For this purpose we have performed a precipitation experiment. As p97 is an abundant protein localized in cytoplasm, nucleoplasm and chromatin, we expressed strep-tagged wildtype p97 (WT) as well as a substrate-trapping p97 mutant (EQ) in HEK293 cells and prepared cytoplasmic (CE), nucleoplasmic (NE) and chromatin (CH) fractions according to the "3-step" protocol (3.4.2.5). The EQ mutant of p97 is able to bind substrates but cannot release them because of its inert ATPase activity.

The efficacy of fractionation was monitored by immunoblotting with cyclophilin A (86) and histone H2A antibodies that were used as markers for the cytoplasmic and chromatin fraction, respectively (Figure 22). The fractionation markers show that the NE fractions were slightly contaminated with both proteins, cyclophilin A and histone H2A (Figure 22 lanes 3 and 4). Moreover, our fractionation protocol gave us a very small amount of proteins in the nucleoplasmic fractions. Due to these reasons we excluded the NE samples from further analysis.

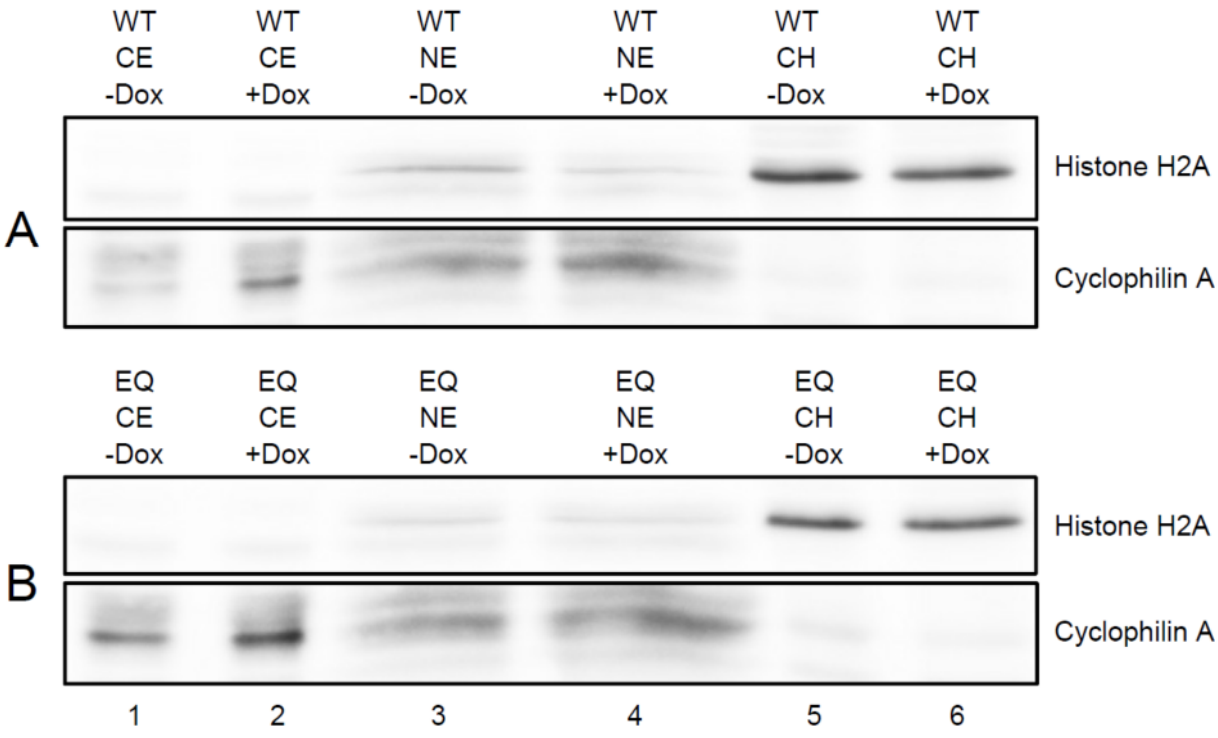


Figure 22: Analysis of fractions prepared according to the "3-step" fractionation protocol. HEK293 cells were induced (+DOX) for strep-p97-WT (WT) and strep-p97-EQ (EQ) expression respectively, or left uninduced (-DOX). Cytoplasmic (CE), nucleoplasmic (NE) and chromatin (CH) fractions were prepared according to the 3-step fractionation protocol. Cyclophilin A and histone H2A were used as fractionation markers. For technical details refer to chapter 3.

Overexpressed strep-p97-WT or strep-p97-EQ was isolated from CE and CH fractions using streptavidine beads (Figure 23, Figure 24). Both p97 constructs were efficiently expressed (Figure 23A and Figure 24A, lanes 2 and 4) and isolated from both fractions (Figure 23A and Figure 24A, lanes 6 and 8). Cells without strep-p97 expression (-DOX) were used as a negative control for the precipitation (Figure 23A and Figure 24A, lanes 1, 3, 5 and 7).

Even though p97 was efficiently isolated from cytoplasm and chromatin, the interaction with 53BP1 was not detected under these experimental conditions. In spite of negative results in terms of p97-53BP1 interaction, these experiments confirmed that p97 binds to chromatin and that it can be isolated from the chromatin fraction for further analysis.

We also tested the presence of total conjugated ubiquitin (FK2 signal) in p97 isolates (Figure 23B and Figure 24B). We were only able to detect p97 association with poly-ubiquitinated substrates in CE (Figure 23B and Figure 24B, lane 6) but not in CH, even though the total level of poly-ubiquitinated substrates was increased on chromatin when p97 ATPase activity was impaired (Figure 24, compare lanes 3 and 4).

Considering the accumulation of poly-ubiquitin conjugates in the P fraction observed upon p97 depletion (chapter 5.2.1), it seems likely that p97 does interact with these conjugates, but that the amount of p97-bound poly-ubiquitinated substrates on chromatin was below the sensitivity level of the FK2 antibody in the present precipitation assay. Moreover, the amount of p97 isolated from CH was much lower than the amount obtained from CE.

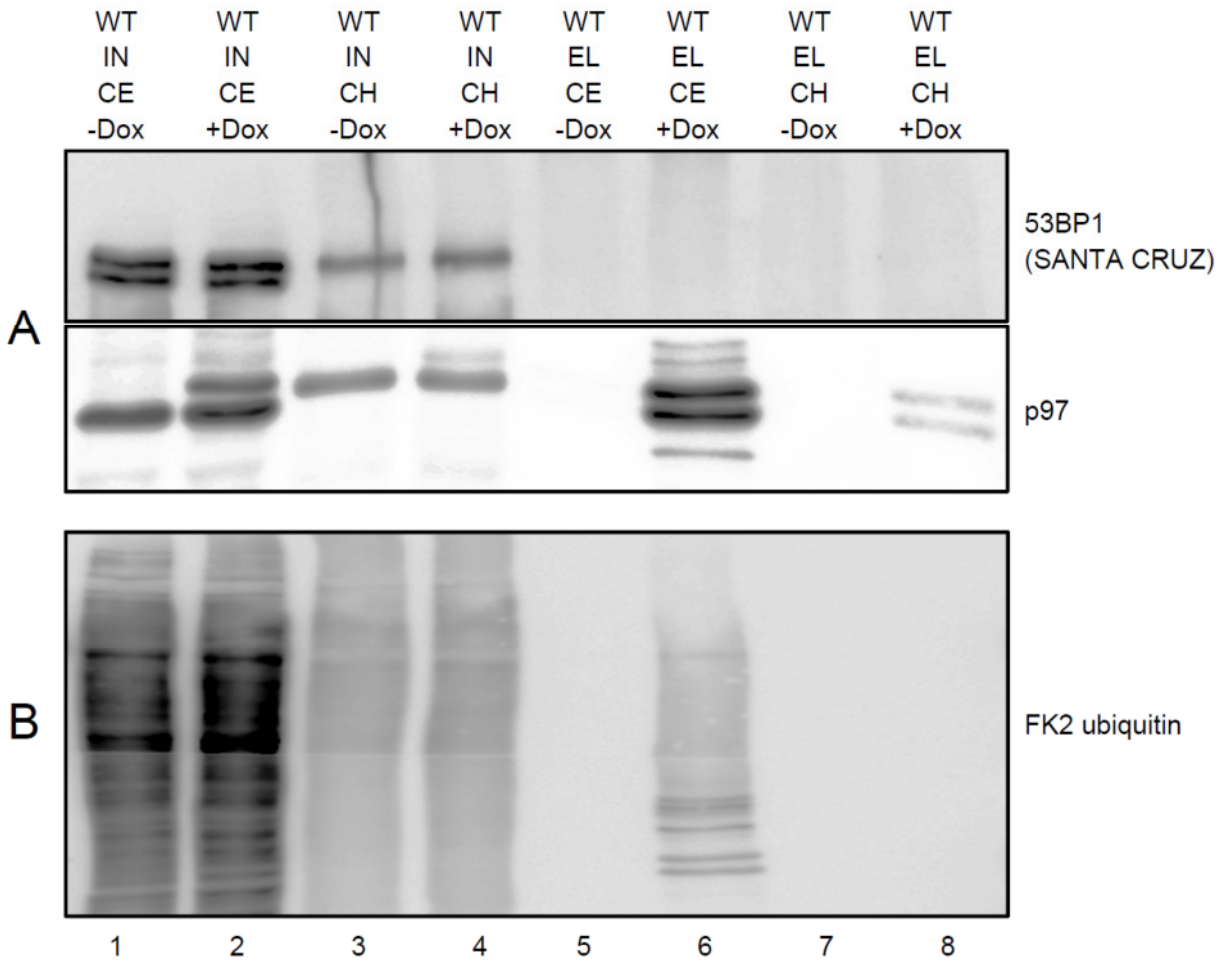


Figure 23: Isolation of strep-p97-WT from the CE and CH fractions characterized in Figure 22A. The levels of the indicated proteins were analyzed using specific antibodies. Lanes 1-4 (IN = input) represent the sample before p97 isolation. Lanes 5-8 (EL = eluate): p97 was purified over streptavidin beads and analyzed for p97, 53BP1 and total conjugated ubiquitin (FK2). For the experimental procedures consult chapter 3.

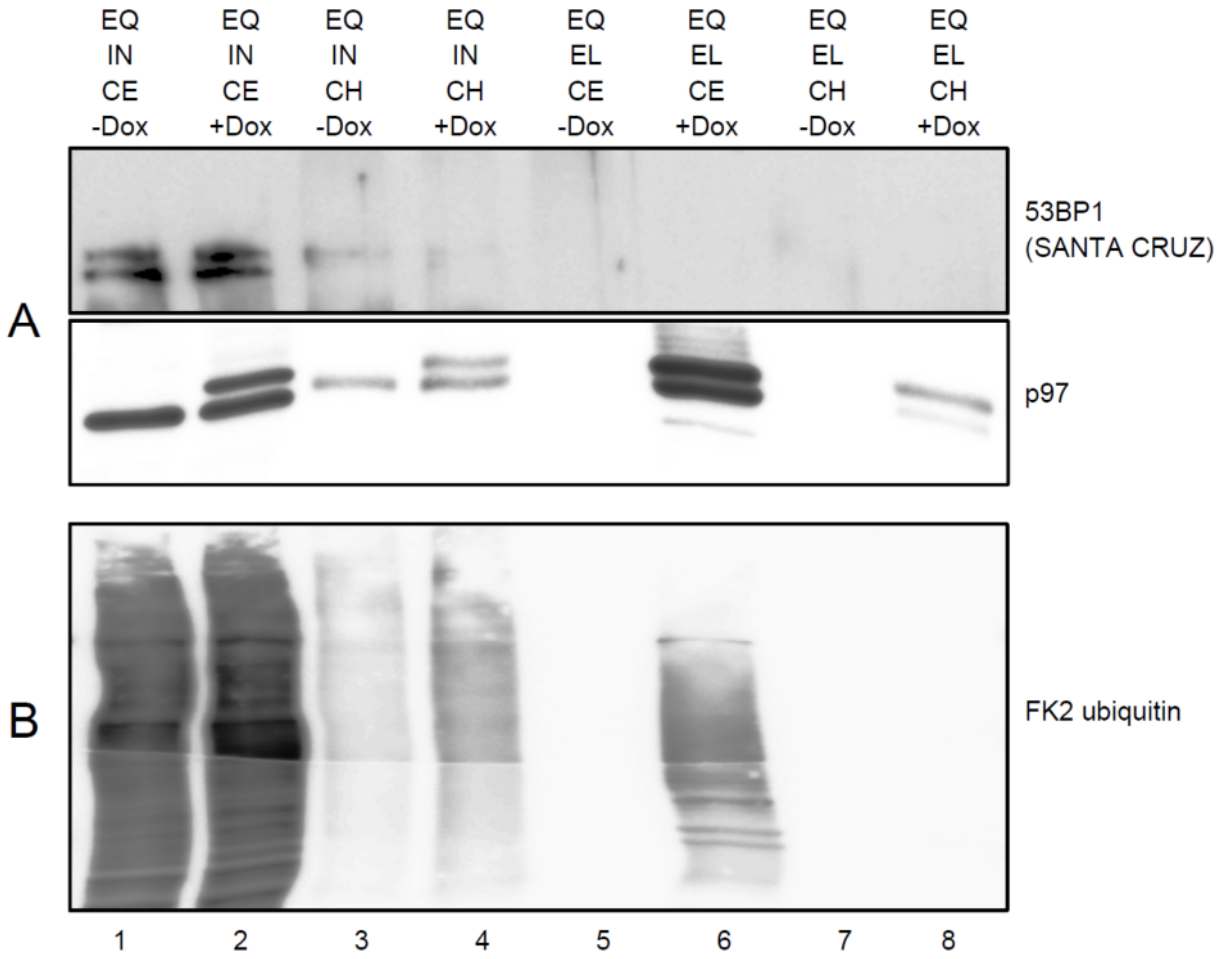


Figure 24: Isolation of strep-p97-EQ from the CE and CH fractions characterized in Figure 7A. The levels of the indicated proteins were analyzed using specific antibodies. Lines 1-4 (IN = input) represent the sample before p97 isolation. Lines 5-8 (EL = eluate): p97 was purified over streptavidin beads and analyzed for p97, 53BP1 and total conjugated ubiquitin (FK2). For the experimental procedures consult chapter 3.

## 5.5 Removal of L3MBTL1 by p97 as a potential mechanism for recruitment of 53BP1 to the tightly packed chromatin

Although the negative results of the co-precipitation experiment do not exclude the possibility that p97 interacts with 53BP1, they also could point to indirect mechanisms by which p97 controls the steady state level and mobility of 53BP1. Indeed, concurrent work of Acs et al. recently provided an explanation how p97 indirectly facilitates recruitment of 53BP1 to sites of DNA damage (87): In accordance with the results from our laboratory (33), they found that p97 localizes to DSB with its UFD1-NPL4 adaptor in a RNF8-dependent manner and is required for 53BP1 recruitment. They showed that p97 removes the ubiquitinated polycomb protein L3BMTL1, which covers the Lysine 20 (di-)methylation mark of histone H4 (H4K20me2), from sites of DNA damage. Since H4K20me2 is the main binding site of 53BP1 on damaged chromatin, this mechanism explains why functional p97 is required for assembly of 53BP1 at sites of DNA damage (87).

It should be noted that in addition to the results of our laboratory (33), Acs et al. found that not only RNF8, but also RNF168 is required for efficient recruitment of p97 to damage sites, and that p97 is dispensable for accumulation of BRCA1 at DSB (87). Their study leaves open by which ubiquitin chain type L3MBTL1 is modified, if it is degraded after removal from chromatin, and if there might be analogous mechanisms for other chromatin-associated substrates in the DDR. In spite of these unsolved questions, Acs et al. proofed the role of p97 as an ubiquitin-dependent segregase at sites of DNA damage.

According to the results shown in chapter 5.2.3, localization of 53BP1 to the P fraction is abolished upon depletion of p97. Notably, this is not only the case after irradiation, but also under physiological conditions. In order to clarify whether displacement of L3MBTL1 by p97 accounts for this observation, we performed another “2-step” fractionation experiment with HEK293 cells depleted for p97, L3MBTL1 and co-depleted for both proteins. Based on the above-mentioned study, it could be expected that co-depletion of L3MBTL1 should compensate the negative effect of p97 depletion on 53BP1 recruitment to the P fraction. However, Acs et al. applied damage conditions for their experiments. Therefore, it was unclear if the same mechanism works out in undamaged chromatin.

The quality of fractionation and the depletion of p97 are demonstrated in Figure 25A and B, respectively. As follows from Figure 25C and D, we were not able to confirm the depletion of L3MBTL1 with two different commercial antibodies. Both pictures show the MW range from approx. 60kDa to 150kDa, which should include L3MBTL1 (predicted MW = 84kDa). A failure of the siRNA transfection seems unlikely, because we neither could show an effect with these antibodies using two additional siRNA sequences against L3MBTL1 (results not shown), because RNAi of p97 was successful in the same experiments, and finally, because the expected effect on 53BP1 is observed.

Acs et al. used antibodies from the same company for their study (87), but they show L3MBTL1 bands only after immunoprecipitation. Therefore it must be assumed that the sensitivity of these antibodies is insufficient to detect endogenous levels of L3MBTL1 and that it recognizes unspecific bands with a much higher affinity.

Hence, although no suitable antibody was available to demonstrate the level of L3MBTL1 depletion in our experiment, Figure 25E and the quantification in Figure 26 show the result that is expected based on the above-mentioned publication. As in the previous experiments, the 53BP1 level in the P fraction is markedly reduced in absence of p97 (compare lines 2 and 4 in Figure 25E). This effect is fully restored by co-depletion of L3MBTL1 (line 6). Therefore, removal of L3MBTL1 from H4K20me binding sites might represent the mechanism by which p97 enables 53BP1 to associate to chromatin not only upon DNA damage, but also under physiological conditions.

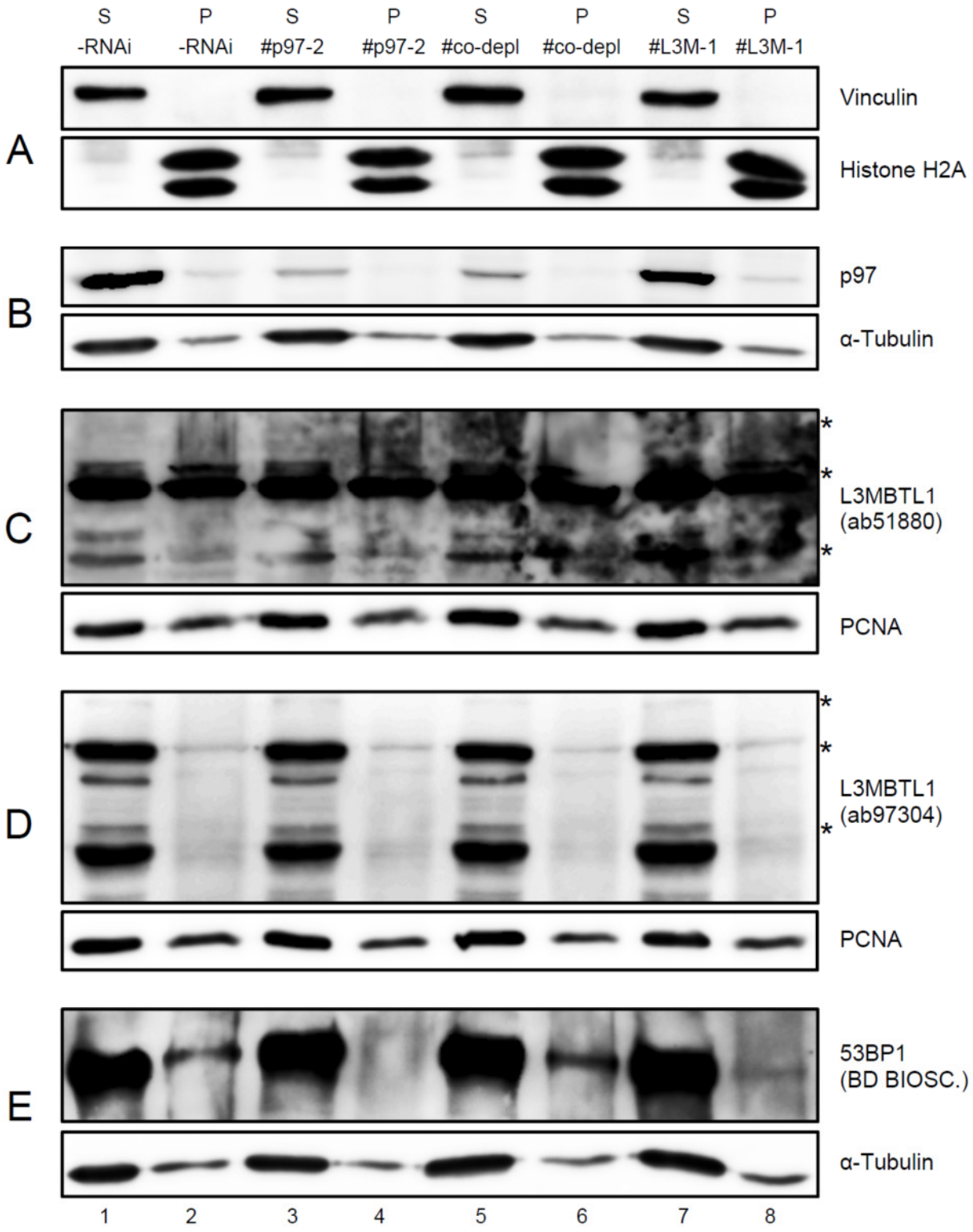


Figure 25: Immunoblots of S and P fractions from HEK293 cells treated with siRNA against p97 (#p97-2), L3MBTL1 (#L3M-1) and both sequences together (#co-depl). The treatment lasted for 3 days and transfection reagent without siRNA was applied to the control cells (-RNAi). Protein levels were analyzed with the indicated antibodies. Vinculin and Histone H2A were detected to confirm the quality of fractionation. α-Tubulin and PCNA were used as loading controls. Stars (*) in panels C and D indicate the positions of 150kDa, 100kDa and 75kDa marker bands (expected size of L3MBTL1 = 84kDa). For technical details refer to chapter 3.

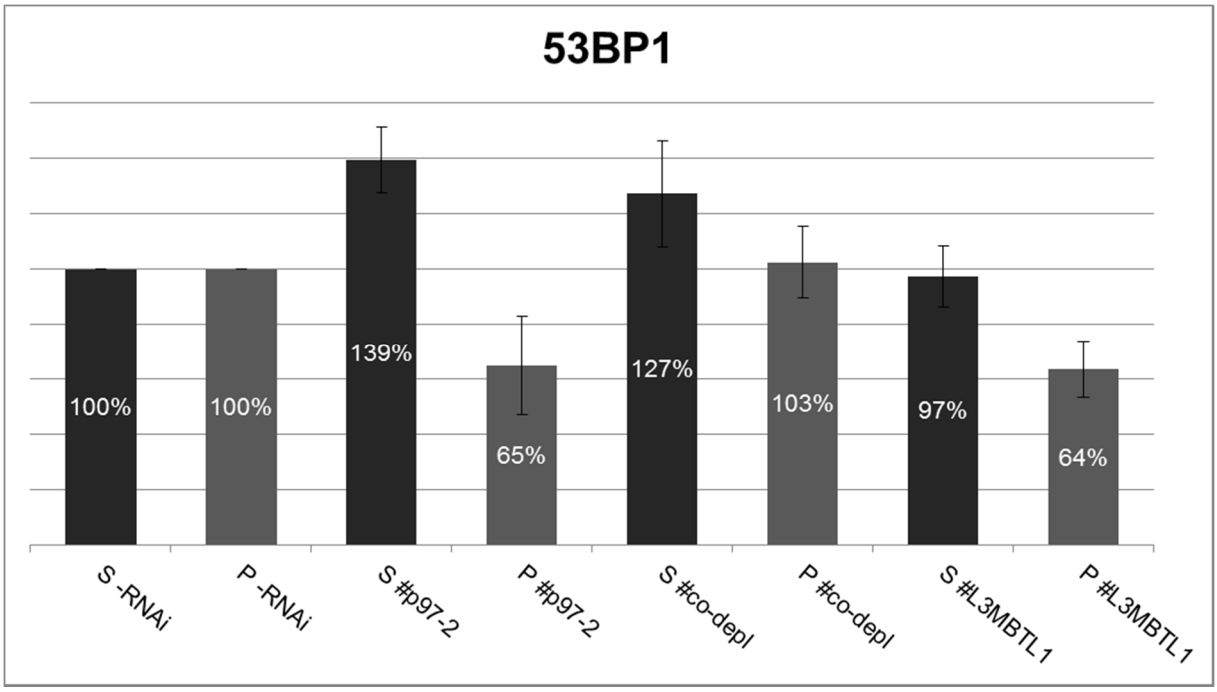


Figure 26: Quantification of 53BP1 levels in the experiment shown in the previous figure and one additional, independent experiment. The second experiment was performed with the siRNA sequence #L3M-2 instead of #L3M-1. Protein levels in the S and P fractions were normalized to the loading control and are depicted as percentage of the corresponding untreated control (S $^{-RNAi}$ and P $^{-RNAi}$, respectively). For technical details refer to chapter 3.

# 6 Discussion

Much progress has been achieved during the past few years in understanding the role of ubiquitin signaling in orchestration of the cellular response to DSBs. In addition to the well-established non-proteolytic K63-linked ubiquitin signal, pioneering work from our laboratory, afterwards confirmed by others, established K48-linked ubiquitin chains, the UPS and p97 as a parallel signaling pathway in orchestration of the DDR (32; 33; 34; 35; 63; 88). In this study, the influence of p97 on the central DDR proteins MDC1, 53BP1 and BRCA1 as well as on chromatin ubiquitin levels was investigated by biochemical methods in HEK293 cells.

## 6.1 p97-independent degradation of MDC1 upon IR

As mentioned in chapter 4, it was previously proposed that MDC1 is modified by K48 poly-ubiquitin chains, removed from sites of DNA damage and degraded by the proteasome in response to IR (54). In the fraction of tightly chromatin-associated proteins obtained with our "2-step" fractionation assay, we observed an increased background signal of the MDC1 antibody 1h after exposure to IR, which was abolished by RNAi of MDC1 and therefore probably corresponds to MDC1 ubiquitination and/or SUMOylation products (chapter 5.3.1). Hence, our results support the idea that MDC1 has to be recruited, but also ubiquitinated and/or SUMOylated and finally removed from sites of DSBs after a certain time. Since the total level of MDC1 was markedly reduced upon IR, it can be speculated that MDC1, which serves as a platform for the amplification of the DNA damage signal, is removed and degraded from sites of DNA damage to ensure a proper orchestration of the DDR. This suggests that the spatiotemporal regulation of MDC1 is an essential step in DDR. Its hyper-accumulation at sites of DNA damage might cause excessive accumulation of downstream molecules, namely genome caretakers. Interestingly, hyper-accumulation of genome caretakers also causes a severe DNA repair defect, chromosomal breakage and genome instability (M. Puumalainen, K. Ramadan and H. Näegeli, personal communications; manuscript submitted). Thus, the UPS serves as a rate-limiting component of DDR pathways by preventing hyper-accumulation of genome caretakers and thus preventing "good guys" to become "bad guys".

Interestingly, p97 inactivation increased the level of modified, probably ubiquitinated and/or SUMOylated MDC1 in the tightly chromatin-bound protein fraction under physiological and genotoxic conditions (chapter 5.2.2). This could point to a novel role of p97 in regulating the steady state level of chromatin-associated MDC1. In particular, it comes into consideration that p97 is required for removal and/or degradation of E3 ubiquitin ligases from chromatin which in turn regulate the level of MDC1. A possible candidate is RNF4, which is known to target SUMOylated MDC1 (88).

Moreover, an example of an E3 ubiquitin ligase that is regulated by poly-ubiquitination itself is given in the case of RNF168 (58). However, since these studies investigated damage conditions, further work will be necessary to clarify if such mechanisms play a role in undamaged chromatin and if they involve p97.

## 6.2 p97 controls the total cellular level and chromatin recruitment of 53BP1

In all experiments shown in chapters 5.1, 5.2.3 and 5.5, depletion of p97 led to a strong increase of 53BP1 total levels, indicating that p97 takes part in the steady-state turnover of 53BP1. This turnover also involves the proteasome, because proteasome inhibition results in 53BP1 accumulation as demonstrated in chapter 5.1. IR caused a marked reduction of the 53BP1 level which was independent of p97 (5.2.3). Together, these results suggest dual degradation pathways for 53BP1: p97-dependent under physiological conditions and p97-independent after genotoxic stress.

The observation of IR-induced 53BP1 degradation is consistent with the literature data since 53BP1 is known as an ubiquitination target (32) and its degradation upon DNA damage was shown to be delayed by the DUB USP28 (56). It might be surprising that 53BP1 decreases by 50% already 1h after irradiation, because 53BP1 belongs to the DDR proteins that operate in IRIF at later time points (15). However, it seems likely that only a small quantity of 53BP1 is effectively required for the DDR and degradation might affect the surplus amount.

Strikingly, p97 depletion not only lead to 53BP1 accumulation on the total cellular level, but also abolished its localization to the tightly chromatin-bound protein fraction in our experiments (chapter 5.2.3 and 5.5). Published studies of our laboratory and of Acs et al. demonstrate that p97 is required to recruit 53BP1 to sites of DNA damage (33; 87). In the work presented here, we detected a chromatin-associated 53BP1 fraction under physiological conditions, and this was dependent on p97, too. Moreover, MDC1 seems to facilitate association of 53BP1 to the tightly chromatin-bound protein fraction not only upon IR, but also under physiological conditions (chapter 5.3.3). This is supported by the finding that MDC1 directly interacts with 53BP1 (17).

The observed, strong effects of p97 depletion on 53BP1 steady-state level and its recruitment to the tightly bound chromatin fraction led us to the question if the two proteins might physically interact. This was not the case under our experimental conditions, see chapter 5.4. There are different explanations for the negative results in terms of 53BP1-p97 complex formation. First, genotoxic stress might be required to boost the interaction as in the case of 53BP1 and Rad18 (89) or p97 and L3MBTL1 (87).

Second, the amount of 53BP1 in the p97 precipitate from chromatin could have been below the detection limit, since the level of chromatin bound p97 isolate was low. The fact that we neither were able to co-precipitate poly-ubiquitinated substrates from the chromatin fraction, although it is known meanwhile that there is an interaction of p97 with ubiquitinated L3MBTL1 (87), supports the suspicion that the sensitivity of the employed assay was insufficient. Nevertheless, the third and most likely explanation is that p97 does not associate with 53BP1 at all, but regulates its function indirectly. The direct interaction of p97 and 53BP1 cannot be definitively excluded, however.

The results in chapter 5.5 indicate that the indirect mechanism proposed for 53BP1 recruitment to DSB, namely removal of L3MBTL1 by p97 (87), might also allow the constitutive binding of 53BP1 to chromatin. It has to be noted that an antibody which detects endogenous levels of L3MBTL1 would have been required to unequivocally proof the depletion of L3MBTL1. Whether 53BP1 has a function on undamaged chromatin (e.g. remodeling) or just is “on standby” there, remains unclear, although constitutive chromatin binding of 53BP1 was described in lymphocytes and interestingly was suggested to depend on RNF168 (18).

Besides L3MBTL1 displacement and direct 53BP1-MDC1 interaction, three additional, recently proposed mechanisms could also contribute to the recruitment of 53BP1 to DSB: Firstly, direct binding to ubiquitinated histone H2A (42); secondly, de-novo methylation of H4K20 by MMSET (18); and thirdly, removal of the lysine de-methylases JMJD2A and JMJD2B by the UPS. JMJD2A and JMJD2B, as L3MBTL1, bind to H4K20me and it is speculated that p97 could participate in their extraction as well (35). This notion is not supported by our data, but since 53BP1 recruitment might be controlled by different mechanisms to a different extent under different conditions, further work on this issue is required.

It will be of special interest to clarify if UPS- and p97-dependent control of the 53BP1 steady state level relies on chromatin recruitment of 53BP1 prior to degradation, or if this degradation pathway is independent from the chromatin recruitment pathway(s).

## 6.3 IR-induced degradation of BRCA1

The physical interaction of p97 and BRCA1 was one of the earliest discoveries that implicated p97 in the DDR (75). BRCA-1 is ubiquitinated and degraded upon IR but also exhibits E3 ubiquitin ligase activity. Therefore, it is speculated that BRCA-1 could function as a p97 substrate, a p97 substrate processing factor or both (34). While the previous results of our laboratory indicated that p97 is needed for the recruitment of BRCA1 to the site of DSBs (33), the publication from Acs et al. suggests no effect of p97 on BRCA1 recruitment (87).

In accordance with the literature (55), we observed that BRCA1 is degraded upon IR (chapters 5.2.4 and 5.3.3). This effect was p97-independent as well, but was mild in comparison to the degradation of MDC1 and 53BP1 1h after irradiation. It seems likely that a stronger decrease would be observed at later time points. The possible increase of the BRCA1 total level upon MDC1 depletion corresponds to a similar observation in the case of 53BP1 (chapter 5.3.3), but probably would require a higher number of experiments to be clearly assessed.

The fractionation assay used in this study appeared to be difficult for monitoring the unmodified form of BRCA1 on chromatin, since this form of BRCA1 was completely extracted within the soluble protein fraction (chapters 5.2.4 and 5.3.3). Under our experimental conditions, it seems that only heavely modified (ubiquitinated and/or SUMOylated) BRCA1 associates to the tightly bound chromatin fraction.

The observation that unmodified BRCA1 is more sensitive to stringent extraction conditions than MDC1 and 53BP1 could also be due to the fact that it does not bind to the chromatin directly, but via RAP80 and K63-linked ubiquitin chains (29). Assuming that the remaining BRCA1 background signal (“smears”) in the P samples of our assay corresponds to ubiquitinated and/or SUMOylated BRCA1, it could be noticed that p97 depletion reduces these smears by approximately 15% (chapter 5.2.4). By this experimental approach, even the depletion of MDC1, a well-characterized upstream factor for the recruitment of BRCA1 to chromatin, reduces BRCA1 “smears” for only 30% (chapter 5.3.3). These results, together with the previous data regarding p97-BRCA1 interaction (75) and p97-dependent BRCA1 recruitment to DSB (33), but in contrary to the findings of Acs et al. (87), suggest that p97 indeed regulated BRCA1 recruitment to chromatin under both, physiological and genotoxic conditions. Further experiments and other methodological approaches would be necessary to completely understand how p97 controls the chromatin association of BRCA1 and its function. The dynamics of BRCA1 after DNA damage might be complex as suggested by the literature data (36). In particular, there might be considerable differences between cell cycle stages (5) or cell lines.

## 6.4 p97 promotes CAD of ubiquitinated substrates

By depletion of p97 by RNAi (chapter 5.2.1), as well as by expression of an ATPase-inactive p97 mutant (chapter 5.4), we were able to demonstrate the significance of p97 for the clearance of ubiquitin conjugates from chromatin both under physiological and genotoxic conditions. Impaired p97 function does not solely increase the level of soluble but especially the amount of tightly chromatin-bound, poly-ubiquitinated substrates. Taking into account the extent of accumulation, it must be assumed that these ubiquitin conjugates severely disturb physiological processes on chromatin and thus lead to PICHROS (57).

As discussed in section 6.1, chromatin-associated p97 substrates possibly include E3 ubiquitin ligases, persistence of which would amplify the effect of ubiquitin accumulation on chromatin if p97 is inhibited. Employing chain-specific ubiquitin antibodies, it would be possible to clarify which ubiquitin linkage types are present among the accumulating substrates under physiological conditions and upon IR. Based on the present knowledge it could be assumed that K48 chains are predominant (34).

Surprisingly, the results in chapter 5.3.2 indicate that also MDC1 depletion causes accumulation of soluble and tightly chromatin-bound ubiquitin conjugates under physiological conditions, although to a lower extent than p97 depletion. To our knowledge, MDC1 was not implicated in ubiquitination processes on undamaged chromatin so far, but only in those related to DNA damage. Our finding thus suggests a novel, general role of MDC1 in the turnover of poly-ubiquitinated proteins on chromatin.

## 6.5 Conclusion and outlook

Our work points to diverse p97 activities on DDR and chromatin-associated proteins in human cells and to an important role of p97 in genome stability. It raises plenty of questions regarding the dynamics of DDR proteins under physiological and genotoxic conditions as well as how their dysregulation influences DNA repair. Notably, our results support the idea that protein degradation is an integral regulation mechanism of the DDR (53). These degradation pathways might be complex and not all of them seem to depend on p97.

DDR proteins are key players in genome stability and their inactivation causes a variety of diseases including neoplasms (3). Implication of p97 in DDR opens a new window for diagnosis, prognosis and therapy of cancer: While the significance of somatic mutations in the p97 gene found in human cancers is currently unknown (90), it seems clear that malignant cells rely on the functions of p97 related to proliferation and proteostasis (57). As mentioned in chapter 2.5, p97 and its adaptors regulate proteins that are critically involved in tumorigenesis (45; 57; 71; 74). It was demonstrated more than a decade ago that high p97 expression levels correlate with the metastatic potential of murine osteosarcoma cells. These finding was associated with enhanced IκBα degradation, constantly activated NFκB and resistance to tumor necrosis factor α (TNFα)-induced apoptosis (91).

The prognostic significance of p97 expression levels was subsequently assessed by a number of clinical studies. In hepatocellular carcinoma (HCC) patients, high p97 levels correlated with invasive behavior of the tumor and poor survival (92). An investigation on gastric carcinoma patients revealed a significant association of p97 expression and tumor size, depth of invasion, histologic differentiation, vascular and lymphatic invasion, and lymph node metastasis (93).

Similar results were obtained from studies on non-small-cell lung carcinomas (NSCLC) (94), gingival squamous cell carcinomas (95), follicular thyroid cancer (96), prostate cancer (97) and colorectal carcinomas, whereas non-metastatic colorectal adenomas showed low p97 expression. Hence, determination of p97 levels by immunohistochemistry was proposed as a prognosticator for the mentioned malignancies in combination with classical tumor staging (98). Moreover, p97 was proposed as a sensitive serum tumor marker for human granulosa cell tumor, ovarian carcinoma, non-Hodgkin's lymphoma as well as breast, colon, and pancreatic cancer. Notably, high p97 levels even identified some granulosa cell tumor, ovarian carcinoma, breast cancer and colon cancer patients who did not display an increase of customary serum markers for their cancer type (99).

Another recent study confirmed elevated p97 levels in HCC tissues and suggested that microRNA-129-5p negatively regulates p97 expression. Down-regulation of p97 by siRNA or microRNA-129-5p was shown to inhibit HCC tumor growth in a mouse model (100). Similarly, the p97 inhibitor Eeyarestatin I (EerI), which disturbs ERAD-associated p97 functions but not ATPase activity (90), reduced tumor growth in a NSCLC xenograft model (80).

Interestingly, high p97 levels were accompanied by accumulation of ubiquitinated proteins in NSCLC tissues and cell lines. It is therefore speculated that p97 overexpression is a consequence of defective proteostasis in cancer cells. It was concluded from this study that p97 is an attractive molecular target for controlling tumor genesis and metastasis of NSCLC and other forms of cancers, because p97 inhibitors may have added potential over existing proteostasis and HDAC inhibitors (80). This idea is supported by the finding that p97 depletion showed pronounced synergistic interactions with standard chemotherapeutic agents, such as DNA-damaging agents, antimitotics and stress-inducing agents. Importantly, cells treated with proteasome inhibitors could bypass defective protein elimination by the UPS via activation of the aggresome-autophagy pathway, accounting for bortezomib resistance observed in multiple myeloma patients. In contrast, p97 inhibitors also interfere with the autophagy process and thus might have an advantage over proteasome inhibitors (81).

Besides EerI, a number of additional p97 inhibitors were discovered and are currently under intense investigation as potential anticancer drugs (90). 2-anilino-4-aryl-1,3-thiazole, which inhibits p97 ATPase activity, was the first of these small, drug-like compounds (101). N2,N4-dibenzylquinazoline-2,4-diamine (DBeQ) is another selective, potent, reversible, and ATP-competitive p97 inhibitor that can enhance the effect of sorafenib, a multikinase inhibitor. The latter is used for HCC treatment and prevents p97 tyrosine phosphorylation, promoting an unbalance of p97 subcellular distribution (90). Furthermore, alkylsulfanyl-1,2,4-triazoles were recently identified as a new class of allosteric p97 inhibitors, with one of the discovered compounds exhibiting anti-proliferative activity in the sub-micromolar range (102).

Chemical expansion of this allosteric class identified NMS-873, the most potent and specific p97 inhibitor described to date. In the same study, NMS-859 was described as a covalent inhibitor that modifies p97 at Cys522 (81). This residue is also targeted by Syk inhibitor III, which irreversibly blocks p97 by trapping the ubiquitinated client protein (90).

In conclusion, the promising effects of p97 inhibitors have been mainly linked to ERAD (81), while the association between increased p97 expression and tumor cell proliferation has been attributed to the role of p97 in regulation of NFκB and p53 (80). However, other cellular functions of p97, especially its recently identified roles in the DDR and in chromatin proteostasis, open a new avenue for exploring the potential of p97 for anti-cancer therapy. Our group is currently focusing on the understanding of how two-hit therapy based on specific p97 inhibitors and IR might be used for the treatment of solid tumors. If p97 is targeted for treatment of cancer or degenerative disorders, the beneficial and adverse effects of such therapeutic strategies need to be assessed. Therefore, further efforts should be made to get a comprehensive understanding of the emerging p97 functions.

# 7 References


1. **Hoeijmakers, Jan H.J.** DNA Damage, Aging, and Cancer. *New England Journal of Medicine.* 2009, 361, pp. 1475-1485.

2. **Ciccia, Alberto and Elledge, Stephen J.** The DNA damage response: making it safe to play with knives. *Molecular cell.* 2010, 40, pp. 179-204.

3. **Jackson, Stephen P. and Bartek, Jiri.** The DNA-damage response in human biology and disease. *Nature.* 2009, 461, pp. 1071-1078.

4. **Basu, Bristi, et al.** Targeting the DNA damage response in oncology: past, present and future perspectives. *Current Opinion in Oncology.* 2012, 24, pp. 316-324.

5. **Polo, Sophie E., and Jackson, Stephen P.** Dynamics of DNA damage response proteins at DNA breaks: a focus on protein modifications. *Genes & Development.* 2011, 25, pp. 409-433.

6. **Bartek, Jiri, and Hodny, Zdenek.** SUMO Boosts the DNA Damage Response Barrier against Cancer. *Cancer Cell.* 2010, 17, pp. 9-11.

7. **Sulli, Gabriele, et al.** Crosstalk between chromatin state and DNA damage response in cellular senescence and cancer. *Nature Reviews Cancer.* 2012, 12, pp. 709-720.

8. **Vijg, Jan, and Suh, Yousin.** Genome Instability and Aging. *Annual Review of Physiology.* 2013, 75, pp. 645-668.

9. **Van Attikum, Haico and Gasser, Susan M.** Crosstalk between histone modifications during the DNA damage response. *Trends in Cell Biology.* 2009, 19 (5), pp. 207-217.

10. **Luo, Kuntian, et al.** Sumoylation of MDC1 is important for proper DNA damage response. *The EMBO Journal.* 2012, 31, pp. 3008-3019.

11. **Pinder, Jordan B., et al.** Reading, writing, and repair: the role of ubiquitin and the ubiquitin-like proteins in DNA damage signaling and repair. *Frontiers in Genetics.* 2013, 4, pp. 1-14.

12. **Price, Brendan D., and D'Andrea, Alan D.** Chromatin Remodeling at DNA Double-Strand Breaks. *Cell.* 2013, 152, pp. 1344-1354.

13. **Stewart, Grant S.** Solving the RIDDLE of 53BP1 recruitment to sites of damage. *Cell Cycle.* 2009, 8, pp. 1532-1538.

14. **Curtin, Nicola J.** DNA repair dysregulation from cancer driver to therapeutic target. *Nature Reviews.* 2012, 12, pp. 801-817.

15. **Bekker-Jensen, Simon, and Mailand, Niels.** Assembly and function of DNA double-strand break repair foci in mammalian cells. *DNA repair.* 2010, 9, pp. 1219-1228.

16. **Hiom, Kevin.** Coping with DNA double strand breaks. *DNA repair.* 2010, 9, pp. 1256–1263.

17. **Coster, Gideon, and Goldberg, Michal.** The cellular response to DNA damage: A focus on MDC1 and its interacting proteins. *Nucleus.* 2010, 1, pp. 166-178.

18. **Noon, Angela T., and Goodarzi, Aaron A.** 53BP1-mediated DNA double strand break repair: Insert bad pun here. *DNA repair.* 2011, 10, S. 1071-1076.

19. **Taleei, Reza, et al.** A kinetic model of single-strand annealing for the repair of DNA double-strand breaks. *Radiation Protection Dosimetry.* 2011, 143, pp. 191-195.

20. **Yelamos, José, et al.** PARP-1 and PARP-2: New players in tumour development. *American Journal of Cancer Research.* 2011, 1, pp. 328-346.

21. **Pears, Catherine J., et al.** The role of ADP-ribosylation in regulating DNA double-strand break repair. *Cell Cycle.* 2012, 11, pp. 48-56.

22. **Chapman, J. Ross, et al.** Playing the End Game: DNA Double-Strand Break Repair Pathway Choice. *Molecular Cell.* 2012, 47, pp. 497-510.

23. **Feng, Lin, et al.** RIF1 Counteracts BRCA1-mediated End Resection during DNA repair. *The Journal of Biological Chemistry.* 2013, 288, pp. 11135-11143.

24. **Stracker, Travis H., and Petrini, John H. J.** The MRE11 complex: starting from the ends. *Nature Reviews.* 2011, 12, pp. 90-103.

25. **Sirbu, Bianca M., and Cortez, David.** DNA Damage Response: Three Levels of DNA Repair Regulation. *Cold Spring Harbor Perspectives in Biology.* 2013, 10.1101, pp. 1-16.

26. **Heijink, Anne Margriet, et al.** The DNA damage response during mitosis. *Mutation Research/Fundamental and Molecular Mechanisms of Mutagenesis.* 2013, http://dx.doi.org/10.1016/j.mrfmmm.2013.07.003.

27. **Jungmichel, Stephanie, and Stucki, Manuel.** MDC1: The art of keeping things in focus. *Chromosoma.* 2010, 119, pp. 337-349.

28. **Vignard, Julien, et al.** Ionizing-radiation induced DNA double-strand breaks: A direct and indirect lighting up. *Radiotherapy and Oncology.* 2013, doi: 10.1016/j.radonc.2013.06.013.

29. **Al-Hakim, Abdallah, et al.** The ubiquitous role of ubiquitin in the DNA damage response. *DNA Repair.* 2010, 9, pp. 1229–1240.

30. **Luijsterburg, Martijn S., and van Attikum, Haico.** Close encounters of the RNF8th kind: when chromatin meets DNA repair. *Current Opinion in Cell Biology.* 2012, 24, pp. 439-447.

31. **Bunting, Samuel F., et al.** 53BP1 Inhibits Homologous Recombination in Brca1-Deficient Cells by Blocking Resection of DNA Breaks. *Cell.* 2010, 141, pp. 243-254.

32. **Ramadan, Kristijan, and Meerang, Mayura.** Degradation-linked ubiquitin signal and proteasome are integral components of DNA double strand break repair: New perspectives for anti-cancer therapy. *FEBS Letters.* 2011, 585, S. 2868–2875.

33. **Meerang, Mayura, et al.** The ubiquitin-selective segregase VCP/p97 orchestrates the response to DNA double-strand breaks. *Nature Cell Biology.* 2011, 13, pp. 1376-1382.

34. **Ramadan, Kristijan.** p97/VCP- and Lys48-linked polyubiquitination form a new signaling pathway in DNA damage response. *Cell Cycle.* 2012, 11, pp. 1062-1069.

35. **Mallette, Frédérick A., and Richard, Stéphane.** K48-linked ubiquitination and protein degradation regulate 53BP1 recruitment at DNA damage sites. *Cell Research.* 2012, 22, pp. 1221-1223.

36. **Brodie, Kirsty M. and Henderson, Beric R.** Differential modulation of BRCA1 and BARD1 nuclear localisation and foci assembly by DNA damage. *Cellular Signalling.* 2010, 22, pp. 291-302.

37. **Zhang, Fan, et al.** MDC1 and RNF8 function in a pathway that directs BRCA1-dependent localization of PALB2 required for homologous recombination. *Journal of Cell Science.* 2012, 125, pp. 6049-6056.

38. **Nakada, Shinichiro, et al.** RNF8 Regulates Assembly of RAD51 at DNA Double-Strand Breaks in the Absence of BRCA1 and 53BP1. *Cancer Research.* 2012, 72, pp. 4974-4983.

39. **Jacq, Xavier, et al.** Deubiquitylating Enzymes and DNA Damage Response Pathways. *Cell Biochemistry and Biophysics.* 2013, 67, pp. 25-43.

40. **Zgheib, Omar, et al.** An Oligomerized 53BP1 Tudor Domain Suffices for Recognition of DNA Double-Strand Breaks. *Molecular and Cellular Biology.* 2009, 29 (4), pp. 1050–1058.

41. **Doil, Carsten, et al.** RNF168 Binds and Amplifies Ubiquitin Conjugates on Damaged Chromosomes to Allow Accumulation of Repair Proteins. *Cell.* 2009, 136, pp. 435-446.

42. **Fradet-Turcotte, Amélie, et al.** 53BP1 is a reader of the DNA-damage-induced H2A Lys 15 ubiquitin mark. *Nature.* 2013, 499, pp. 50-54.

43. **FitzGerald, Jennifer E., et al.** 53BP1: function and mechanisms of focal recruitment. *Biochemical Society Transactions.* 2009, 37, pp. 897-904.

44. **Bologna, Serena, and Ferrari, Stefano.** It takes two to tango: Ubiquitin and SUMO in the DNA damage response. *Frontiers in Genetics.* 2013, 4, pp. 1-18.

45. **Haines, Dale S.** p97-containing complexes in proliferation control and cancer: emerging culprits or guilt by association? *Genes Cancer.* 2010, 1, pp. 753-763.

46. **Yang, Yili, et al.** Targeting the ubiquitin-proteasome system for cancer therapy. *Cancer Science.* 2009, 100, pp. 24-28.

47. **Panier, Stephanie and Durocher, Daniel.** Regulatory ubiquitylation in response to DNA double-strand breaks. *DNA Repair.* 2009, 8, pp. 436-443.

48. **Clague, Michael J. and Urbé, Sylvie.** Ubiquitin: Same Molecule, Different Degradation Pathways. *Cell.* 2010, 143, pp. 682-685.

49. **Franz, André, et al.** Create and preserve: Proteostasis in development and aging is governed by Cdc48/p97/VCP. *Biochimica et Biophysica Acta.* 2013, doi: 10.1016/j.bbamcr.2013.03.031.

50. **Wojcik, Cezary, Yano, Mihiro and DeMartino, George N.** RNA interference of valosin-containing protein. *Journal of Cell Science.* 2004, 117, pp. 281-292.

51. **Finley, Daniel.** Recognition and Processing of Ubiquitin-Protein Conjugates by the Proteasome. *Annual Review of Biochemistry.* 2009, 78, pp. 477–513.

52. **Bergink, Steven and Jentsch, Stefan.** Principles of ubiquitin and SUMO modifications in DNA repair. *Nature.* 2009, 458, pp. 461-467.

53. **Kouranti, Ilektra, and Peyroche, Anne.** Protein degradation in DNA damage response. *Seminars in Cell & Developmental Biology.* 2012, 23, pp. 538-545.

54. **Shi, Wei, et al.** Disassembly of MDC1 Foci Is Controlled by Ubiquitin-Proteasome-dependent Degradation. *Journal of Biological Chemistry.* 2008, 283, pp. 31608-31616.

55. **Liu, Weijun, et al.** Turnover of BRCA1 Involves in Radiation-Induced Apoptosis. *PLoS ONE.* 2010, 5 e14484, pp. 1-11.

56. **Zhang, Dong, et al.** A Role for the Deubiquitinating Enzyme USP28 in Control of the DNA-Damage Response. *Cell.* 2006, 126, pp. 529-542.

57. **Vaz, Bruno, et al.** Role of p97/VCP (Cdc48) in genome stability. *Frontiers in Genetics.* 2013, 4, pp. 1-14.

58. **Gudjonsson, Thorkell, et al.** TRIP12 and UBR5 Suppress Spreading of Chromatin Ubiquitylation at Damaged Chromosomes. *Cell.* 2012, 150, pp. 697-709.

59. **Lukas, Jiri.** The interface between the ubiquitin family and the DNA damage response. *EMBO reports.* 2010, 11, pp. 907-909.

60. **Vyas, R., et al.** RNF4 is required for DNA double-strand break repair in vivo. *Cell Death and Differentiation.* 2013, 20, pp. 490-502.

61. **Guzzo, Catherine M., et al.** RNF4-Dependent Hybrid SUMO-Ubiquitin Chains Are Signals for RAP80 and Thereby Mediate the Recruitment of BRCA1 to Sites of DNA Damage. *Science Signalling.* 2012, 5, pp. 1-7.

62. **Galanty, Yaron, et al.** Mammalian SUMO E3-ligases PIAS1 and PIAS4 promote responses to DNA double-strand breaks. *Nature.* 2009, 462, pp. 935-939.

63. —. RNF4, a SUMO-targeted ubiquitin E3 ligase, promotes DNA double-strand break repair. *Genes & Development.* 2012, 26, pp. 1179-1195.

64. **Wang, Qing, Song, Changcheng and Li, Chou-Chi H.** Molecular perspectives on p97-VCP: progress in understanding its structure and diverse biological functions. *Journal of Structural Biology.* 2004, 146, pp. 44-57.

65. **Chia, Wei Sheng, et al.** ATP Binding to p97/VCP D1 Domain Regulates Selective Recruitment of Adaptors to Its Proximal N-Domain. *PLOS ONE.* 2012, 7, e50490.

66. **Chapman, Eli, et al.** The complexities of p97 function in health and disease. *Molecular BioSystems.* 2011, 7, pp. 700-710.

67. **Jentsch, Stefan and Rumpf, Sebastian.** Cdc48 (p97): a 'molecular gearbox' in the ubiquitin pathway? *Trends in Biochemical Sciences.* 2006, 32, pp. 6-11.

68. **Meyer, Hemmo, et al.** Emerging functions of the VCP/p97 AAA-ATPase in the ubiquitin system. *Nature Cell Biology.* 2012, 14, pp. 117-123.

69. **Ewens, Caroline A., et al.** Structural and functional implications of phosphorylation and acetylation in the regulation of the AAA+ protein p97. *Biochemistry and Cell Biology.* 2010, 88, pp. 41-48.

70. **Livingstone, Mark et al.** Valosin-Containing Protein Phosphorylation at Ser784 in Response to DNA Damage. *Cancer Research.* 2005, 65, pp. 7533-7540.

71. **Alexandru, Gabriela, et al.** UBXD7 Binds Multiple Ubiquitin Ligases and Implicates p97 in HIF1α Turnover. *Cell.* 2008, 134, pp. 804-816.

72. **Yamanaka, Kunitoshi, et al.** Recent advances in p97/VCP/Cdc48 cellular functions. *Biochimica et Biophysica Acta.* 2012, 1823, pp. 130-137.

73. **Cao, Kan, et al.** The AAA-ATPase Cdc48/p97 Regulates Spindle Disassembly at the End of Mitosis. *Cell.* 2003, 115, pp. 355-367.

74. **Ramadan, Kristijan, et al.** Cdc48/p97 promotes reformation of the nucleus by extracting the kinase Aurora B from chromatin. *Nature.* 2007, 450, pp. 1258-1262.

75. **Zhang, Hongtao, et al.** VCP, a Weak ATPase Involved in Multiple Cellular Events, Interacts Physically with BRCA1 in the Nucleus of Living Cells. *DNA and Cell Biology.* 2000, 19, pp. 253-263.

76. **Indig, Fred Eliezer, et al.** Werner syndrome protein directly binds to the AAA ATPase p97/VCP in an ATP-dependent fashion. *Journal of Structural Biology.* 2004, 146, pp. 251-259.

77. **Watts, Giles D. J., et al.** Inclusion body myopathy associated with Paget disease of bone and frontotemporal dementia is caused by mutant valosin-containing protein. *Nature Genetics.* 2004, 36, pp. 377-381.

78. **Weihl, Conrad C., et al.** Valosin-containing protein disease: Inclusion body myopathy with Paget's disease of the bone and fronto-temporal dementia. *Neuromuscular Disorders.* 2009, 19, pp. 308-315.

79. **Johnson, Janel O., et al.** Exome Sequencing Reveals VCP Mutations as a Cause of Familial ALS. *Neuron.* 2010, 68, pp. 857-864.

80. **Valle, Christopher W., et al.** Critical Role of VCP/p97 in the Pathogenesis and Progression of Non-Small Cell Lung Carcinoma. *PLoS ONE.* 2011, 6, e29073.

81. **Magnaghi, Paola, et al.** Covalent and allosteric inhibitors of the ATPase VCP/p97 induce cancer cell death. *Nature Chemical Biology.* 2013, 9, pp. 548-556.

82. **Postow, Lisa, et al.** Ku80 removal from DNA through double strand break-induced ubiquitylation. *The Journal of Cell Biology.* 2008, 182, pp. 467-479.

83. **Goldmann, Wolfgang H., et al.** Vinculin, cell mechanics and tumour cell invasion. *Cell Biology International.* 2013, 37, pp. 397-405.

84. **Peng, Aimin, and Chen, Phang-Lang.** NFBD1, Like 53BP1, Is an Early and Redundant Transducer Mediating Chk2 Phosphorylation in Response to DNA Damage. *Journal of Biological Chemistry.* 2003, 278, pp. 8873-8876.

85. **Sobhian, Bijan, et al.** RAP80 Targets BRCA1 to Specific Ubiquitin Structures at DNA Damage Sites. *Science.* 2007, 316, pp. 1198–1202.

86. **Bannon, John H., et al.** The peptidyl prolyl isomerase cyclophilin A localizes at the centrosome and the midbody and is required for cytokinesis. *Cell Cycle.* 2012, 11, pp. 1340-1353.

87. **Acs, Klara, et al.** The AAA-ATPase VCP/p97 promotes 53BP1 recruitment by removing L3MBTL1 from DNA double-strand breaks. *Nature Stuctural & Molecular Biology.* 2011, 18, pp. 1345-1351.

88. **Yin, Yili, et al.** SUMO-targeted ubiquitin E3 ligase RNF4 is required for the response of human cells to DNA damage. *Genes and Development.* 2012, 26, pp. 1196-1208.

89. **Watanabe, Kenji, et al.** RAD18 promotes DNA double-strand break repair during G1 phase through chromatin retention of 53BP1. *Nucleic Acids Research.* 2009, 37, pp. 2176-2193.

90. **Fessart, Delphine, et al.** P97/CDC-48: Proteostasis control in tumor cell biology. *Cancer Letters.* 2013, 337, pp. 26-34.

91. **Asai, Tatsuya, et al.** VCP (p97) Regulates NFκB Signaling Pathway, Which Is Important for Metastasis of Osteosarcoma Cell Line. *Japanese Journal of Cancer Research.* 2002, 93, pp. 296-304.

92. **Yamamoto, Shinji, et al.** Elevated Expression of Valosin-Containing Protein (p97) in Hepatocellular Carcinoma Is Correlated With Increased Incidence of Tumor Recurrence. *Journal of Clinical Oncology.* 2003, 21, pp. 447-452.

93. —. Expression Level of Valosin-Containing Protein Is Strongly Associated With Progression and Prognosis of Gastric Carcinoma. *Journal of Clinical Oncology.* 2003, 21, pp. 2537-2544.

94. —. Expression Level of Valosin-Containing Protein (p97) Is Correlated With Progression and Prognosis of Non–Small-Cell Lung Carcinoma. *Annals of Surgical Oncology.* 2004, 11, pp. 697-704.

95. —. Expression level of valosin-containing protein (VCP) as a prognostic marker for gingival squamous cell carcinoma. *Annals of Oncology.* 2004, 15, pp. 1432-1438.

96. —. Increased Expression of Valosin-Containing Protein (p97) Is Correlated With Disease Recurrence in Follicular Thyroid Cancer. *Annals of Surgical Oncology.* 2005, 12, pp. 925-934.

97. **Tsujimoto, Yuichi, et al.** Elevated Expression of Valosin-Containing Protein (p97) Is Associated with Poor Prognosis of Prostate Cancer. *Clinical Cancer Research.* 2004, 10, pp. 3007-3012.

98. **Yamamoto, Shinji, et al.** Expression of Valosin-Containing Protein in Colorectal Carcinomas as a Predictor for Disease Recurrence and Prognosis. *Clinical Cancer Research.* 2004, 10, pp. 651-657.

99. **Laguë, Marie-Noëlle, et al.** Proteomic Profiling of a Mouse Model for Ovarian Granulosa Cell Tumor Identifies VCP as a Highly Sensitive Serum Tumor Marker in Several Human Cancers. *PLoS ONE.* 2012, 7, e42470.

100. **Liu, Yu, et al.** VCP/p97, Down-Regulated by microRNA-129-5p, Could Regulate the Progression of Hepatocellular Carcinoma. *PLoS ONE.* 2012, 7, e35800.

101. **Bursavic, Matthew G., et al.** 2-Anilino-4-aryl-1,3-thiazole inhibitors of valosin-containing protein (VCP or p97). *Bioorganic & Medicinal Chemistry Letters.* 2010, 20, pp. 1677-1679.

102. **Polucci, Paolo, et al.** Alkylsulfanyl-1,2,4-triazoles, a New Class of Allosteric Valosine Containing Protein Inhibitors. Synthesis and Structure-Activity Relationships. *Journal of Medical Chemistry.* 2012, 56, pp. 437-450.

# 8 Abbreviations

| | |
|---|---|
| AAA | ATPase associated with diverse cellular activities |
| ADP | adenosine diphosphate |
| ALS | amyotrophic lateral sclerosis |
| APS | ammonium persulfate |
| ATM | ataxia telangiectasia mutated (kinase) |
| ATP | adenosine triphosphate |
| ATR | ataxia telangiectasia and Rad3-related (kinase) |
| BARD1 | BRCA1-associated RING domain protein 1 |
| BER | base-excision repair |
| BRCA1/BRCA2 | breast cancer type 1/2 susceptibility protein |
| BRCT | BRCA1 C-terminus (domain) |
| BSA | bovine serum albumin |
| BLM | Bloom syndrome (helicase) |
| CAD | chromatin-associated degradation |
| Cdc48 | cell division cycle 48 (p97 ortholog in yeast) |
| CDKs | cycline-dependent kinases |
| CHK1/CHK2 | checkpoint kinase 1/2 |
| $CO_2$ | carbon dioxide |
| CPT | camptothecin |
| CSR | class-switch recombination |
| DDR | DNA damage response |
| DMEM | Dulbecco's modified Eagle's medium |
| DMSO | dimethyl sulfoxide |
| DNA | deoxyribonucleic acid |
| DNA-PKcs | DNA-dependent protein kinase, catalytic subunit |
| DSB | DNA double-strand break |
| DTT | DL-dithiothreitol |
| DUB | de-ubiquitinating enzyme |
| DUF | DNA unwinding factor |
| DVC1 | DNA damage-associated VCP/p97 cofactor 1 |
| EDTA | ethylenediaminetetraacetic acid |
| EGTA | ethyleneglycoltetraacetic acid |
| EQ | p97-E578Q (ATPase deficient mutant) |
| ERAD | endoplasmic reticulum-associated degradation |
| ex-polyQ | expanded poly-glutamine region |
| FANC | Fanconi anemia proteins |
| FCS | fetal calf serum |

| | |
|---|---|
| FHA | forkhead-associated (domain) |
| HCC | hepatocellular carcinoma |
| HCl | hydrochloric acid |
| HDAC6 | histone deacetylase 6 |
| HECT | homologous to the E6AP carboxylterminus (family of E3 ubiquitin ligases) |
| HEK | human embryonic kidney (cell line) |
| HEPES | 4-(2-hydroxyethyl)-1-piperazineethanesulfonic acid |
| HIF1α | hypoxia-inducible factor 1α |
| HR | homologous recombination (DNA repair pathway) |
| H3K79/H4K20 | lysine 79 of histone H3/lysine 20 of histone H4 |
| IB | immunoblotting |
| IBMPFD | inclusion body myopathy associated with Paget's disease of bone and frontotemporal dementia (disease caused by p97 mutations) |
| ICL | interstrand crosslink (DNA) |
| IgG | immunoglobulin G |
| IP | immunoprecipitation |
| IR | ionizing radiation |
| IRIF | ionizing radiation-induced foci |
| KCl | potassium chloride |
| kDa | kilodalton |
| $K_2HPO_4$ | dipotassium phosphate |
| K11/K29/K48/K63 | ubiquitin chain linkage types (lysine residues 11/29/48/63) |
| L3BMTL1 | lethal(3)malignant brain tumor-like protein 1 |
| MAD | mitochondria-associated degradation |
| MDC1 | mediator of DNA damage checkpoint protein 1 |
| $MgCl_2$ | magnesium chloride |
| MGMT | $O^6$-methylguanine DNA methyltransferase |
| MHC | major histocompatibility complex |
| MIU | motif interacting with ubiquitin |
| MJD | Machado-Joseph disease |
| MMC | mitomycin C |
| MMEJ | microhomology-mediated end joining (DNA repair pathway) |
| MMR | mismatch repair |
| MMS | methyl methanesulfonate |
| MRE11 | meiotic recombination 11 |
| MW | molecular weight |
| NaCl | sodium chloride |
| $NaHCO_3$ | sodium hydrogen carbonate |
| $Na_2HPO_4$ | disodium hydrogen phosphate |

| | |
|---|---|
| $NaN_3$ | sodium azide |
| NBS1 | Nijmegen breakage syndrome 1 |
| NER | nucleotide-excision repair |
| NF-κB | nuclear factor κB |
| NHEJ | non-homologous end joining (DNA repair pathway) |
| NPL4 | nuclear protein localization homolog 4 (p97 core adaptor) |
| NSCLC | non-small-cell lung carcinoma |
| OMM | outer mitochondrial membrane |
| PAGE | polyacrylamide gel electrophoresis |
| PAR/PARP | polyADP-ribose/polyADP-ribose polymerase |
| PBS | phosphate buffered saline |
| PBS-T | phosphate buffered saline containing Tween 20 |
| PCNA | proliferating cell nuclear antigen |
| PIAS1/PIAS4 | protein inhibitor of activated STAT-1/4 (SUMO E3 ligases) |
| PICHROS | protein-induced chromatin stress |
| PIKK | phosphatidylinositol 3-kinase-related kinases |
| PLAP | phospholipase A2-activating protein |
| PMSF | phenylmethanesulfonylfluoride |
| PNGase | peptide:N-glycanase |
| PUB | p97 binding motif of PNGase, RING finger 31 and UBXD1 (45) |
| PUL | p97 binding motif in PLAP (human), Ufd3 (yeast), and Lub1 (*Schizosaccharomyces pombe*) (45) |
| PVDF | polyvinylidene fluoride |
| RAD | ribosome-associated degradation |
| RIDDLE | radiosensitivity, immunodeficiency, dysmorphic features and learning difficulties (syndrome caused by RNF168 mutations) |
| RING | really interesting new gene (family of E3 ubiquitin ligases) |
| RNA | ribonucleic acid |
| RNAi | RNA interference |
| RNF8/RNF168 | RING finger protein 8/168 (E3 ligases) |
| RPA | replication protein A |
| SAE1/SAE2 | SUMO-activating enzyme subunit 1/2 |
| SDS | sodium dodecyl sulfate |
| SIM | SUMO-interacting motif |
| siRNA | small interfering RNA |
| SSA | single-strand annealing (DNA repair pathway) |
| SSB | DNA single-strand breaks |
| ssDNA | single-strand DNA |
| SUMO | small ubiquitin-like modifier |

| | |
|---|---|
| TDP-43 | transactive response DNA-binding protein 43 |
| TEMED | tetramethylethylenediamine |
| TRIP12 | thyroid hormone receptor interactor 12 (E3 ubiquitin ligase) |
| UBA | ubiquitin-associated domain |
| UBD | ubiquitin-binding domain |
| UBL | ubiquitin-like protein |
| UBR5 | ubiquitin protein ligase E3 component n-recognin 5 (E3 ubiquitin ligase) |
| UBX | ubiquitin-X domain (of p97 adaptors) |
| UFD1 | ubiquitin fusion degradation 1 (p97 core adaptor) |
| UPS | ubiquitin proteasome system |
| UV | ultraviolet (radiation) |
| VCP | valosin-containing protein (p97) |
| WRNp | Werner syndrome helicase |
| WT | HEK 293 cells stably transfected with strep-p97-WT (wildtype form) |
| 53BP1 | p53 binding protein 1 |

# Acknowledgments

First of all, I would like to thank my supervisor Dr. Kristijan Ramadan, who always kept his optimism about my work and encouraged me to continue, even if I had obtained some disappointing results or unexpected problems arose in the laboratory. I am especially grateful for the freedom that Kristijan granted me to organize my project in a flexible way, which allowed me to fulfill my other commitments at the same time.

My thanks also go to the members of our research group, Dr. Bruno Vaz, Zuzana Garajova, Judith Oehler, Swagata Halder and Regina Fertig, for their helpfulness, friendliness and for all the interesting discussions about methodical or conceptual aspects of our work as well as about the everyday life in a lab.

Furthermore, I have to address special thanks to my referee, Prof. Dr. Hanspeter Nägeli, and to the director of the Institute of Veterinary Pharmacology and Toxicology, Prof. Dr. Felix Althaus, for giving me the possibility to carry out my dissertation project here. I also would like to thank Prof. Dr. Ulrich Hübscher from the Institute of Veterinary Biochemistry and Molecular Biology for being available as a co-referee.

Likewise, I want to express my sincere thanks to all members of the Institute of Veterinary Pharmacology and Toxicology who were not mentioned so far, for every kind of support they granted me, for their consideration, helpful advices and for the pleasant working atmosphere at the institute.

Last but not least, I have to thank my family for the great support during the whole time of my dissertation project.

# Curriculum vitae

## Personal data

| | |
|---|---|
| Name: | Sebastian Martin Koller |
| Date of birth: | April 8, 1988 |
| Place of birth: | St. Gallen, Switzerland |
| Nationality: | Swiss |
| Hometown: | Wil SG, Switzerland |

## Education

| | |
|---|---|
| 2012 - 2013: | Dissertation project, Institute of Veterinary Pharmacology and Toxicology, University of Zürich |
| 2011: | Federal diploma in veterinary medicine |
| 2010 - 2011: | Focal course in biomedical research, Institute of Veterinary Pharmacology and Toxicology, University of Zürich |
| 2006 - 2011: | Studies in veterinary medicine, Vetsuisse Faculty, University of Zürich |
| 2002 - 2006: | Gymnasium, Kantonsschule Wil, SG |
| 2000 - 2002: | Secondary school, Wil, SG |
| 1994 - 2000: | Primary school, Wil, SG |